A TRANSMISSION ELECTRON MICROSCOPE STEREOLOGICAL ANALYSIS OF THE BLOOD VESSELS AND NERVES IN THE HUMAN MANDIBULAR PREMOLAR PERIODONTAL LIGAMENT

A RESEARCH THESIS
submitted in partial fulfilment
of the requirements for the degree of
Master of Dental Surgery

by

KELVIN W.C. FOONG
B.D.S.
(Singapore)

Department of Dentistry
The University of Adelaide
South Australia

FEBRUARY 1994

Awarded 1995

ADDENDUM

page x : Add "Venous capillaries (VC) made up 27.3% of the total luminal volume." after the last sentence of the first paragraph.

page xi, paragraph 1 : Götze's method was inaccurate because the low magnification histological sections used did not facilitate the identification of all blood vessels.

page xi, paragraph 2, line 1 : Lateral distribution of axons in the tooth third, mid third and bone third are 5%, 80% and 15%. The differences between the respective thirds are comparable to the lateral distribution of luminal vessel volume at 9%, 78% and 13%, respectively.

page 12, last paragraph, line 1 : Insert "characteristic" between "own" and "microcirculatory".

page 89, 6.2.3 : Insert "A longer staining period of 10 minutes, compared with 8 minutes of staining with Reynolds' Lead (Parlange and Sims, 1993), was adopted to improve contrast in the EM histological sections." after first sentence.

page 100, paragraph 2, last 4 lines : Insert a separate sentence before the beginning of sentence "Therefore, in reviewing the studies of Götze (1976, 1980)..." with "The electron microscope offers a higher magnification and better resolution when viewing histological structures when compared to the light microscope."

Include into Discussion on page 108, continue from last sentence of paragraph 2 : "The findings provided a measure of the vascular anatomy of the human PDL. However, the present data from non-functional teeth posed a dilemma over whether they were relevant for extrapolation to normal functioning teeth, and whether these observations taken from a single individual would be representative of other individuals."

With dedications to:

My wife, Sandra,
whose love and encouragement
has been a source of strength during
the preparation of the thesis;

and

My parents,
who made possible my education.

TABLE OF CONTENTS

TABLES

FIGURES

THESIS SUMMARY

RATIONALE

The few histological studies into the vascular volume of the human PDL have provided overall values ranging from 1.63% to 3.5% (Götze, 1976 ,1980) and regional estimates of up to 20% (Sims, 1980). By contrast, stereological TEM animal data show luminal values ranging from 7.5% to 11.3% for mice, rats and marmosets depending on tooth and PDL region (Freezer and Sims, 1987; Lew et al., 1989; Clark et al., 1990; Chintakanon, 1990; Weir, 1991; Parlange and Sims, 1993). The discrepancy between animal and human data may be attributed to a number of factors including species differences, tooth type, the location of PDL examined, different techniques of specimen preparation, and the different patterns of masticatory function.

While the work of Götze (1965, 1976, 1980) has provided a measure of the human PDL blood volume, his work has not been re-evaluated using recently developed techniques to provide an accurate evaluation of the PDL vasculature (Nyengaard et al., 1988). In view of the reasons cited above, the data obtained from the studies of Götze (1976, 1980) may not accurately reflect the vascular volume in the human PDL. In addition, the animal models used to analyse the PDL may, therefore, not be valid for studying vascular anatomy and function for extrapolation to human PDL.

OBJECTIVES

Therefore, this investigation was undertaken utilising standard point counting techniques to obtain blood vessel and nerve data for the human PDL between the alveolar crest and the root apex. Stereological parameters for vessel and nerve, ie. volume (V_V), surface (S_V), length (L_V) densities, number per unit area (N_A), and the mean caliper diameters were to be determined. The human stereological data were also compared with animal data to determine the statistical relevance of animal models to study the human PDL.

MATERIALS AND METHODS

The distal PDL halves of 4 human mandibular premolars, derived from left and right mandibular surgical segments of a 20 year old male burns victim, were immersion fixed in 2.5% glutaraldehyde, and demineralised at 4°C in 0.1M EDTA in 0.06M cacodylate buffer and 2.5% glutaraldehyde solution at pH 6.0. Each distal half was then subdivided into 6 equal vertical wedge-shaped segments, with the two most distal wedged-shaped segments selected for horizontal sectioning from the alveolar crest to the root apex to produce 9 equal levels or 8 wedge-shaped blocks per distal segment. Each block was postfixed with 2% OsO_4, immersed in 1% uranyl nitrate, and processed for embedding in Agar 100 (Ladd). Horizontal sections in the silver - gold interference range from each block were stained with 1% uranyl acetate and Reynolds' lead, and viewed under a Jeol 100S transmission electron microscope (TEM). Micrographs at x3000 magnification were taken of the tooth, middle and bone circumferential thirds of the PDL in each randomly selected grid square, and were subsequently printed at x8500 magnification for point counting of blood vessels and nerve profiles with a 140 square lattice grid with points spaced at 17 mm. A total area of 110,000 μm^2 of PDL tissue was analysed. Blood vessels were identified according to their luminal diameter and wall structure (Rhodin, 1968; Freezer and Sims, 1987; Cooper et al., 1990; Parlange, 1991). Nerves were identified and classified according to their proximity to the vessel endothelium or location within the PDL space. The width of the PDL at each level was measured in a straight line across the sampling zone from the cementum to the alveolar bone. A generalised linear regression statistical model with binomial distribution was performed on the point counting data. An ANOVA was also carried out on blood vessel diameters. The mean luminal diameter of each vessel type was used to derive the V_v, S_v, and L_v densities for each category of blood vessel.

RESULTS

The mean luminal volume ranged from 8.97 ± 2.05% (SE) to 9.52 ± 2.28%. Endothelial volume added another 3.39% to give a mean abluminal volume ranging from 12.26 ± 2.49% to 12.91 ± 2.76%. Significant differences were observed between

luminal and abluminal volumes ($p<0.05$). The middle circumferential third of the PDL contained 78% of the blood volume, with 13% in the bone third, and the remaining 9% in the tooth third. Blood volume distribution was 50.4% in the apical third of the PDL while the coronal third contained the least blood volume at 18.7%. Venous vessels accounted for 96.4% of the vessel cohort. Arterial capillaries (AC) contributed the remaining 3.6%. Postcapillary - sized venules (PCV) were the most common vessel type, occupying 69.1% of the total luminal volume.

Axons accounted for 0.53% of the total periodontal ligament (PDL) volume. Nerve cells added another 0.48%. The mean diameters for unmyelinated and myelinated axons were 0.55 μm and 3.20 μm, respectively. Eighty-five per cent of the axons were unmyelinated and 15% were myelinated. The middle circumferential third contained 80% of the axons, with 15% and 5% in the bone and tooth circumferential thirds, respectively.

DISCUSSION

The four experimental premolars were derived from one person, and were essentially non-functional teeth. The mean luminal volume range of 8.97% to 9.52% found in immersion-fixed human premolar PDL was lower than the 11.26% mean luminal volume reported for the perfusion-fixed marmoset incisor PDL (Parlange and Sims, 1993). The predominance of blood volume in the middle circumferential third of the PDL suggested that physiological exchange was most efficient in this region. The linear increase in blood volume between the vertical thirds with increasing depth contrasted with the quadratic gradient reported in mouse (Sims, 1987) and in marmoset PDL (Parlange and Sims, 1993). Stereological data suggested that venular - sized vessels (PCV and CV) contained four times more blood per unit area of endothelial surface than capillary - sized vessels (AC and VC) in the human PDL. While the venular - sized vessels functioned as a blood reservoir, the capillary - sized vessels were considered to be more adept at providing physiological exchange.

The histological estimations of blood volume by Götze (1976, 1980), based on x400 magnification photomicrographs, included vessel wall volume. On the basis of the present findings, the volumetric estimations of 1.63% to 3.5% by Götze (1976, 1980) were low and, therefore, suggested the methodology he employed was inaccurate.

The lateral distribution pattern of axons compared favourably with the distribution pattern of vessel volume across the respective circumferential thirds. This similarity suggested an intimate neurovascular association in the regulation of physiological exchange and blood flow.

CONCLUSIONS

This investigation was the first TEM stereological study to quantify the vessel and nerve volume in the human premolar PDL. The findings of Götze (1976, 1980) were re-examined and it is concluded that they were erroneous when compared with the present finding of 8.97% to 9.52%. Venous blood volume was 26 times greater than arterial volume. The predominance of blood volume (78%) in the middle circumferential third suggested a regionalisation of physiological exchange. The linear volumetric gradient along the vertical length of the non-functional human PDL contrasted with the quadratic increase in blood volume reported for the marmoset incisor PDL (Parlange and Sims, 1993). The V_V and S_V densities showed that venular - sized vessels contained four times more blood per unit area of endothelium than capillary - sized vessels, while the latter were considered to be more efficient for physiological exchange.

This study confirmed the anisotropic nature of the human PDL. Comparable vascular characteristics between human and marmoset PDL in terms of V_v (9.52% vs 11.26%), the lateral vascular distribution, and the relative proportion of blood volume carried in venular - sized vessels and capillary - sized vessels, were observed. On the basis of these data, the marmoset PDL model might be recommended as the most appropriate substitute for studying the human PDL.

SIGNED STATEMENT

This MDS research report contains no material which has been accepted for the award of any other degree or diploma in any university or other tertiary institution and, to the best of my knowledge and belief, the report contains no material previously published or written by another person, except where due reference has been made in the text.

KELVIN FOONG
B.D.S. (Singapore)

NAME: KELVIN FOONG COURSE: MDS Orthodontics

I give consent to this copy of my research report, when deposited in the University Library, being available for photocopying and loan.

SIGNATURE ..... DATE: 17.2.95

ACKNOWLEDGEMENTS

I wish to thank the following people for their help and support over the last 2 years :

1. Dr M.R. Sims, my supervisor, for the intellectual stimulation and for sharing his vast experience that has made this study a worthwhile challenge.

2. Dr W.J. Sampson, my co-supervisor, for his many gentle ways that helped to pushed this project along.

3. Mr Ken Crocker, for his invaluable instruction and technical back-up on the Jeol 100s electron microscope.

4. Ms Sandra Pattison, for her excellent statistical analysis of the data, who helped made sense of the mountain of impersonal numbers.

5. Mrs Margaret Leppard, for her instruction and technical assistance on the use of the ultramicrotome, which helped speed up the laboratory stages of the experiment.

6. Ms Vicki Hargreaves, for her instruction on the use of the enlarger and on the staining procedures, and technical assistance whenever and wherever it was needed; many thanks also for decalcifying the teeth.

7. The Department of Anatomy, for allowing the use of their ultramicrotome.

8. My dear wife, Sandra, for her editorial support, and encouragement throughout the preparation of the thesis.

CHAPTER 1 INTRODUCTION

Götze (1965) was the first and only person to comprehensively quantify the human PDL vasculature. Using the light microscope, he estimated the blood vessel volume to be 1% to 2.5% of the total volume of the PDL. Further histological studies by Götze (1976, 1980) updated total vascular volumes with ranges from 2% to 3.5%. Sims (1980) histologically estimated the human vascular volume at a mean of 11%, with regional estimates reaching 20%. By contrast, stereological TEM rodent and primate data show mean vascular volumes ranging from 7.5% to 11.3% (Douvartizidis, 1984; Freezer and Sims, 1987; Lew et al., 1989; Clark et al., 1990; Parlange, 1991; Weir, 1991; Parlange and Sims, 1993).

The work of Götze (1976) has not been re-evaluated. Recently developed stereological techniques applied to TEM sections (Gundersen et al., 1988a,b) provide superior accuracy to low magnification histological estimations. Furthermore, the differences in reported data between animal and human PDL might be attributed to species variation, the tooth and the location of the PDL examined, the variation in specimen preparation, and the pattern of mastication.

Animal models have generally been used to study the PDL. The data obtained from such animal studies may not accurately reflect the vascular characteristics of the human PDL. Therefore, these species may not be valid models for studying vascular anatomy and function for extrapolation to human PDL.

CHAPTER 2 AIMS OF INVESTIGATION

AIMS

The aims of the investigation were to :

1. Collect blood vessel and nerve data at each sectioned level of the periodontal ligament (PDL) from the alveolar crest to the apex of the root.

2. Quantify vessel and nerve profiles within the tooth, middle, and bone circumferential thirds of the PDL using standard point counting techniques.

3. Measure the mean caliper diameter ($\overline{d}$) of blood vessels and nerves to provide stereological data for the volume (V_V), surface (S_V), and length (L_V) densities.

4. Establish the vessel and nerve number per unit area (N_A).

5. Compare human stereological data with animal data, and determine if animal models are relevant to an understanding of the ultrastructure and possible function of the human PDL.

CHAPTER 3 LITERATURE REVIEW

3.1 STEREOLOGY

3.1.1 Definition

Stereology is defined as a method of quantitative morphology which uses measurements from two-dimensional sections to describe the morphology of the original three-dimensional tissue (Bertram, 1989). It is highly objective and reliable in its description of cellular and tissue structures. Stereological methods are those which are used to derive three-dimensional information from a consideration of two-dimensional images. Methods of reconstructing structures from serial sections and methods used in extrapolating quantitative data have been termed "quantitative stereology" by Underwood (1970). The concept of stereology originated from the Delesse principle (Delesse, 1848). It asserts that on average the fractional area of a feature on sections taken of a solid body is directly proportional to the fractional volume of that feature in the original solid body. Therefore, stereological methods are based on mathematical and probabilistic ideas and stereological equations on geometric probability theory. The parameters used in stereological techniques are the volume density (V_V), surface density (S_V), length density (L_V) and numerical density (N_A).

3.1.2 Applications In Biological Science Research

Stereological methods can be used to provide estimates of morphometric quantities of cellular organelles, tissue structures and biochemical estimates of enzyme activities (Weibel 1981). Just as it is applicable to "normal" tissues, it can be used to detect pathological alterations (Gundersen et al., 1988a,b) not appreciable through the qualitative examination of sections (Bertram 1989). Newer and more efficient stereological techniques (Sterio, 1984; Gundersen and Jensen, 1985; Baddeley et al., 1986; Gundersen, 1986; Cruz-Orive, 1987; and Gundersen et al 1988a,b) are able to analyse organelles with complex shapes as well as minimize the effects of sampling bias. The stereological basis of the present research assumes blood vessels

and nerves to be three-dimensional tubular structures (Nyengaard et al., 1988) Vascular and neural volume can, therefore, be obtained from the cross-sectional area of these structures.

3.1.3 Sources Of Errors In Stereology

Potential problems include biased sampling and variance in the sections. Problems also arise when the interpretation of data is subjective. The thickness of tissue sections, shrinkage or the presence of swelling artefacts, the angle at which the tissue structure was cut, the resolution of the electron microscope (Weibel, 1981) and compression of the section during tissue processing all affect the accuracy of the measurements.

3.2 THE HUMAN PERIODONTAL LIGAMENT

3.2.1 Nomenclature

Gomphosis, pericementum, dental periosteum, peridental membrane, alveolo-dental ligament, periodontal membrane and desmodont have been some of the names by which the periodontal ligament (PDL) was called (Schroeder, 1986). German literature calls the PDL the *Periodontium*. Frohlich (1958) referred to the PDL as a syndesmotic joint-like structure between tooth and bone.

3.2.2 Function

The properties of the PDL influence the type of functions performed as an attachment between tooth and alveolar bone. Schroeder (1986) listed the properties of the PDL to be tensile strength, viscoelasticity, and hydrodynamic damping, and "an extra-ordinary potential for the various cellular activities related to remodelling". As such, the functions of the PDL are as follows:

1. Tooth support in that it plays a part in tooth eruption and it acts as a cushion for forces displacing tooth eg. during mastication.
2. Proprioception via its sensory nerve endings and mechanoreceptors.

3. Nutritive function is provided through the blood vessels in that cementoblasts and cementocytes are kept vital.
4. Homeostasis is carried out in that cellular functions are well regulated in response to functional demands placed on the PDL.
5. Reparative function in that self-regeneration is possible in tooth movement and cemental deposition in the repair of root resorption and root fracture.

3.2.3 Age Changes In The PDL

Qualitative histological studies to assess the age changes in the marmoset PDL (Bernick 1962; Grant and Bernick 1970, 1972b; Levy et al., 1972a,b) and in the human PDL (Severson et al., 1978) suggested that the main age changes in the PDL to be a collagen fibrosis, decreased cellularity, a decreased number of principal collagen fibres, and a tendency for the blood vessels to become arteriosclerotic - Grant and Bernick's (1970) definition of arteriosclerosis included the thickening of the vessels as well as a narrowing of the luminal diameter. Gathercole and Keller (1982) found that the collagen fibril diameter decreased more than 50% from about 70nm to about 30nm with age. Bernick (1962) used rat molar teeth (age of rats ranged from 1 to 18 months) and found that the PDL of the older rats showed a progressive decrease in the number of interstitial vessels and their perforating branches. Severson et al. (1978) examined eighty human cadaver PDL (age ranges from 20 to 90 years) and found that numerous periodontal fibres surrounded small, vascularized interstitial spaces in the young specimens. The older specimens showed larger vascularized spaces and these encroached upon areas formerly occupied by PDL fibres and bone.

However, these qualitative studies suffer from subjectivity, and information presented may be inaccurate. The only quantitative study on age changes in the PDL microvascular bed to date was by Sims et al. (1994). Using four one day old and four one year old male mice, a stereological TEM analysis was carried out to quantify the effects of age on the mandibular molar mesial PDL. There was an apparent 2.3x increase in the total luminal vascular volume of the older animals. Of significance was a four fold increase in the number of collecting vessels as compared to the

younger mice. However, this has to be viewed in the light that the reference volume of PDL tissue was half as much in the old mice as in the young mice, ie. the mean PDL width was half as much in the old mice as in the young mice. Therefore, with a slight increase of blood volume in half the volume of PDL tissue, there was a relative increase in the vascular volume of 2.3x. This study also refuted the claim by Grant and Bernick (1970) that vessels become arteriosclerotic with age.

3.3 THE PERIODONTAL VASCULAR BED

3.3.1 An Overview Of The Methods Used To Study The Microvasculature Of The PDL

The periodontal ligament has undergone many and varied types of investigation and examination. Routine histologic preparations, however, do not permit complete visualization of the vascular supply of these tissues. Carranza et al. (1966) used the light microscope to study the periodontal vascularization of different laboratory animals. Under the TEM, a two-dimensional image of the cross-section of the microvessels is seen, but the pathways of these vessels are difficult to visualize. However, with the advent of stereological techniques (Baddeley et al., 1986; Nyengaard et al., 1988), a model of the vascular arrangement can be built up using principles of mathematical probability (Freezer and Sims, 1987; Gundersen et al., 1988a,b; Parlange and Sims, 1993). PDL vessels can also be observed in the longitudinal dimensions. Injection techniques, using dye solutions (Keller and Cohen, 1955; Quintarelli, 1959; Castelli, 1963; Castelli and Dempster, 1965), gelatin preparations (Schuback and Goldman, 1957), radio-opaque substances (Schuback and Goldman, 1957; Saunders, 1966), microspheres (Folke and Stallard, 1967; Meyer and Tschetter, 1966) and the intravascular precipitation technique (Boyer and Neptune, 1962) have also been employed to demonstrate vascular pathways.

A 3-dimensional picture of the periodontal microvasculature can be observed under the SEM with corrosive castings. Corrosive castings of the PDL arrangement

have been produced by injection of latex (Kindlová, 1965; Kindlová and Matena, 1959; Lenz, 1968), and methylmethacrylate (Weekes and Sims, 1986b; Wong and Sims, 1987; Lee et al., 1990; Stanley, 1993).

Most perfusion methods by which blood vascular patterns have been delineated, in situ, involved replacement of blood by an injection of a substance circulated under pressure or by pressure produced by a pump to overcome backflow pressure within the artery. The pressures so produced, unless calibrated to and maintained at the exact intra-arterial pressure, could cause endothelial and intimal disruption as well as increased fluid diffusion through capillary walls into the tissues (Turner et al., 1969).

As with all techniques, significant dimensional changes can occur. Lindskog, Branemark and Lundstrom (1968) reported that the vessel diameters in perfused specimens varied significantly at 10-15% from values obtained using vital microscopy. Zweifach (1961) argued that neither perfusion nor histological techniques should be used alone to measure vessels that are less than 30μm in diameter. Kindlová and Matena (1959) claimed that precise details of the vascular pattern could be determined from corrosive specimens of the latex injected vessels. Weekes and Sims (1986b) and Wong and Sims (1983 and 1987) identified postcapillary-sized venules from the endothelial cell imprints on the microvascular castings and lumen patterns. However, Edwall (1982) highlighted the inherent disadvantage of the corrosive specimens that they do not permit the localization of the blood vessels in relation to other tissue elements.

3.3.2 Arterial Blood Supply To The PDL

The arterial vessels supplying the maxillary PDL are derived mainly from the posterior superior alveolar artery and those that supply the mandibular PDL come mainly from the inferior alveolar artery (Cohen, 1959a; Castelli, 1963). These arteries are branches of the maxillary arteries. The inferior dental artery terminates as the mental and incisive arteries. Anteriorly, the buccal gingiva and PDL are supplied

by the mental artery and by perforating branches of the incisive artery. The lingual gingiva and PDL are supplied by perforating branches from the inferior dental artery and by the lingual artery of the external carotid. In the maxilla, the posterior superior alveolar artery courses tortuously over the maxillary tuberosity before entering bony canals to supply molar and premolar teeth. The middle superior alveolar artery, when present, arises from the infra-orbital artery and terminates near the canine where it anastomoses with the anterior and posterior alveolar arteries. The anterior teeth PDL are supplied by the anterior superior alveolar artery, also a branch of the infra-orbital artery. A secondary vascular supply to the maxillary PDL arises from the greater palatine artery via the palatal gingiva and from the superior labial branches of the facial and infra-orbital arteries.

Kindlová (1965) reported that the distribution and blood supply to the PDL of the Macaca rhesus monkey closely resembles that of man. In contrast, Castelli and Dempster (1965) found that the maxillary and mandibular incisor ligaments of monkeys are each supplied by a single artery. Kindlová (1965) provided evidence to the contrary to show that the blood supply of the incisor PDL of macaque monkey was not singular.

That there is a rich accesory blood supply to the PDL from intraosseal and periosteal sites has been reported by Boyer and Neptune (1962), Kindlová and Matena (1962), and Fölke and Stallard (1967). These are arterioles that have diameters less than 100μm which run in the marrow spaces of the alveolar bone and enter the periodontal ligament at different levels. Birn (1966), after having examined eighty-four human tooth sockets, reported that the periodontal tissues of the posterior teeth seemed to be more vascular than those of anterior teeth. Furthermore, he reported that the blood supply was greatest in the cervical part of the periodontal ligament and least marked in its middle third. In a differing view offered by Castelli and Dempster (1965), they observed that the perforating arterioles generally enter the PDL through the apical two-thirds of the alveolus. Birn's (1966) findings were made on the assumption that the diameter of the vessels corresponded to the size of the

alveolar perforations, and that the diameter and number of these perforations could be taken as an expression of the blood supply to the PDL. A sceptical view was offered by Edwall (1982) in that the number of wide bore vessels per unit surface area did not reveal much about the blood flow but rather was an indication of the capacity of the PDL to store blood. Furthermore, Kishi and Takahashi (1977) refuted Birn's concept of periodontal blood supply on the basis of their findings. They showed that the blood supply changed with different locations around the tooth, and that other vessels originating inferiorly from the apical PDL and superiorly from the cervical gingiva were involved in providing the blood supply to the PDL.

3.3.3 Venous Drainage Of The PDL

A venous reservoir system linking the PDL with the bone marrow, and venous anastamoses with the gingiva have been described by Castelli and Dempster (1965). Cohen (1959a) reported that the main mandibular venous drainage is via the periosteal veins into the jugular veins. Secondary mandibular venous drainage occurs through the inferior alveolar vein anteriorly through the mental foramen into the facial vein or posteriorly through the mental foramen into the pterygoid venous plexus. The maxillary veins accompany the superior alveolar arteries and drain either anteriorly into the facial vein or posteriorly into the pterygoid venous plexus (Edwall, 1982). Castelli (1963) and Castelli and Dempster (1965) noted close similarities in the venous drainage of the PDL between monkey and man. The veins in the alveolar bone and in the PDL drain into veins in the interalveolar and interradicular septi. These veins do not follow the arteries but join to form larger veins in the interalveolar septi which in turn are connected to a rich venous network surrounding the apex of each alveolus.

3.3.4 Vascular Arrangement In The PDL

Kindlová (1965) and Lenz (1968) noted in monkeys that the main vessels are arranged in palisades and run parallel to the long axis of the tooth. These vessels

branch to form a flat network of capillaries. This basket-like network of vessels surrounds the root surface and is located approximately in the center of the PDL space, most often nearer the alveolar wall than the root surface. Lenz (1968) estimated that these vessels have diameters between 15μm and 100μm, with the wider-bore vessels predominating. A slightly different arrangement in the cervical region of the PDL has been observed by Kindlová (1965). The flat capillary network was condensed into a narrow band from which single capillaries were given off to form structures resembling glomeruli. Anastomeses with gingival vessels were also observed in this area. Kindlová and Matena (1962) described the vascular arrangement of the PDL vessels to be a paired arterial and venous mirror image. SEM analyses of methacylate vascular castings of the rat (Weekes and Sims, 1986b) and of the mouse (Wong and Sims, 1987) PDL did not confirm Kindlová and Matena's (1962) description of morphologically paired arterial and venous systems.

Using latex castings of the rat PDL vasculature, Kindlová and Matena (1962) reported there was no direct, fine anastomoses between periodontal and gingival arteries. On the contrary, Wong and Sims (1983), Weekes and Sims (1986b), Lee et al. (1990), and Stanley (1993) using methylmethacrylate castings of the marmoset PDL vasculature, discovered distinct trans-alveolar vascular communications between the PDL vessels and those of the labial gingiva.

Under light microscopy, Carranza et al. (1966) reported that in all species, a vascular plexus located close to the bone was seen running parallel to the long axis of the tooth. Perforating vessels were most commonly seen in the middle and apical thirds of the alveolus. Vascular communications were seen between the periodontal and pulpal vessels in the rat and mouse (Carranza et al., 1966) and similar communications were reported in man by Sicher (1966).

Provenza et al. (1960) reported the greatest number of glomeruli-like structures were found in the inter-radicular ligament, superior to the alveolar septi. They believed these to be arteriovenous anastomoses. Kindlová (1965) observed

glomeruli-like structures between the alveolar crest and the junctional epithelium in the monkey, as did Kindlová and Matena (1962) in a corresponding location in the rat. However, Weekes and Sims (1986b) did not observe glomeruli-like vascular structures in the rat molar ligament but noted that these structures were present at the interdental gingiva. On the other hand, Waerhaug (1954) observed that the 'glomeruli' in the PDL were branching vessels which perforated the alveolar wall.

The work of Folke and Stallard (1967) used injections of plastic microspheres of diameter 15 μm to 35 μm ($\pm$5 μm) to examine PDL blood vessel diameter in the squirrel monkey. They reported that the spheres of 35$\pm$5 μm do not enter the terminal periodontal vasculature. Smaller diameter spheres of 15$\pm$5 μm were trapped in branching vessels of the PDL network. Kennedy (1969) perfused the vasculature with indian ink after injecting microspheres, and found that most of the vessels in the PDL contained the ink. This finding, as reviewed by Edwall (1982), is suggestive of the "presence of preferential channels and/or arteriovenous shunts which are wider than the corresponding vessels in the gingiva and the periosteum."

3.3.5 Ultrastructural Morphology Of PDL Microvessels

Bevelander and Nakahara (1968) reported that the human PDL vasculature comprised thin walled vessels that showed marked variation in lumen diameter. The observations of Frank et al. (1976) in the rat molar PDL principally recorded the existence of continuous blood capillaries and few fenestrated capillaries. In man, Griffin and Spain (1972) reported that the PDL blood vessels were closely associated with nerves (myelinated and unmylinated) and suggested that these complexes were a form of mechanoreceptor. These complexes were supplied by encapsulated terminal arterioles, metarterioles and capillaries. However, innervation of the terminal arterioles and metarterioles was not shown in this study. Oxytalan fibres, (Sims, 1975), often terminated in blood vessel walls and it was postulated that the oxytalan-vascular association may form part of a periodontal receptor mechanism which mediated vascular control (Sims, 1973; 1975; 1983).

Weekes (1983), using the SEM corrosion cast technique, described the rat molar PDL as comprising predominantly postcapillary venules of luminal diameter of ≈20μm. Similarly, Gilchrist (1978) and Sims and Weekes (1985) described the PDL of the human and rat as essentially venous microcirculatory beds. Barker (1979) in a regional TEM study of the human PDL, observed small and large vessels which were described as pericytic venules and lymphatics, respectively. Avery et al. (1975) and Corpron et al. (1976) described finger-like projections that protruded into the lumen of pericytic venules. The cytoplasmic contents of endothelial cells consisted of numerous vesicles, ribosomes and oval-shaped mitochondria. The endothelial cells were surrounded by a continuous basement membrane, each cell being united by tight junctions.

3.3.6 Classification Of Blood Vessels

a. Introduction

Improved techniques in the preparation of tissues for examination under the electron microscope have revealed new information about capillary structure. For example, the presence of micropinocytic vesicles (Palade, 1960), endothelial cell fenestrae (Rhodin, 1962b) and intercellular junctions (Luft, 1965) have been demonstrated. This knowledge has enabled the classification of the different types of capillaries to be established (Bennett et al., 1959; Majno, 1965). Rhodin (1967, 1968) further developed the classification of the microcirculation. Microcirculation is a collective name of the smallest components of the cardiovascular channels comprising the arterioles, the blood capillaries, and the venules (Majno, 1965; Rhodin, 1974,1980). Lymphatics are usually not included as a component although they have been shown to intermesh with blood capillaries (Rhodin and Lim Sue, 1979). Together with the microcirculation, the lymphatics and the connective tissue spaces are termed the microvascular bed (MVB) (Rhodin, 1981).

Each organ has its own microcirculatory bed (Wolff et al., 1975) and the blood vessels vary even within different parts of the same microcirculation (Simionescu et al., 1975). Although the arterioles and venules of the microcirculatory beds in

various organs have many structural similarities, the capillary beds vary greatly from organ to organ, both in their three-dimensional architecture and in their ultrastructure as it pertains to the endothelial cytoplasm (Luft, 1973).

b. Ultrastructural Classification of Blood Vessels

Most classifications of the microcirculation are based on a few criteria. Fernando and Movat (1964) used the criterion of vascular position to define a terminal vascular bed as comprising that part of the vascular tree lying between terminal arterioles and venules. Bennett et al. (1959) provided a definitive morphological classification of vertebrate blood capillaries based on several criteria:

1. Basement Membrane

   Type A-has a complete continuous basement membrane.

   Type B-without a complete continuous basement membrane.

2. Endothelial Cell Type

   Type 1-without fenestrations or perforations.

   Type 2-with intracellular fenestrations or perforations.

   Type 3-with intercellular fenestrations or gaps.

3. Presence or Absence of Pericapillary Cellular Investment.

   Type alpha: without a complete pericapillary cellular investment interposed between parenchymal cell and capillary.

   Type beta: with a complete pericapillary cellular investment interposed between parenchymal cell and capillary.

However, Bennett et al. (1959) defined the word "capillary" to mean any small blood vessel, including sinusoids, where a major part of the exchange of materials and substances between parenchymal cells and blood plasma took place. As such, what Bennett et al. (1959) classified as "capillaries" may be the postcapillary-sized venules described by Rhodin (1968).

In view of the shortcomings and complexity of the classification proposed by Bennett et al. (1959), Majno (1965) redefined capillaries as having a diameter of <8μm. He classified capillaries into 3 groups based on the type of endothelial wall: Type I (continuous), Type II (fenestrated) and Type III (continuous). However, Type I and Type III vessels appear to be similar.

Simionescu and Simionescu (1984) further redefined capillaries as the smallest ramification of the microvascular system, with a "luminal diameter of 5-10 μm and a wall reduced to endothelium, basal lamina and a few pericytes".

There is however, a difficulty in differentiating between postcapillary-sized venules and capillaries. Movat and Fernando (1964) maintained that venules can only be distinguished from capillaries by their size. Weideman (1963), using the bat wing as a model, claimed that at any one time, 80% of the blood is on the venous side of the circulation, and that the number of postcapillary-sized venules is 3 times that of capillaries. However, this is not to be taken as a general rule because the bat wing has an atypical venous microcirculation. Interestingly, the average diameter of each microvascular segment under Weideman's classification (1963) is comparable to that of Rhodin's classification (1967, 1968), a summary of which is outlined in Table 3.1.

Freezer (1984), in a stereological TEM study of the mouse molar PDL, provided a comprehensive classification of the PDL microvasculature. He described 4 distinct vessel types:

i. Capillary-sized vessels vessels (luminal diameter of 4 μm to 7 μm) with a partial or complete pericytic cellular investment.
ii. Capillary-sized vessels without a pericytic cellular investment.
iii. Postcapillary-sized vessels (luminal diameter of 8 μm to 30 μm) with associated pericytes being few in number or absent.
iv. Postcapillary-sized vessels with a complete pericytic investment.

An interesting finding was that although postcapillary-sized vessels comprised 69% of the total blood vessel endothelial surface, they contained 88% of the blood volume. The remaining 31% of vessel endothelial surface (formed by capillary-sized vessels) carried 12% of the blood volume. This finding implied that the postcapillary-sized vessels handled approximately 3 times more blood volume per unit surface area of endothelium than capillary-sized vessels and that the arterial elements were responsible for pumping up this periodontal reservoir (Lew, 1986).

Blood Vessel Type	Lumen Calibre	Wall Thickness	Endothelial Cell Morphology	Peri-endothelial Cells	Other
Arteriole	100-50μm	Greater than 6μm	Cell 0.15 to 2μm in width, few pinocytotic vesicles, upstream cell usually overlaps downstream cell.	2-3 layers of smooth muscle cells, some eosinophils, mast cells and macrophages.	Well developed elastica interna, non-myelinated nerves extending to smooth muscle layer.
Terminal Arterioles	Less than 50μm	Less than 6μm	Generally as above but with many filaments parallel to the long axis of the blood vessel and with more pinocytotic vesicles.	One layer of smooth muscle cells.	Little elastic interna, nerves closer to vessel wall with more frequent contacts with the smooth muscle layer, some myoendothelial junctions.
Precapillary	7-15μm	Less than 5μm	Cell protrudes towards vessel lumen, nucleus shorter, thicker and more lobulated than above, some cytoplasmic filaments, many pinocytotic vesicles.	One layer of smooth muscle cells.	An increased number of unmyelinated nerves associated with a decrease in lumen diameter, frequent neuromuscular and myo-endothelial junctions.
Venous Capillary	4-7μm	0.3-1.3μm	Some rough endoplasmic reticulum, free ribosomes, mitochondria, vesicles, granules and filaments.	Occasional veil cells and pericytes. Some macrophages, leukocytes, lymphocytes and plasma cells.	Endothelium may be fenestrated.
Post-capillary venule	8-30μm	1-5μm	Cell rarely less than 0.2μm thick and generally larger than that of venous capillary. Slight over-lapping of adjoining cells.	More pericytes and veil cells than above. Some primitive smooth muscle cells around larger vessels.	Endothelium generally lacks fenestrae. Leukocytes may adhere to endothelial wall.
Collecting Venule	30-50μm	1.7μm	As above.	Continuous layer of pericytes and veil cells around vessel. More primitive smooth muscle than above. Smooth muscle cells around larger vessels.	Single layer of veil cells and some collagenous fibrils surround blood vessels.
Muscular Venule	50-100μm	2.0μm	As above.	1-2 layers of smooth muscle cells.	Veil cells form a complete layer around vessel wall. Myoendothelial junctions present.
Small collecting vein	100-300μm	2-3μm	As above but with specific endothelial granules.	2 or more layers of smooth muscle cells.	Unmyelinated nerves situated 5-10 microns from muscular layer.

Table 3.1 Classification of blood vessels in the microcirculation. Adapted from Rhodin (1967,1968)

3.3.7 Quantification Of PDL Microvasculature

Götze (1965) pioneered the quantification of the PDL blood vessels in his work on human cadavers. Using the point counting procedure on low magnification histological sections, he reported that the vascular proportion of the PDL amounted to 1% to 2% and that this proportion decreases with age. In a quantitative study of human PDL microvasculature of maxillary and mandibular anterior and premolar teeth, Götze (1976) revised his earlier estimates of PDL vessel volume, and reported blood vessel volume ranging from 1.63% to 3.5%, of which a chart representing the lower premolar is shown in Fig. 3.1.

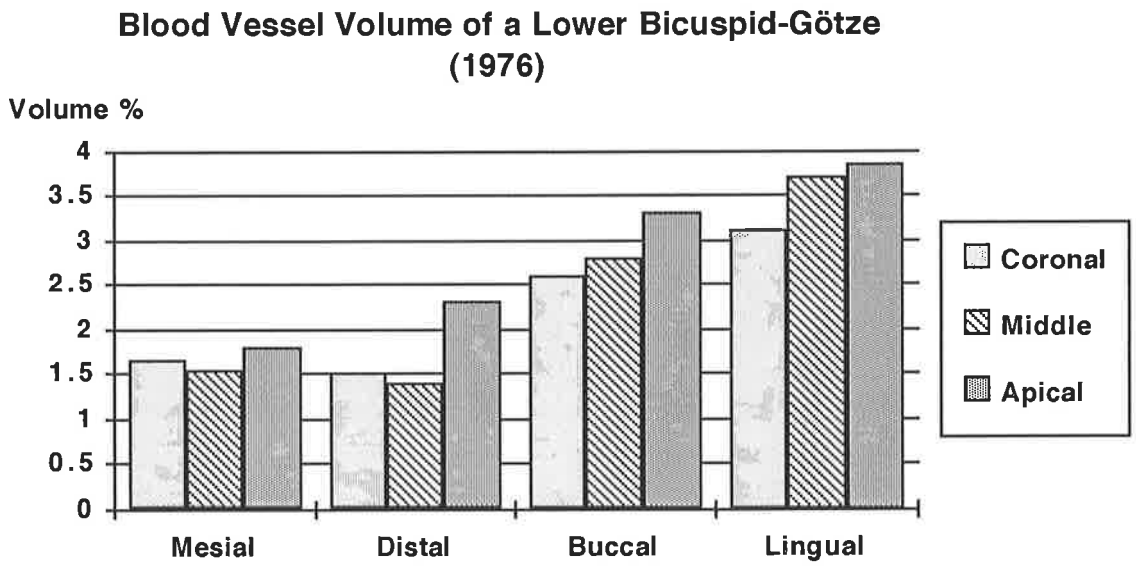

Fig. 3.1. The variability of blood vessel volume among the four quadrants in the vertical axis of a human mandibular bicuspid as observed by Götze (1976) under the light microscope.

His findings indicate that:

(i) the vascularity of the labial/buccal and lingual aspects is higher than the corresponding mesial and distal surfaces; and

(ii) the vascular proportion decreases from the apical to the coronal region, except in the mesial and distal aspects of the mandibular premolars when the middle portion showed the lowest vascular volume.

In contrast, Sims (1980) reported a higher regional mean vascular volume of 11% in some human mandibular premolars, and exceeding 20% along the buccal aspects of maxillary bicuspids. The work of Götze (1965, 1976, 1980) implied that the ligament contained an inherently low vascular volume (Sims, 1980). Table 3.2 presents a summary of the studies examining the vascular volume of the mammalian PDL.

STUDY	REGION OF PDL	VASCULAR VOLUME (%)
HUMAN		
•Götze (1976, 1980)	Anterior and premolar teeth	1.63%-3.50%
•Sims (1980)	Mandibular premolars	11%
MONKEY		
•Wills et al. (1976)	Mandibular incisors	0.5-1%
•Douvartzidis (1984)	Md second molar	8.3±0.4%
•Crowe (1989)	Mx incisor apex	2.6-19.7% Mean 11.0%
•Weir (1990)	Mx incisor (distal)	10.80%
•Parlange & Sims (1993)	Mx incisor (mesial)	11.26%
MOUSE		
•Gould et al. (1977)	Md first molar (mesial)	7.7±0.6%
•Sims (1980)	Md first and second molars	17%
•McCulloch & Melcher (1983b)	Md first molar (mesial)	7.25±0.75%
•Freezer (1984)	Md first molar (mesial)	7.46±1%
•Sims (1987)	Md first molar	10.9%
•Sims et al. (1994)	Md first molar (mesial)	8.5% (with PDL past apex)
RAT		
•Moxham et al. (1985)	Md first molar	22.1%
•Lew (1986)	Mx first molar apical region	19.9%
•Clark (1986)	Mx first molar apical region	23.1%
•Sims (1988)	Mx first molar (unpublished data)	10.2-24.6%

Table 3.2. Summary of studies on the vascular proportion of mammalian PDL.

The results of the study by Götze (1976) suffer from a lack of accuracy as the x400 magnification histological sections used could not reveal the nature and quality of blood vessels. Furthermore, his estimations were based only on three sampling levels, ie. apical, middle and coronal portions. A feature not included in both studies

(Götze, 1976; Sims, 1980) was that the portion of PDL between the apex and socket limit was not examined. As such, an accurate estimation of the total PDL volume on each tooth region eg. mesial or distal, cannot be made. Wills et al. (1976) estimated the PDL blood volume of adult macaque monkeys to be about 0.5% to 1.0%. Their estimation was based on the degree of reduced tooth displacement after injecting a vasoconstrictor. They believed that a 1% blood volume would account for a 30% of tooth displacement change when the tooth was subjected to intrusive forces.

3.3.8 Initial Lymphatics

According to Lindhe (1985), initial lymphatics are difficult to identify in an ordinary histological section because the walls of initial lymphatic are similar in structure to blood capillary endothelium in that they consist of a single layer of endothelium. However, Schroeder (1986), in referring to the work of several authors, stated that histological observations and perfusion studies provided evidence for lymphatic vessels in the ligament. Levy and Bernick (1968b) examined celloidin sections of decalcified jaw specimens of adult marmosets, and reported that "lymph capillaries, composed of a single layer of flattened endothelial cells, originated in the PDL as blind endings in the stroma. These lymph capillaries flowed into collecting vessels, which were slender, thin-walled structures composed of a single layer of endothelial cells surrounded by scattered fibroblasts and collagenous fibres.

Using tracer substances to identify the PDL lymphatic vessels of dead human fetuses, Schweitzer (1907) reported a rich network of lymphatic capillaries. However, one could argue about the validity of his specimens as fetuses did not contain mature ligaments. Box (1949), after a thorough review of the then current literature, concluded that histological and perfusion studies provided substantial evidence for the existence of lymphatic vessels in the PDL. Ruben et al. (1971) back-perfused carbon black suspension into the deep cervical lymphatic vessels of young mongrel dogs and demonstrated with retrograde lymphography the presence of periodontal lymphatic vessels in histological sections. Most of these vessels occured

proximal to the alveolar bone, they drained apically, and were found in the "apical phase" of the PDL.

Using a combination of intravital microscopy and electron microscopic techniques to examine the rat mesentry, Rhodin and Lim Sue (1979) observed that the lymphatic capillary wall consisted of endothelial cells and that it lacked smooth muscles. As a consequence of this feature, no simultaneous changes in capillary lumen were observed. Inter-endothelial gaps were present, and these were suggested to be a possible "gateway" for transport of substances in and out of the lymphatic capillaries.

Casley-Smith (1977a) listed several distinguishing features of initial lymphatics when viewed under the TEM. They:

1. have a tenuous basal lamina which is absent in regions of high lymphatic activity;
2. have abluminal projections where collagenous filaments attach to endothelial cells;
3. are usually larger than blood capillaries;
4. exhibit frequent open junctions;
5. are free of fenestrae;
6. contain fewer red blood cells and plasma proteins than blood capillaries;
7. are usually partially or totally collapsed;
8. have an irregular outline; and
9. have an endothelial lining that usually stains less intensely than endothelial lining of blood vessels.

Using the TEM, Barker (1979) observed 'initial lymphatic' vessels in the cancellous spaces of alveolar bone, and that these vessels protruded into the bone circumferential third of the PDL via foramina in the lamina dura. His observation posed the suggestion that alveolar bone was unique in that it contained lymphatic vessels with endothelial lining in the medullary spaces.

3.4 PERIODONTAL LIGAMENT INNERVATION

3.4.1 Introduction

An excellent review of the structure and function of periodontal innervation was given by van Steenberghe (1979). Nerve endings in the PDL are served by fibres from branches of coarse bundles ascending through the apical region, or from finer branches arriving from the lateral foramina of the alveolus (Bernick, 1957; Rapp et al., 1957; Dubner et al., 1978). The sensory nerves come from the maxillary and mandibular divisions of the trigeminal nerve and also by branches of the superior cervical nerves in some regions of the apical bases. It is also shown by Robinson (1979) that the nerves supplying one tooth do not all travel in the same branch.

The endings of the nerve fibres can be classified as "free" nerve endings, while other fibres terminate in some organized structures. The latter can be categorised as enlargements of the neural endings which are called spindle- or knob-like (Simpson, 1966) or coiled or twisted nerve endings (Griffin and Harris, 1968).

Hannam (1976) categorised receptors found in the periodontal tissues according to three locations: the gingiva, the periosteum of the alveolar bone, and the periodontal ligament. The gingiva and periosteal innervation share common morphological and physiological features with the periodontal innervation.

The terms used to describe the putative nerve terminals in the PDL have been wide-ranging. This can be attributed to species differences as well as to the differences in the techniques and standards of preparation (Hannam, 1982). Bonnaud et al. (1978) highlighted the problem of accurately identifying the type of nerves in the PDL. The difficulty lies in determining whether a terminal or subterminal region has been sectioned, and therefore whether one is looking at a collection of fine axons en route to the endings, or at components of an organised receptor, or at free endings. The relationship of nerve fibres to blood vessels and collagen fibres in a rat molar ligament are shown in Fig. 3.2.

3.4.2 Microscopic Anatomy Of PDL Innervation

Lewinsky and Stewart (1937) identified nerve endings in the human PDL, and described them as spindle-shaped. Simpson (1966), using the apoxestic technique, described thick parallel nerve bundles which run parallel to the long axis of the tooth, and which gave off branches to form plexuses and bundles of fibres. These fibres travelled considerable distances randomly, and then looped back along their original

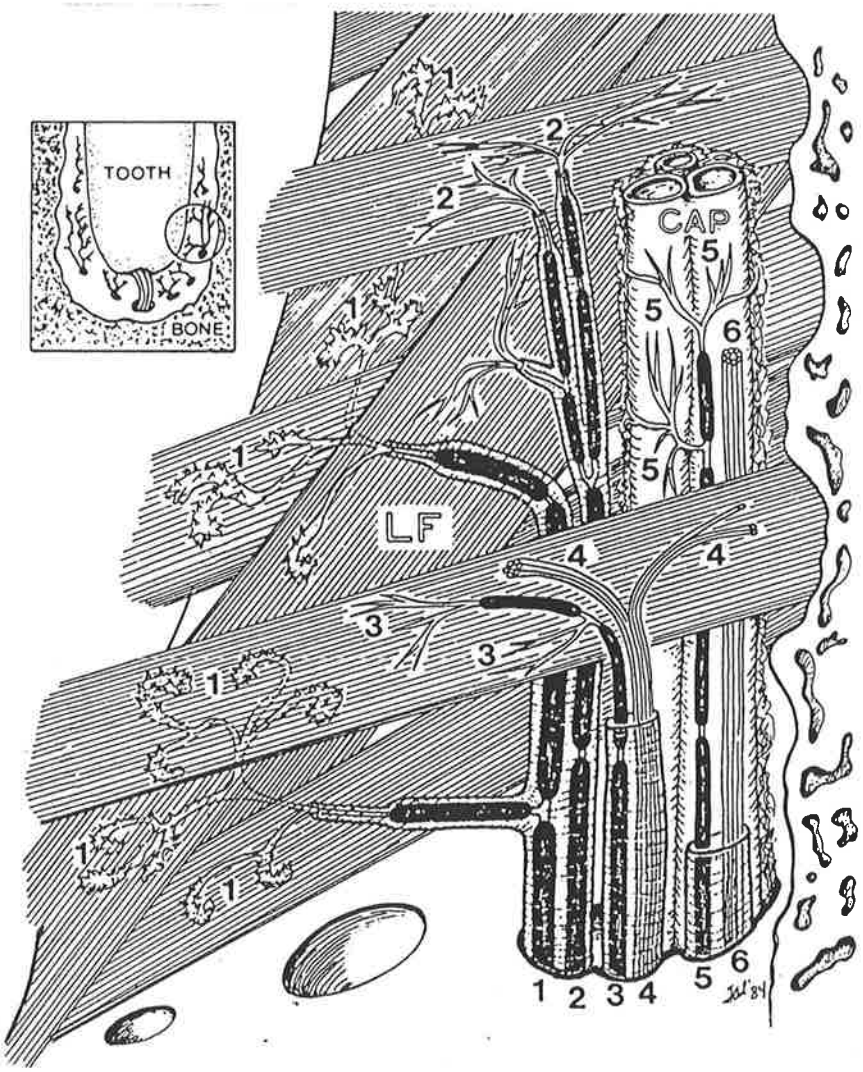

Fig. 3.2. A schematic drawing of the types of preterminal axons and sensory endings in the PDL of a rat molar. PDL collagen fibers are indicated by (*LF*). 1. Complex Ruffini-like endings, myelinated preterminal axon; 2, simple Ruffini-like endings, myelinated preterminal axons; 3, simple Ruffini-like endings, branching from free small myelinated axon; 4, bundles of free unmyelinated axons, receptors in loose connective tissue around capillaries (*CAP*); 5, simple Ruffini-like endings, branching from free small myelinated axons; 6, bundles of free unmyelinated axons. *[Taken from Schroeder (1986)as adapted from Byers (1985)]*

course in a complicated pattern. Some fibres terminated in free unmyelinated extremities while others joined to form a network. Other unmyelinated nerve fibres occasionally ended in knob-like enlargements, whilst others broke up into irregularly branching endings of variable form.

'K' or 'kidney' cells in mouse, as described by Everts et al. (1977) have been observed to surround neurons, and similar cells have been observed by Berkovitz and Shore (1978) and are considered to be atypical Schwann cells.

In a definitive electron microscopic study on the mouse PDL, Everts et al. (1977) observed the presence of organised nerve endings. These endings contained numerous mitochondria and it was suggested that they may be part of a receptor system. This observation had been confirmed by Berkovitz and Shore (1978) in their study in the rat incisor PDL.

Griffin and Harris (1968) demonstrated the ultrastructural characteristics of nerve endings of developing and functioning human PDL. Unmyelinated fibres were found in the developing PDL while both unmyelinated and myelinated nerve fibres are present in the functioning PDL. In the developing PDL of unerupted third molar teeth, unmyelinated nerve endings consisted of many small vesicles 40 nm to 100 nm in diameter. These axons also contained filaments of about 6 nm in diameter and microtubles of about 20 nm in diameter. The mean diameter of unmyelinated nerve fibres was approximately 720 nm.

Myelinated and unmyelinated axons were observed in the functional periodontium. The myelinated nerve fibres were A-delta fibres with a diameter ranging between 1 μm to 6 μm. Towards their endings, the nerve fibres lose their myelin sheath and divided into several branches of uniform diameter which were surrounded by Schwann cell cytoplasm. These were observed to terminate as several axonal swellings approximately 0.5 μm to 1.5 μm in diameter covered by basement membrane. The axonal cytoplasm appeared to contain numerous vesicles, vacoules with electron-dense bodies and mitochondria. Unmyelinated

nerves were observed to be in close proximity to myelinated nerves. Some nerve fibres were enclosed by an envelope of Schwann cell cytoplasm whilst others were exposed to the ground substance. The exposed axons corresponded with nerve endings and their diameters ranged between 100 nm to 600 nm. The mean diameter of all the unmyelinated nerve fibres measured in the developing and functioning PDL was 463 nm.

In a later ultrastructural study, Griffin (1972) showed that the end-ring (also known as encapsulated nerve ending) in the human PDL consisted of myelinated nerve fibres completely or partially surrounded by unmyelinated fibres. The diameters of the myelinated nerve fibres varied between 2 μm and 3 μm, and were enclosed in Schwann cell cytoplasm and basal lamina. They were separated from the unmyelinated nerve fibres by a relatively sparse endoneurium. The neural tissue was separated from the extraneural tissue by cell bodies and processes of capsular cells. The myelinated nerve fibres appeared to lose their myelin sheaths, to branch repeatedly and to surround adjacent myelinated nerve fibres.

Harris and Griffin (1974b), examined the fine structure of complex mechanoreceptors in the human PDL and reported on the capillary vascularization of a nerve unit in the complex mechanoreceptor containing exposed nerve endings. The complex derived its blood supply from a metarteriole which terminated in a capillary complex. The metarteriole became encapsulated along its course. The discrete encapsulation consisted of very fine processes of capsular cells which not only enclosed the metarteriole but also included the myelinated nerve fibres.

In a recent TEM study of the human PDL, Lambrichts et al. (1992) found three types of nerve endings: free nerve endings, Ruffini-like endings and lamellated corpuscles. The free nerve endings are mostly derived from unmyelinated fibres. The axon is partly covered by a Schwann cell envelope which has fingerlike processes projecting far into the surrounding connective tissue of the PDL. Ruffini-like receptors, simple and compound, are observed in the PDL. Simple receptors

lack any form of a capsule and are very small with a diameter ranging from 5 μm to10 μm. These simple Ruffini-like receptors contain numerous mitochondria and have neural herniations touching the basement membrane. These herniations are known to be part of the membrane transducing mechanism. Compound Ruffini-like receptors have a mean diameter of 50 μm and are supplied by myelinated nerves. Inside these receptors, the myelin is shed and the unmyelinated branches show neural thickenings that contain abundant accumulations of mitochondria. These neural endings are encased by cells with a large multiform, often kidney-shaped nucleus. Lamellated corpuscles are not encapsulated and the neurite contain numerous mitochondria. It has been suggested by Lambrichts et al. (1992) that free nerve endings act as receptors for pain and heat, the Ruffini-like receptors are thought to be slowly adapting mechanorecptors and the lamellated corpuscles may be mechanoreceptors of the rapidly adapting type.

3.4.3 Distribution Of PDL Terminals

Byers and Holland (1977) and Dubner et al. (1978) suggested that nerve endings are not evenly distributed along the PDL but are most frequently observed around the root apices. This is suppported by histological evidence on innervation density provided by Kubota and Osanai (1977) on the Japanese shrew mole. They found that the apical innervation is far denser than that in the intermediate zone. This is in agreement with the findings of Bernick (1957) who reported that organized neural endings are more frequent in the apical region. However, in an ultrastructural study of the tooth related part of the human PDL, Lambrichts et al. (1992) found that the amount of neural tissue was least in the apical region, and highest in the intermediate region. Kubota and Osanai (1977) reported that the relative densities of the upper dentition (8:1) is greater than that found for the lower dentition (5:1). It is inferred that teeth with different functional demands may exhibit different innervation densities (Hannam, 1982). In the mouse incisor, which had continual eruption, Everts et al. (1977) have shown that neural elements were found exclusively in the lateral alveolar compartment of the ligament around and between the vascular spaces.

Linden and Scott (1989a) suggested that the mechanoreceptors with cell bodies in the trigeminal ganglion are distributed in the cat PDL much more evenly around the tooth root. As for mechanoreceptors with cell bodies in the mesencephalic nucleus, they were located in a discrete area of the PDL between the fulcrum and the apex of the tooth (Linden and Scott, 1989a). None was found in the apical part of the cat incisor ligament, which is in contrast to the observations made by Byers et al. (1986).

3.4.4 Peripheral Innervation Of The PDL

Peripheral sensory nerves can be considered as long cellular extensions of centrally located cell-bodies. Cell bodies of the trigeminal neurones are found in the trigeminal ganglion, and other neurones serving the PDL are found in the trigeminal mesencephalic nucleus (Byers et al., 1986). Cell bodies in the trigeminal ganglion project to the trigeminal sensory complex of the brainstem for synaptic relay to the thalamus and cerebral cortex.

3.4.5 Autonomic Innervation Of The PDL

Matthews and Robinson (1979, 1980) have shown that sympathethic nerve fibres reach the PDL arterial microvessels by branches of the external carotid artery as well as by terminal branches of the superior and inferior dental nerves.

Matthews and Robinson (1980) described the PDL sympathetic nerves as mostly myelinated with a diameter range of 0.2 μm to 1 μm. They become varicose on approaching their destinations and branch into long terminal fibres of $\approx$ 0.1 μm to 0.5 μm in diameter (Burnstock and Bell, 1974). These varicosities are known to synthesize, contain and release noradrenaline, and exert its effects on the alpha-adrenergic receptors sites in the underlying smooth muscles.

In a recent electron microscopic study, Nakamura et al. (1992) demonstrated the presence and the ultrastructure of adrenergic nerve endings in the apical PDL of the human premolar teeth. These unmyelinated adrenergic nerve endngs were

identified by their size and shape, and the presence of small dense-cored vesicles containing noradrenaline. These endings were in close proximity to terminal arterioles, and were suggested to regulate blood flow in the human PDL.

Rhodin (1967) demonstrated the presence of unmyelinated nerves around the arterioles, and that the number of unmyelinated nerves increased simultaneously with the decrease in diameter of terminal arterioles. These nerves were particularly abundant near precapillary sphincters. All of these unmyelinated axons contained heavily stained small granules and these were commonly accepted to represent the ultrastructural evidence for an adrenergic transmitter or its precursor. Some of these axons had club-like terminations with a clear cytoplasm containing aggregations of granulated and nongranulated small vesicles together with somewhat larger empty vesicles. These club-like structures undoubtedly represented nerve endings.

The major influence of the autonomic innervation of the PDL blood vessels is upon the regional blood flow. Edwall and Kindlova (1971) showed in the dog and cat dental pulp that sympathetic nerve stimulation can be measured by the rate of disappearance of radioactive tracers injected into the PDL. Consequently, a reduction of blood flow was demonstrated in the dental pulp and the PDL. Baez et al. (1976) showed that stimulation of the CNS would provoke a response gradient of smooth muscle contraction in the terminal microvessels, and the contraction increased toward the last muscular outpost of the arteriolar tree. It has also been suggested that the metarteriole and precapillary sphincter can completely obliterate the lumen in response to CNS stimulation and actively regulate local blood flow. The study by Wills et al. (1976) indicated that tooth mobility can either be increased or decreased under the influence of angiotensin or noradrenaline, respectively. Vasoconstriction and vasodilatation due to variable sympathetic activity have also been known to affect the discharge of the mechanosensitive units in the PDL (Hannam, 1982).

3.4.6 Function Of Periodontal Innervation

At the brainstem level, periodontal signals are processed so that alone (or in combination with inputs from other orofacial site) they may result in transient, reflex inhibition of the activity of the jaw-closing muscles. This is mediated via the trigeminal sensory complex. The mesencephalic nucleus of the trigeminal nerve, besides being the residence of cell-bodies of the periodontal nerves, also contain cell bodies of afferents supplying the muscle spindles of the jaw-closing muscles. This suggests that they play a role in the control of the elevator muscle activity during function. Brainstem-mediated effects associated with periodontal innervation are not limited to jaw-opening reflexes only. Reflex, lateral jaw movements in response to dental stimuli have also been reported by Lund et al. (1971). Periodontal innervation, via its thalamo-cortico projection, also contributes to the conscious perception of interocclusal forces, and postulated by Hannam (1979a) to be able to perceive very small particles between the teeth. However, this is disputed by Dubner et al. (1978), that thickness estimation is largely a function of input from joint and muscle. Periodontal mechanoreceptors have been proven to be involved in the masticatory-salivary reflex in both man and animals (Anderson and Hector, 1987; Jensen Kjeilen et al., 1987). Gustatory input from the facial and glossopharyngeal nerves provide a greater stimulus than that provided by mechanical stimuli alone in the control of salivary secretion (Watanabe and Dawes, 1988).

Functionally single C-fibres (unmyelinated) originating from the PDL have been identified by Jyvasjarvi et al.(1988). These fibres are not stimulated by forces known to excite periodontal mechanoreceptors but responded to noxious stimulation of chemical and heat. These fibres had similar properties to A-delta fibres described by Mei et al. (1977). It is thus suggested by Jyvasjarvi et al. (1988) that the C-fibres could be polymodal nociceptors involved in nociceptive mechanisms.

3.5 FIBRES OF THE PERIODONTAL LIGAMENT

3.5.1 Collagen

Black (1887) described the PDL as consisting of large bundles of collagenous fibres which are arranged in groups and are orientated in a slightly wavy course from root cementum to the alveolar bone proper. Biochemically, Type I collagen is the predominant type of collagen found in the PDL and it comprises 80% of the total collagen (Berkovitz, 1990). The remaining 20% of PDL collagen is comprised of Type III collagen (Butler et al., 1975). Using bovine PDL, Dublet et al.(1988) demonstrated the presence of Type XII non-linking collagen, although its functional significance is not known. Freezer and Sims (1987), in a stereological study of the mouse molar PDL, found that collagen fibre bundles occupied about 51% of the total ligament volume.

The topographical arrangement of the collagenous fibre groups was categorised by Kronfeld (1936) as alveolar crest fibres, horizontal fibres, transseptal fibres, oblique fibres and apical fibres. These principal fibre groups, as viewed with the light microscope, are shown in Fig. 3.3.

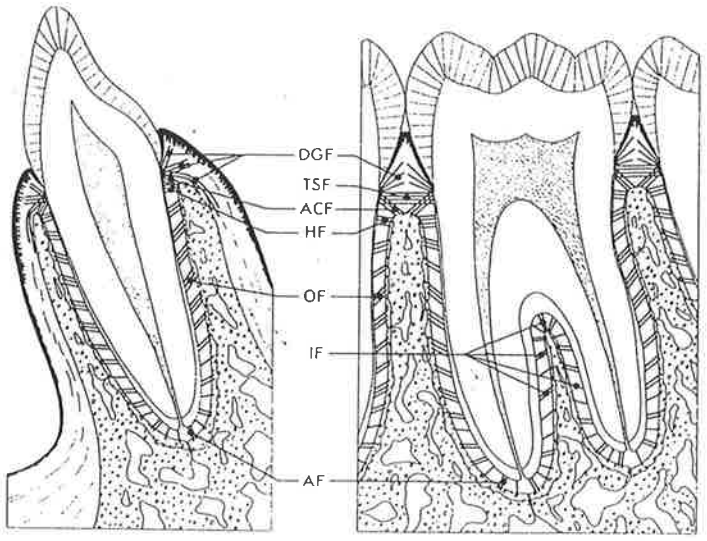

LEGEND
DGF:Dentogingival fibres
TSF:Transseptal fibres
ACF:Alveolar crest fibres
HF:Horizontal fibres
OF:Oblique fibres
AF:Apical fibres
IF:Inter-radicular fibres

Fig. 3.3 A schematic drawing showing the arrangement and distribution of the different groups of principle fibre bundles in the human PDL of a single-rooted tooth (left) and multi-rooted tooth (right). [Taken from Schroeder (1986)]

Electron microscopy studies have revealed a much more complex arrangement of the periodontal fibres. Bevelander and Nakahara (1968) examined TEM transverse sections of the human periodontal ligament and found that bundles of collagen fibrils cut in the longitudinal, transverse and tangential planes intermingle with one another, and that fibroblasts are found among the fiber bundles. Three-dimensional arrangement of the collagen fibre bundles was revealed with the scanning electron microscope. Observing the rabbit incisor ligament in the transverse, oblique and median planes under the LM and SEM, Sloan (1978) found three distinct zones of periodontal fibre arrangement ie., the alveolar, middle, and cemental zones, each occupying about 40%, 50%, and 10% respectively, of the total width of the PDL, as shown in Fig. 3.4. Using monkey and human material, Sloan (1982) observed the network arrangement of highly oriented principal fibres between blood vessels. However, due to the frequent branching and anastomosing of the fibers, it was not possible to trace an intact network across the PDL width.

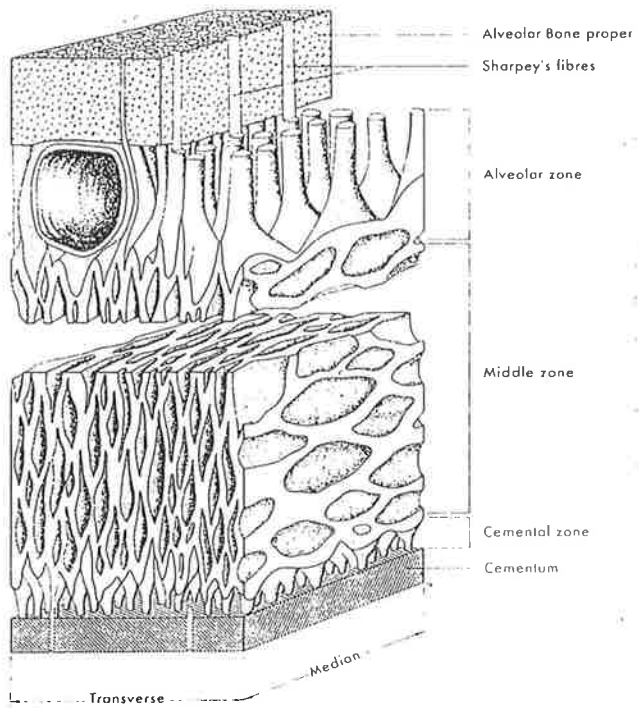

Fig. 3.4. A schematic drawing showing the arrangement of the principal collagen fibres in the PDL, close to the alveolar crest around mouse incisors. The fibres in the cemental and alveolar zones are organized into bundles, whereas those in the middle zone are arranged into sheets enclosing compartments. (Taken from Schroeder 1986 as adapted from Sloan 1978)

The periodontal fibre bundles are comprised of numerous collagen fibrils at 50 nm to 80 nm in diameter each (Furseth et al., 1986). Berkovitz et al. (1981) found that the periodontal collagen fibril diameters show a sharp unimodal distribution with a peak around 45 nm. Collagen bundle diameters vary depending upon their location. Zwarych and Quigley (1965), Shackleford (1971) and Sloan (1982) found that the

collagen bundles close to the cementum were 3 μm to 10 μm in diameter, and they increased in size to 10 μm to 20 μm when nearer the alveolar bone. The majority of the remaining PDL collagen bundles ranged from 1 μm to 4 μm in diameter.

Biochemical and autoradiographic techniques demonstrated that collagen turnover in the PDL is one of the most rapid in the body. Sodek (1976), using the rate of incorporation of ^{3}H proline as an indicator of collagen synthesis, observed the rate of collagen synthesis in the PDL to be twice as fast as in gingiva and four times as fast as in skin. The rate of ^{3}H proline incorporation into ligament collagen being five times as fast as in gingiva and alveolar bone, and thirty-five times as fast as in skin. The turnover times of the PDL collagen are known to range from about 2 days to 45 days, and this could be attributed to the method used in assessing the turnover (biochemical or autoradiography), species differences, tooth, age, site and sampling differences (Berkovitz, 1990). The significance of a high rate of collagen turnover in the PDL is poorly understood. It may be related to tooth movement as in secondary tooth eruption, or it may be related to masticatory force (Kanoza et al., 1980). Duncan et al. (1984) reported a significant increase in the proportion of Type III collagen when the tooth was subjected to orthodontic loading. Furthermore, collagen at different regions along the length of the tooth have different turnover rates. Comparing young and old rat molars, Rippin (1976) found that the average half lives for collagen in the crestal and apical regions of the PDL were 6.5 days and 2.5 days, respectively, in erupting and young molars. Adult rat molar PDL values were increased to 11 days and 7 days, respectively. Finally, Limeback et al. (1978) suggested that the high turnover rate may be the result of mechanical stresses derived from intermittent occlusal forces that cause microtrauma in the PDL.

3.5.2 Oxytalan

Shuttleworth and Smalley (1983) described oxytalan as pre-elastin type fibres. Sampson (1979) reported that oxytalan fibres and elastic fibers are similar on the basis of the ability of the oxytalan fibers to stain with a wide range of dyes that also stain elastic fibres. Oxytalan fibres are distinguished from collagen fibres in that

they contain variable amounts of amorphous interfibrillar material and show no banding. They are also distinguished from elastic fibers in that the oxytalan fibrils lack an amorphous core (Berkovitz, 1990). Sims (1977b) assessed the PDL of the lathyritic mouse and found that, despite the severe pathological changes in the collagen and elastic fibres, the oxytalan fibre system of the functioning molar persisted and retained its histochemical properties, and possessed a high degree of permanence and stability.

Ultrastructurally, oxytalan fibrils have a mean diameter of 15 nm (Carmichael and Fullmer, 1966). Sims (1984a) and Shore et al. (1984) reported the mean values of the major and minor axes of oxytalan fibres vary from about 0.6 μm to 1.5 μm and 0.2 μm to 0.5 μm, respectively, according to site and species. At the light microscopic level, Beertsen et al. (1974a) reported that oxytalan fibers in the rat PDL ranged from 0.5 μm to 2.5 μm, and from 0.1 μm to 1.4 μm in man (Sims, 1984a). Using the apoxestic technique, Simpson (1967) found human oxytalan fibres to be several millimeters in length and about 0.5 μm to 1.0 μm in diameter.

By means of stereological methods, Jonas and Reide (1980) quantified human oxytalan fibers as occupying 3% of the extracellular matrix. By contrast, animal models showed a lower percentage of extravascular oxytalan fibres. In the rat incisors, Shore et al. (1982) reported that rat oxytalan fibres occupied approximately 0.3% volume of the extracellular matrix. However, Freezer and Sims (1987) reported a higher percentage of oxytalan fibres in the mouse molar ligament at 0.45%.

Freezer and Sims (1988) reported two distinct groups of oxytalan fibres, one group as fibres in the endothelial lining of PDL blood vessels and the other group as discreet fibres adjacent to cells. They suggested the two groups of oxytalan fibres might indicate a possibility of having two physiologically distinct operant oxytalan fibre systems present within the mouse molar PDL. Sims (1975) observed that oxytalan fibres were associated with two types of blood vessels, one associated with individual vessels, the other surrounding a complex of arteries, veins, and lymph

vessels. Sims (1984b) has also demonstrated the affiliations of oxytalan fibers with unmyelinated endoneurium and myelinated nerve fibres in the endoneurium.

Berkovitz (1990), in his review article on the update of the periodontal ligament, ascribed three functions of the oxytalan fiber system:

1. The oxytalan fibres provide tooth support by means of increasing the rigidity of the PDL (Fullmer et al., 1974; Jonas and Reide, 1980). This was possible due to the close relationship of oxytalan fibres to collagen fibre bundles, and that increased number of oxytalan fibres were found in ligaments of teeth subjected to increased functional demand.

2. Due to the proximity of oxytalan fibres to fibroblasts, oxytalan fibres may serve as guides for cell migration during tooth eruption (Beertsen et al., 1974a).

3. Sims (1973, 1977b, 1984b) and Freezer and Sims (1988) reported a close relationship of oxytalan fibers to the PDL blood vessels and putative nerve endings (K-cells), and suggested that oxytalan-vascular-nervous association acted as part of a mechanoreceptive system which regulated the vascular flow according to functional tooth movement, either directly or by production of a more general neural response.

3.5.3 Elastin

Few elastic fibres are found in the periodontal ligament (Lindhe, 1985). They are observed to be associated with blood vessels (Furseth et al., 1986). Together with the oxytalan fibres, they form the approximately 20% of the non-collagenous ligament proteins (Schroeder, 1986). The elastic fibres do not contribute to the suspension of the tooth (Furseth et al., 1986).

3.6 INTERSTITIAL TISSUE OF THE PDL

3.6.1 Ground Substance

Berkovitz et al.(1981) analysed from electron micrographs and reported that ground substance amounted to an average of 65% within the bundles, fibres or sheets of collagen fibrils.

Its biochemical constituents include glycosaminoglycans such as hyaluronic acid, chondroitin sulfates, and heparin monosulfate (Munemoto et al. 1970). Gillard et al. (1977) found that chondroitin sulphates predominated in areas of tissue compression. Pearson (1982), in his review article on PDL ground substance, reported that dermatan sulphate was the major component of the sulphated galactosaminoglycan in bovine PDL, while chondroitin sulphate was not detected. Other constituents are the proteoglycans (Pearson and Gibson 1979), and glycoproteins such as fibronectin (Hynes, 1985). Using immunofluorescent techniques, Takita et al. (1987) demonstrated the general distribution of fibronectin throughout the PDL in both erupted and non-erupted teeth. Important functions have been ascribed to fibronectin. Jones et al. (1986) observed that fibronectin may promote attachment of cells to collagen fibrils. As cells preferentially adhere to fibronectin, it may be involved in cell migration and orientation.

3.6.2 Interstitial Matrix

The interstitial matrix comprises loose connective tissue, extra-cellular spaces and fluid. Some of the blood vessels, nerves and lymphatics reside in this matrix. The fluid component of the matrix is produced by fibroblasts and mast cells. The matrix is the medium in which the connective tissue cells are embedded and is essential for the maintenance of the normal function of the connective tissue. Thus, exchange of nutrients, electrolytes and metabolites occur to and from the cells within the matrix (Lindhe, 1985).

3.7 PERIODONTAL LIGAMENT CELLS - AN OVERVIEW

3.7.1 Vascular and Perivascular Cells

a. Endothelial Cells

The endothelial lining of PDL blood vessels consists of a sheet of flattened cells. These cells are held together by tight junctions (Leeson et al., 1988). The two plasma membranes are separated by approximately 20 nm at each of these tight junctions (Cliff, 1976). Bruns and Palade (1968a) observed that true desmosomes do not occur in endothelial junctions of higher vertebrates. However, this was noted in the endothelial intercellular junctions of the blood vessels of the rete mirabile of the teleost swim bladder (Fawcett, 1963). The relationship of one endothelial cell to another at the junctions may show considerable variety. There could be a simple abutment of the margins or that the margin of the upstream cell could overlap the margin of the downstream cell on the luminal surface. "Seamless" cells were observed by Wolff (1964) and consisted of a single endothelial cell with no apparent cell junction. Avery et al. (1975) reported tortuous intercellular junctions between endothelial cells in rat molar ligament vessels. Fine endothelial cytoplasmic processes were observed to extend into the vessel lumen, particularly at junctional regions (Cliff, 1976). This characteristic feature was also noted by Avery et al. (1975) in the mouse molar PDL.

Each endothelial cell has a high surface-to-volume ratio. Willmer (1945) observed that this characteristic feature of endothelial cells was also shared by the mesothelial cells of the pleura, peritoneum and pericardium.

The ultrastructure of endothelial cells reveals a poorly developed Golgi complex and rough endoplasmic system (Fawcett, 1959). Microtubular material, termed "Weibel and Palade bodies" (Weibel and Palade, 1964) are peculiar inclusions in the endothelial cells. Their functional significance is not known. Numerous caveolae and pinocytic vesicles are also observed in the cytoplasm (Casley-Smith, 1968). Vascular permeability at the endothelial level is attributed to the vesicular

system, the endothelial cellular junctions and the fenestrae (Cliff, 1976). Renkin (1977) provided a good review of the various pathways of capillary permeability. Fenestrae only occur in the thinnest regions of the endothelial membranes ie. capillaries (Fawcett, 1963; Lew, 1986) and at times more specifically in venous capillaries (Rhodin, 1968).

Rhodin (1967, 1968) studied vascular wall morphology in rabbit medial thigh muscle fascia and rabbit skin, respectively, and identified four specialized perivascular cell types:

1. *Veil cells* are a form of fibroblasts. They are located near the venous circulation. They are distinguished by sheets of flatly extending cytoplasm, having a diameter of 0.2 μm.
2. *Pericytes.*
3. *Primitive smooth muscles* which are considered to be an intermediate cell type between smooth muscle cells and pericytes.
4. *Smooth muscle cells.*

b. Pericytes

Pericytes are a morphologically diverse class of pericapillary cells which have several morphological, developmental, and biochemical similarities to smooth muscles cells of larger vessels (Buchanan and Wagner, 1990). These cells are distinct from smooth muscle cells in that they are enclosed by a basement membrane system which at times is continuous with the endothelial basement membrane (Cliff, 1976; Weibel, 1974). Rhodin (1968) observed that pericytes can differentiate into smooth muscle cells under appropriate conditions.

Majno and Palade (1961) and Cotran et al. (1965) described pericytes as non-contractile cells with well developed phagocytic powers. More recently, in situ histochemical studies have demonstrated that contractile proteins similar to those of smooth muscle are present in significant amounts within pericytes (Joyce et al., 1984, 1985a,b; Herman and Jacobson, 1988). Using heavy mero-myosin labelling, actin

and myosin-like filaments have been identified in rat brain pericytes (LeBeux and Willemot, 1978).

Cliff (1976) described the ultrastructure of the pericytes as consisting of an elongated nucleus showing the same curvature about the vessel wall as the cell as a whole. It characteristically forms a bulge on the abluminal surface of the cell. Golgi complexes are scant, and mitochondria are few in number. The cytoplasm contains small quantities of fine fibrils and microtubules. On TEM examination of the pericytes of the eel rete mirabile, Buchanan and Wagner (1989) found numerous cytoplasmic filaments. Plasmalemmal vesicles were also observed in the pericytes. Pericytes form cell-to-cell attachments of the zonula adherens type both between themselves (Farquhar and Palade, 1962) and with endothelial cells in regions where the basement membranes are absent (Rhodin, 1968).

Various functions have been ascribed to pericytes (Cliff, 1976):

1. Pericytes have a primary role in providing mechanical support within the walls of minute blood vessels.
2. They produce additional basement membrane condensations external to the endothelium to reinforce their primary role of tooth support.
3. Phagocytosis is carried out within the vessel wall.
4. Pericytes may represent a source of undifferentiated mesenchymal cells which participate in the repair process and inflammation.
5. The close similarity between pericytes and smooth muscles and the arrangement of pericytes along the capillaries suggested a regulatory influence on the blood flow. Moffat (1967) observed the presence of tracts of intracytoplasmic fibrils in medullary pericytes of mammalian kidneys and termed them 'myofibrils'. He suggested that the pericytes control medullary blood flow through the smooth muscle-like regions, and that these pericytes react both to humoral factors and to local sampling by pinocytic vesicles.

3.7.2 Neural And Perineural Cells (Adapted from Leeson et al., 1988)

a. Schwann Cells

Schwann cells ensheath both myelinated and unmyelinated axons. The ultrastructure of each Schwann cell reveals a small Golgi apparatus and few mitochondria. The heterochromatic nucleus is flattened and elongated. In myelinated nerves, the individual Schwann cell and its myelin cover an intermodal segment. Nodes of Ranvier are points of interruptions along the Schwann sheath and myelin.

b. Myelin Sheath

At the electron microscopic level, myelin is formed by fused, spiral laminae of Schwann cell plasmalemma. Mature myelin shows a repeating pattern of dark and light lines. The 3 nm dark lines are the major dense lines formed by fusion of inner cytoplasmic surfaces, while the less dense lines that bisect the spaces between them are the intraperiod lines, formed by apposition of the outer leaflets of the Schwann cell plasma membrane.

3.7.3 Connective Tissue Cells

a. Fibroblast

The most numerous cell population in the mammalian PDL is the fibroblast (Schroeder 1986). In the mouse and rat incisor ligament, they occupy about 50% of the volume of the densely collagenous portions (Beertsen and Everts, 1977; Shore and Berkovitz, 1979). However, in a TEM stereological study of the mouse molar ligament, Freezer and Sims (1987) estimated the volumetric proportion of fibroblast-like cells to be 10% to15% less than the 50% to 60% range reported in the tooth-related ligament of continuously erupting mouse incisors by Beertsen and Everts (1977) and the 46% reported for selected areas of rat molar periodontium by Deporter et al. (1982).

Using ultrathin TEM sections of the rat incisor and molar ligaments, Shore and Berkovitz (1979) estimated the mean diameter of the fibroblast to be 30 μm.

Longitudinal and transverse TEM sections reveal the average nuclear and cytoplasmic length to be 8 μm and 22 μm, respectively.

Intracellular collagen profiles in mice and guinea pig fibroblasts were first reported by Ten Cate (1972b), and it is believed that these intracellular collagen profiles are linked to collagen degradation (Beertsen et al., 1974a; Beertsen and Everts, 1977; Shore and Berkovitz, 1979) through the process of phagocytosis.

Various functions have been ascribed to the periodontal fibroblast:

1. *Collagen synthesis and degradation.*

   Using cultured PDL fibroblasts, Limeback et al. (1983) reported that these cells produced different ratios of type I and type III collagen, and even some type V collagen was produced. Bienkowski et al. (1978) observed that fibroblasts produce collagen in excess of their normal requirements, and the excess being broken down intracellularly. In another experiment, Bienkowski (1983) found that only type I collagen is broken down and that 10% to 49% of newly synthesised procollagen may be degraded intracellularly before processing into collagen fibrils.

2. *Aids tooth eruption.*

   The cell motility / contractility hypothesis of tooth eruption proposed by Melcher and Beertsen (1977) is based on autoradiographic evidence that periodontal fibroblasts move occlusally at a rate equal to that of eruption. Majno et al. (1971), in examining monkey PDL fibroblasts, observed ultrastructural features characteristic of myofibroblasts. The contractile nature of these fibroblasts is derived from the the microfilamentous material in the cytoplasm (Bellows et al., 1982b). Azuma et al. (1975) reported the presence of myofibroblasts in the rat molar ligament. Stopak and Harris (1982) suggested that a combination of migration and contraction generated "tractional forces" for eruption. Furthermore, Beertsen et al. (1974a) and Bellows et al. (1981) suggested that the contractile nature of fibroblasts

provided the major force for tooth eruption. By contrast, Shore and Berkovitz (1979) showed no evidence that fibroblasts generated the eruptive force by their migratory activity.

b. Osteoblast

PDL osteoblasts occur in varying numbers at and along the surface of the alveolar bone proper. Their presence is indicative of bone formation (Schroeder, 1986). During osteogenesis, a distinct layer of columnar shaped osteoblasts lines the alveolar bone surface, surrounding the newly synthesized osteoid. In periods of quiesence, osteoblasts alter their columnar shape to become flattened cells with scanty cytoplasm (Berkovitz and Shore, 1982).

According to Berkovitz and Shore (1982), the ultrastructural features of the osteoblast include an extensive rough endoplasmic reticulum. The Golgi complex appears more localized and extensive. Prominent microfilaments are observed beneath the cell membrane distally at the secreting surface. Desmosomes and tight junctions are the main junctional complexes found between osteoblasts. Numerous fine cytoplasmic processes from the osteoblasts form tight junctions with osteocytes in the bone , and is postulated by Holtrop and Weinger (1972) that these tight junctions form part of the transport system throughout bone.

In a recent excellent review on bone remodelling, Kahn and Patridge (1987) provided evidence to show that the osteoblast plays a pivotal role on bone remodelling by regulating osteoclast resorptive activity and contributing directly to matrix dissolution. They questioned the prevailing view that bone deposition and bone resorption were carried out solely by osteoblasts and osteoclasts, respectively.

c. Osteoclast

The majority of bone resorption is carried out by osteoclasts. These large multinucleated cells reside in resorption Howship's lacunae. Miura (1993), in an in vitro study of bone remodelling using rat calvaria bone, showed that osteoclasts

changed morphology to that of a drill-like structure boring into alveolar bone when prostaglandins were introduced. Using tissue cultured osteoclasts, Hancox (1972) observed that these cells are mobile. Owen and Shetlar (1968) also observed that osteoclasts do not cover the entire resorbing bone surface at any one time. In a later experiment, Owen (1971) found uninucleated cells populating the bone surface between osteoclasts and postulated these cells to be osteoclast precursors.

At the ultrastructural level, a typical osteoclast is observed to have between ten and twenty nuclei, though the number can range from as few as two to several hundreds (Hancox, 1972). A light microscopic feature of the osteoclast when in contact with bone is the "brush border". At the TEM level, this brush border is made up of numerous tightly packed microvilli coated with fine bristle-like structures (Kallio et al., 1971). Numerous mitochondria are distributed throughout the cytoplasm except beneath the brush border. Golgi complexes are prominent but the rough endoplasmic reticulum is less well developed than in osteoblasts. Numerous vesicles containing lysozymes are observed throughout the cytoplasm. Intracellular collagen profiles are scant suggesting an extra-cellular degradation of collagen. Heersche and Deporter (1979) suggested that osteoclasts may only be involved in the initial bone resorption, and final collagen degradation carried out by adjacent fibroblasts.

d. Cementoblast

Cementoblasts resemble osteoblasts, and it is also difficult to distinguish between cementoblasts and fibroblasts. Recently, in a definitive morphometric TEM study on human premolar and third molar roots, Yamasaki et al. (1987) were able to distinguish the two cell types. They found that cementoblasts were a group of immature or resting collagen-producing cells (CPC) which had a poorly define rough endoplasmic reticulum and Golgi complex. In addition, cementoblasts have a higher mean volume density than fibroblasts. However, the appearance of cementoblasts depend on their functional state (Berkovitz and Shore, 1982). During cementogenesis, the cementoblasts are observed to form a cellular layer adjacent to

cementum. Cells depositing acellular cementum lack prominent cytoplasmic processes (Berkovitz and Shore, 1982).

e. Progenitor Cells

Progenitor cells can be identified by their ability to incorporate tritiated thymidine. A range of 0.5% to 3% of the PDL cells was initially labelled after an injection with tritiated thymidine (McCulloch and Melcher, 1983c). Using the rat molar ligament, Gould et al., (1977, 1980) found that the fibroblasts are continuously replaced by progenitor cells during wound healing as well as under physiological conditions. About 40% of these dividing cells are located in a paravascular location (ie. within 10 μm of PDL vessels) and migrate to the surfaces of bone and cementum (McCulloch and Melcher, 1983b).

Gould et al. (1980) and Gould (1983) have studied the morphology of progenitor cells in the PDL and reported that most cells were undifferentiated in that they are small in size, have a high nuclear/cytoplasmic ratio, and have little intracellular organelles. Some of the cells that have incorporated tritiated thymidine were reported to be relatively differentiated and to contain intracellular collagen profiles (Gould, 1983). Using nuclear size as a marker, Roberts et al. (1982) was able to distinguish larger nuclei preosteoblasts from smaller nuclei pre-fibroblasts.

3.7.4 Epithelial Cells

The epithelial cells rests of Malassez (Malassez, 1884) are found in the developing and mature periodontal ligament. They are derived from the disintegrating root sheath of Hertwig. Valderhaug and Zander (1967) reported that the epithelial rests of human and mammalian PDL form a dense network surrounding the root surface at a distance of 30 μm to 40 μm away from the root surface. The average distance away from the cementum in man was 27 μm in the cervical region increasing to 41 μm apically.

The effect of aging on the epithelial cells has been documented in man by Reeve and Wentz (1962). They obeserved that epithelial cells predominated in the apical region during the first and second decade of life. Between the third and seventh decade, the majority of cells were located cervically above the alveolar crest. They ascribed the change to chronic inflammation of the surrounding area. However, in human subjects aged 11 to 27 years, Valderhaug and Zander (1967) noted that most of the epithelial cells resided in the cervical region while Tertel-Kalweit and Donath (1985) found most of the cells in the cervical and middle-root region. Using the apoxestic technique, Simpson (1965, 1967) demonstrated a change in arrangement and number of cells with age. He described the change from a sheet of cells in a newly erupted tooth to that of a net in adult ligament. Disintegration of the net with increasing age resulted in scattered strands and islands of cells.

Light microscopy reveals the arrangement of the epithelial cell as cords and clusters. Each cluster consists of 2 to 10 cells. The ultrastructural morphology of epithelial cells was examined by Valderhaug and Nylen (1966) and Valderhaug and Zander (1967). A basement membrane surrounds the cluster of epithelial cells, with hemidesmosomes and fibrils anchoring the basement membrane to the plasma membrane. Desmosomes and tight junctions connect between cell membranes. Mitochondria are distributed throughout the cytoplasm but the rough endoplasmic reticulum and Golgi complex are poorly developed. Histochemical studies by Ten Cate (1965, 1967) show these epithelial cells to be metabolically inactive. On the function of the epithelial rests in the PDL, Leedham et al. (1990) suggested that these cells become active and have a role to play in the repair of root surface pathology eg, following resorption, fracture.

3.7.5 Inflammatory Cells

a. Macrophages

Macrophages are derived from blood monocytes (Sutton and Weiss, 1966) and their primary function is to phagocytose particulate debris. They are important defence agents. When they encounter a large foreign body, they fuse together and

form the multinucleated foreign body giant cells. Macrophages are irregular in shape with short and blunt cellular processes. When stimulated, they are capable of amoebid movement wih numerous extending pseudopodia. They are about 10 μm to 30 μm in diameter

At the light microscope level, they are distinguished readily from fibroblasts when stimulated. Macrophages take up colloidal tryphan blue dye while fibroblasts do not (Leeson et al., 1988). Ultrastructurally, distinguishing features of a macrophage include:

(1) Lack of rough endoplasmic reticulum.

(2) Presence of thin finger-like projections from the cell surface

(3) Characteristic presence of many lysosome-containing vesicles.

b. Mast Cells

Mast cells are often associated with blood vessels (Berkovitz and Shore, 1982). They are readily identified by their intense staining reaction with basic aniline dyes such as toluidine blue. This staining reaction is attributed to the presence of a large number of intracytoplasmic granules. Mast cells are known to produce histamine, heparin and factors of anaphylaxis eg. eosinophil chemotactic factor of anaphylaxis (ECF-A), and the slow-reacting substance of anaphylaxis (SRS-A), (Austen, 1974). Prostaglandins are also produced which regulate the release of histamine (Whittle, 1977).

3.8 CRITIQUE OF THE T.E.M. TECHNIQUE

3.8.1 Fixation

According to Hayat (1970), the aims of fixation are (1) to preserve the structure of cells with minimum alteration from the living state, (2) to protect them against disruption during embedding and sectioning, and (3) to prepare them for subsequent treatments including staining and exposure to the electron beam. The quality of

fixation depends not only on the type of fixative used or the method of fixation but also on the thickness of the specimen to be fixed.

Gluteraldehyde as a fixative

An ideal fixative should kill tissues quickly and cause minimum shrinkage or swelling. Gluteraldehyde causes shrinkage of both cell and nucleus (Hayat, 1970). Hopwood (1967a) reported an approximately 6% shrinkage of rat liver in 18 hours at 4°C when 4% gluteraldehyde was used as a fixative at pH 7.4. It has no staining action, and accordingly is unable to impart sufficient contrast and density to tissues. Post-fixation with osmium tetroxide imparts contrast and adds sharpness. However, Trump and Bulger (1966) reported that prolonged washing in buffer solution between pre-fixation with gluteraldehyde and post-fixation with osmium tetroxide produced uneven fixation, and cell shrinkage with widened intercellular spaces. Gluteraldehyde is also known to preserve fine structure. It stabilises intra-cellular systems of smooth endoplasmic reticulum, pinocytic vesicle and mitotic spindles. Chambers et al. (1968) reported that gluteraldehyde stabilises blood plasma with little shrinkage of blood clots and attendant collapse of vessel walls. Furthermore, gluteraldehyde prevents gross distortion during embedding and increases the permeability of tissues to embedding media.

Lipids are not preserved by glutaraldehyde and unless a second fixation with osmium tetroxide is used as much as 95% of the lipid in a specimen may be extracted during dehydration (Stein and Stein, 1971). A serious side effect with double fixation comes in the form of myelinic figures. The most probable reason was given by Trump and Ericsson (1965) when they reported that glutaraldehyde appeared to cause phospholipids to pass into solution and myelinic figures then form when osmium tetroxide interacts with these phospholipids during the second fixation.

Osmium tetroxide as a fixative

Osmium tetroxide penetrates and reacts with tissues very slowly and considerable changes in structure can occur before fixation is complete. As such,

fixation with osmium tetroxide as the primary fixative is not recommended. It still plays an essential role, however, as a second fixative. During the second fixation the slow rate of penetration of osmium tetroxide is not critical to the stability of the specimen because gluteraldehyde would have already stabilised most of the structures.

Osmium tetroxide fixation alone produces shrinkage of the myelin sheath of nerves as reported by Moretz et al. (1969). This is due to the significant loss of lipid during dehydration following a fixation with osmium tetroxide. Combination fixatives of gluteraldehyde and osmium tetroxide have been shown to reduce the number of artefacts arising from lipid extraction and cellular shrinkage (Trump and Bulger, 1966).

Comparing the various methods of Fixation - An Overview

Biological specimens must be fixed as soon as possible after death of the organism since alterations in the fine structure could occur rapidly. Many fixatives, including gluteraldehyde and osmium tetroxide, penetrate tissues slowly and in consequence the central region of a large specimen is rarely well fixed. The vehicle of the fixative usually penetrated more rapidly than the fixating agent itself and may cause damage before fixation had effectively started. Palade (1956) described a "wave of acidification' which preceded the osmium during fixation with unbuffered osmium tetroxide. These damaging effects could be kept to a minimum by making the specimen as small as possible and by careful choice of the vehicle for the fixing agent (Glauert, 1978).

Maunsbach et al.(1962) reported that *in vivo* fixation allowed greater penetration of the fixative into tissues than tissues fixed *in vitro*. Hayat (1970) observed that prolonged gluteraldehyde fixation in *in situ* fixation did not seem to affect the tissue adversely. Gluteraldehyde worked best where fixation was carried out by injection, flooding or by vascular perfusion. Bone and Denton (1971) suggested a slightly hypertonic solution of 330-360 m osmol of fixative to be best in

preserving mammalian cells, and recommended that not more than 60% of the osmolarity should be due to buffer salts.

Hayat (1970) reviewed the advantages of *in situ* fixation :

1. Prevents alterations in the fine structure from effects of anoxia and post-mortem changes.
2. Minimises autolytic changes.
3. Appears to increase depth of fixation of tissues considerably.

In contrast, conventional immersion fixed tissues showed closed blood vessel lumina, and was probably attributed to slow penetration of osmium tetroxide into the deeper layers.

Immersion Fixation

Glauert (1978) stated that a tissue was mechanically tougher after aldehyde (gluteraldehye) fixation and that mechanical damage produced during cutting into cubes was considerably less compared with osmium tetroxide as a primary fixative.

The relative volumes of the specimen and the fixative were important; if there was too little fixative the effective concentration of the fixative would be reduced by dilution with soluble components of the specimen. Glauert (1978) recommended that the fixative should be at least 10 times greater in volume than the specimen.

3.8.2 Sectioning

a. Section Thickness

The thickness of the sections can affect the resolution of an image. A thick section will absorb the energy of the electron beam, and the loss in energy from the electron beam will involve a change in the associated de Broglie wavelength of the electron. This results in a spectrum of electron velocities in the electron beam which leads to chromatic errors in the image. In principle, the higher the resolution desired, the thinner the section should be, since this reduces scattering or loss of

electrons as they pass through the section. On the other hand, a decrease in section thickness is accompanied by a decrease in contrast.

Section thickness is commonly estimated by observing the interference colour in light reflected from the section while it is floating on the water bath. Peachey (1960) reported that the estimation of section thickness based on the interference colour is reliable within a range of 10 nm to 20 nm for sections greater than 60 nm. Each interference colour represents a range of approximately 30 nm.

b. Cutting Speed

The speed at which the tissue block is cut also affects the quality of the ultrathin sections. A high cutting speed with its inherent vibrations will result in variations in section thickness. Too high a cutting speed may also cause wrinkles and fine chatter parallel to the cutting edge. As a severe shear strain is produced during cutting, too high a cutting speed may produce an excessive rise in temperature, which in turn may cause permanent deformation of fine structures. The optimal speed for sectioning epoxy resin embedded tissues range from 1 to 2 mm/s.

3.8.3 Staining for Electron Microscopy

Different parts of an electron micrograph are recognizable because they differ in electron density, and the contrast in turn is a result of differential electron density. Staining stabilizes certain components so that they become more resistant to the damage caused by the electron beam. This selective stabilization, in turn contributes to an increased image contrast. Hayat (1975) believed that one of the necessary requirements for successful positive electron stain would be that the stain should increase the local electron-scattering power of the specimen sufficiently so that an appreciable increase in image contrast would result. Maximum contrast is apparently achieved when a stain is applied both en bloc and as a post-stain for ultrathin sections.

a. Staining with uranyl acetate (UA)

The treatment of ultrathin sections with aqueous uranyl acetate following double fixation with gluteraldehyde and osmium tetroxide markedly improves the appearance of membranous structures (Hayat, 1975). Uranyl acetate completely penetrates through a section. When a grid is floated, section-side down, on a drop of the uranyl acetate solution, the stain permeates the entire thickness of the section and cell components are stained throughout the section depth

(i) Reaction with proteins

Collagen fibres stain intensely with UA. Interaction between membranes and UA indicate that the protein part rather than the phospolipid part of the membrane is responsible for the staining.

(ii) Overall effect on tissues

Block staining of the specimen with UA prior to dehydration, irrespective of the type of fixative used, results in an increase in contrast as well as stabilisation of the fine structure, eg. membranous and nucleic acid-containing structures (Hayat, 1969).

b. Staining with lead nitrate (Reynolds' lead)

Lead stains are widely used for electron microscopy. The effective application of lead stains is somewhat limited by the fact that upon exposure to air all solutions of lead salts become clouded by the formation of lead carbonate. The insoluble contaminant is deposited on the surface of sections as electron-opaque (black) fine needle-like crystals, small granules, or large amorphous or polygonal precipitates. Lead shows a strong affinity to stain ground substance, and this tendency is much more prevalent with tissues that have been fixed either primarily or secondarily with osmium tetroxide. This problem can be readily overcome with sodium hydroxide pellets.

Chapter 4 MATERIALS AND METHODS

4.1 THE EXPERIMENTAL TISSUE

4.1.1 History and Procurement of Human Tissue

The specimens were collected on the day of surgery on 01/07/87 from a 20 year old South Korean male. The subject was a burns victim at the age of four years. The resultant scar tissue formation pulled his mandible downwards and backwards during development (Fig. 4.1). Mandibular resection surgery was performed on him, and blocks of bone incorporating teeth 34 and 35, and 44 and 45 were removed and contributed as waste material for this investigation. These resected portions of the mandible were immediately rinsed with normal saline and placed in a container with 10% formalin. Radiographs of these segments were taken after collection (Figs. 4.2 and 4.3). Consent had been given by the patient and approval granted for research into the human tissue.

Fig. 4.1 Subject from whom the four premolar segments were removed during surgical correction of the facial deformity. The left photograph shows the extent of the scarring and the consequent dermal contraction at the mandibular area. This scarring resulted in an extensive deformity of the mandible, whereby the lower dentition was out of static and functional occlusion with the maxillary dentition. The teeth used in this research project are considered to be non-functional teeth. (Taken from The Australian magazine, August 1-2, 1992)

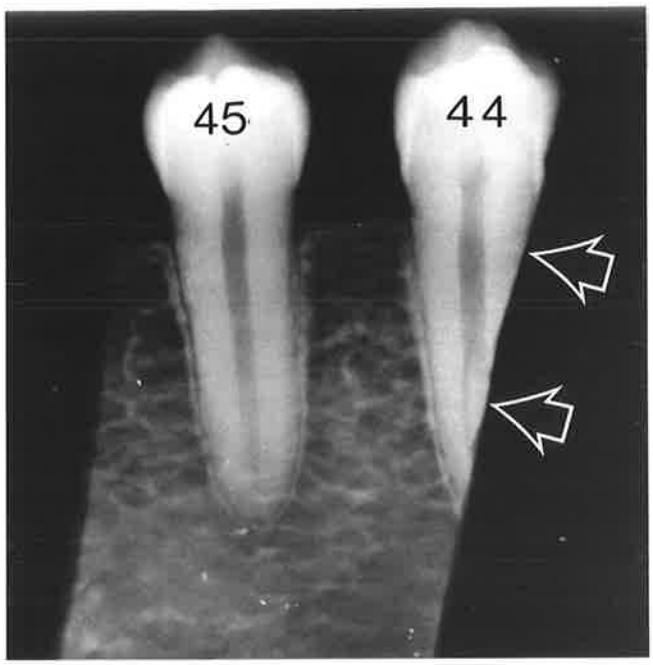

Arrows indicate the line of cut across root

Fig. 4.2. The right mandibular resected segment incorporating the first (44) and second (45) bicuspids. Tooth 44 is designated by the code RPM1 (right first premolar) and tooth 45 by RPM2 (right second premolar). The root lengths of 44 and 45 from alveolar crest to root apex were 13.0mm and 12.5mm, respectively. The surgeon's bone saw had sliced off the mesial portion and apex of the root of 44. Accordingly, the TEM analysis along the distal ligament of RPM1 did not include the root apex.

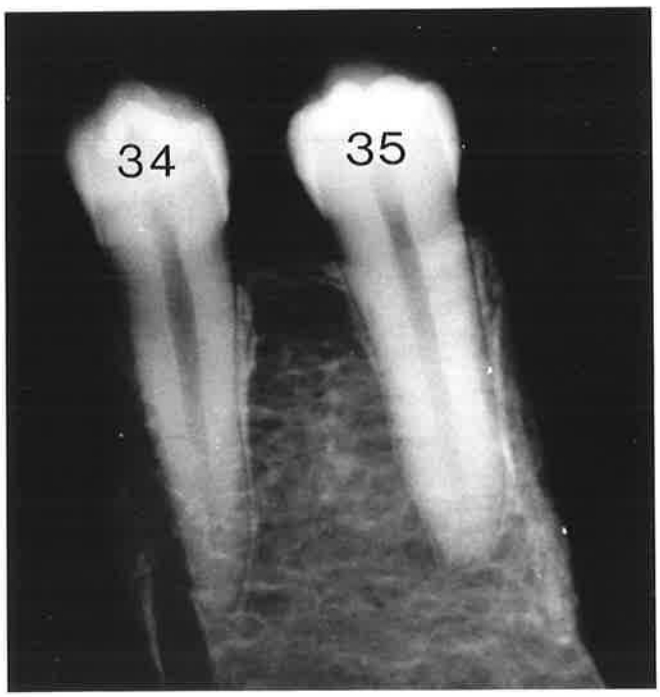

Fig. 4.3. The left mandibular resected segment incorporating the first (34) and second (35) bicuspids. Tooth 34 is designated by the code LPM1 (left first premolar) and tooth 35 by LPM2 (left second premolar). The root lengths of 34 and 35 from alveolar crest to root apex were identical at 14.0mm. A similar situation is observed here where the line of surgical excision was very near the mesial ligament of 34. However, the root apex was intact.

4.2 LABORATORY STAGES

4.2.1 Fixation

Immediately after surgical removal, the mandibular segments were *immersion fixed* in 2.5% glutaraldehyde solution (Appendix 3) for twenty-four hours. Glutaradehyde belongs to the aldehyde family of organic compounds. In tissue this fixative reacts with the active or free hydrogen groups of the amino, imino, and polyhydroxyl alcohols. These reactions form crosslinks or intermolecular bridges which bind the ultracellular structure to produce images free of artifacts.

4.2.2 Demineralization

The resected mandibular portions together with the attached premolars, were demineralized in 4°C 0.1M EDTA and 2.5% glutaraldehyde solution at pH 6.0 with a 0.06M cacodylate buffer. The solution was continuously agitated with a magnetic stirrer and changed daily. Demineralization of enamel was completed on all teeth after several months. The end point of demineralization varied between the samples and was determined by using dental radiographic equipment and needle pricking. Appendix 1 shows the end points of the various specimens.

4.2.3 Trimming

Following demineralization, the samples were sectioned with new razor blades. Each cut was made with a new razor blade. A stereodissection microscope facilitated the trimming. As the mesial root portion of RPM1 had been sliced off during surgery, and that the distal root portions of all teeth were intact, it was determined that the distal half of each tooth be used for the investigation. The first incision was made in the bucco-lingual plane of the premolar down the longitudinal axis to produce mesial and distal halves. Each distal half was then subdivided into 6 equal vertical wedge-shaped segments, with the two most distal wedged-shaped segments selected for horizontal sectioning from the alveolar crest to the root apex. A cutting regime for each tooth was calculated so that the final sections would be at approximately the same percentage levels down the length of the teeth. This was estimated to be at 0% (Level 1-alveolar crest), 12.5% (L2), 25% (L3), 37.5% (L4), 50%

(L5), and so on, in multiples of 12.5% until the 100% level (Root apex-Level 9), to produce a total of nine equal levels or 8 wedge-shaped blocks per distal segment (Fig. 4.4). As the segments approached the apex the semicircular portions became smaller and fewer wedges were cut out. The 100% or the end level was estimated by the disappearance of cellular cementum which is representative of the most apical portion of the root. A notch was placed in the apical aspect of the tooth portion of each numbered wedge-shaped PDL segment, and diagrams were drawn of each section to facilitate orientation during embedding. Dehydration was avoided by continuously bathing the tissue with chilled 0.06M cacodylate buffer. The tissue segments were then transferred to labelled 2ml soda glass vials containing 1.0ml 0.1M EDTA. Prior to processing, the solution was replaced with 0.06M cacodylate buffer and left overnight.

4.2.4 Tissue Processing and Embedding

During processing, the tissue portions were continuously rotated in separate vials and solutions were changed at room temperature using soda glass Pasteur pipettes. The tissue processing regime is outlined in Appendix 2. Propylene oxide is a highly volatile and toxic compound. Adequate ventilation and care in handling are imperative. Fresh Agar 100 resin, prepared for final embedding, was allowed to stand overnight. Each silicone rubber mould was filled with 1ml of resin. The tissue samples were removed from their vials and with the aid of a stereomicroscope, placed with known orientation into the embedding resin. When all tissue pieces were arranged, the moulds were completely filled with resin to form a convex surface. The filled moulds were incubated at 37°C for 48 hours, and then at 60°C for a further 48 hours before being coded and stored at room temperature. The blocks were removed from the moulds and placed in labelled vials.

4.2.5 Ultramicrotome Sectioning

Each specimen block was secured in a Reichert specimen holder for flat trimming, and mounted on a Reichert-Jung OM-U4 ultramicrotome. Initial trimming to remove excess resin on the most coronal portion of the block was carried

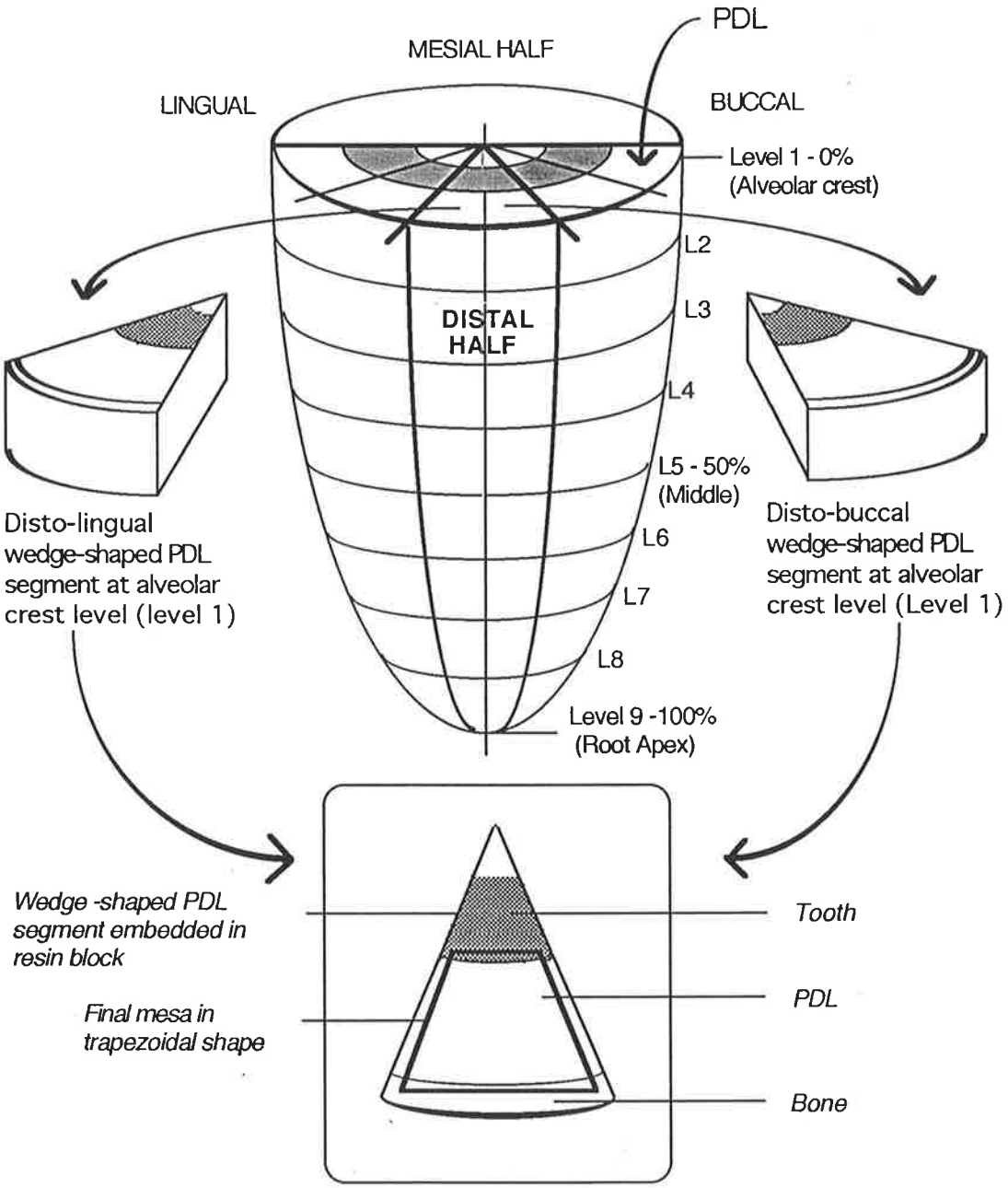

Fig. 4.4. The cutting regime adopted to produce a wedge-shaped PDL segment at each level (L1 to L9) of the tooth root. The PDL segment taken from the disto-buccal side of the root (eg. left first premolar) at level 1 was given the code LPM1 Buccal (Bu) Level 1. The corresponding PDL segment from the disto-lingual side was designated LPM1 Lingual (Li) Level 1. Each wedge-shaped PDL segment from the disto-buccal and disto-lingual sides from L1 to L9 were then embedded in a block of resin. Each resin block was then trimmed to give a trapezoidal shaped final mesa which included bone, PDL and tooth.

out with a double-edged razor blade. After the resin had been removed from the tissue surface, a number 11 scapel blade was used to trim the most coronal aspect of the block face to a divergent sided trapezoidal mesa (Fig. 4.4). Bone and tooth substance were included at the base and top of the trapezium to strengthen the section, facilitate orientation, and to standardize sampling during TEM viewing.

The block and chuck were then transferred to the specimen arm of the ultramicrotome and a glass knife aligned in the knife holder. Glass knives were prepared using a LKB Type 780 1B knifemaker. One micron thick orientation sections were cut at a speed of 2 mm per second and were transferred with tweezers to a pool of millipored, double-distilled water on a clean glass microscope slide. These sections were then flattened on glass slides on top of a 70°C hotplate, and stained for two minutes at 70°C with millipored solutions of 0.5% toluidine blue and 1% borax. Sections were then rinsed with millipored double-distilled water and dried on the hotplate.

An Olympus EHT light microscope was used to examine the sections and to check for the correct orientation within the resin block. Appropriate orientation photographs were taken with a Polaroid Type 107 black and white Land film. Any blocks that were incorrectly orientated were restubbed.

Ultrathin sections in the silver/gold interference range, approximately 70 nm thick were cut with a Diatome diamond knife at a clearance angle of 6° and a cutting speed of 2 mm per second and three of these sections were placed on each copper grid.

At each level, a total of 36 ultrathin sections were cut. These sections were floated on a bath of millipored double distilled water, flattened with chloroform vapour and picked up on uncoated R150A mesh copper grids. Three sections were collected on each grid by holding the copper grid with its dull surface towards the bath, slowly lowering the grid to contact the sections and then lifting the grid and

attached sections perpendicularly from the water surface. Grids were then dried face upwards on Whartman's grade 1 filter paper in a covered petri dish and stored in a LKB specimen grid holder until viewing. Altogether, twelve copper grids were taken at each level.

4.2.6 Grid Staining

Dried grids with complete sections were selected and stained. Staining was initiated by placing the grids, tissue side down for 25 minutes in a microfiltered droplet of freshly prepared 0.5% uranyl acetate (Appendix 12) on Parafilm 'M' laboratory film. The staining procedure was performed in a covered petri dish that had been preheated to 37°C on a thermostatically controlled hotplate. Grids were then rinsed by agitating them vigorously for 45 seconds in each of four beakers containing 100 ml millipored, double-distilled water at 37°C.

Grids were then stained with lead citrate for 10 minutes by floating the grid tissue side down in a microfiltered droplet of freshly prepared modified Reynolds' lead (Appendix 12) on a square of Parafilm 'M' laboratory film in a covered petri dish. Also enclosed in this petri dish were sodium hydoxide pellets to absorb contained carbon dioxide to minimise the formation of lead carbonate precipitate on tissue sections. The tissue was again rinsed in four beakers of freshly double-distilled, millipored water and dried, tissue surface uppermost, on fine grade filter paper. Grids were then stored in a LKB specimen grid holder until required for transmission electron microscopy.

4.2.7 Transmission Electron Microscopy

A Jeol 100S transmission electron microscope was used to examine the tissue sections. Grids were placed tissue side downwards in the vacuum column of the microscope and conditioned in the electron beam before being examined.

4.2.8 Surveying and Selection of quadrat

The survey (Fig. 4.5) was always started from the right hand side of the copper grid with the tooth circumferential third facing superiorly. The surveying process was systematic in that each row of square grids was surveyed before proceeding to the next row. The systematic way of surveying ensured that each square grid had an equal chance of being selected. The number of sections on each copper grid did not affect the random selection process. What affected the randomness of the selection process was the unsystematc way of carrying out the surveying. If one could imagine each row of square grids were joined end to end instead of being stacked upon each other as in the copper grid, a long length of square grids would result. The logical way of surveying all the square grids would be to start at one end and proceed progressively down the chain of squares until the last square was reached. As each row of square grids was surveyed, the row where the ligament of each section was found had a 50% chance of being surveyed from the left to right or vice versa. *It must be borne in mind to start on the same side when surveying each copper grid.*

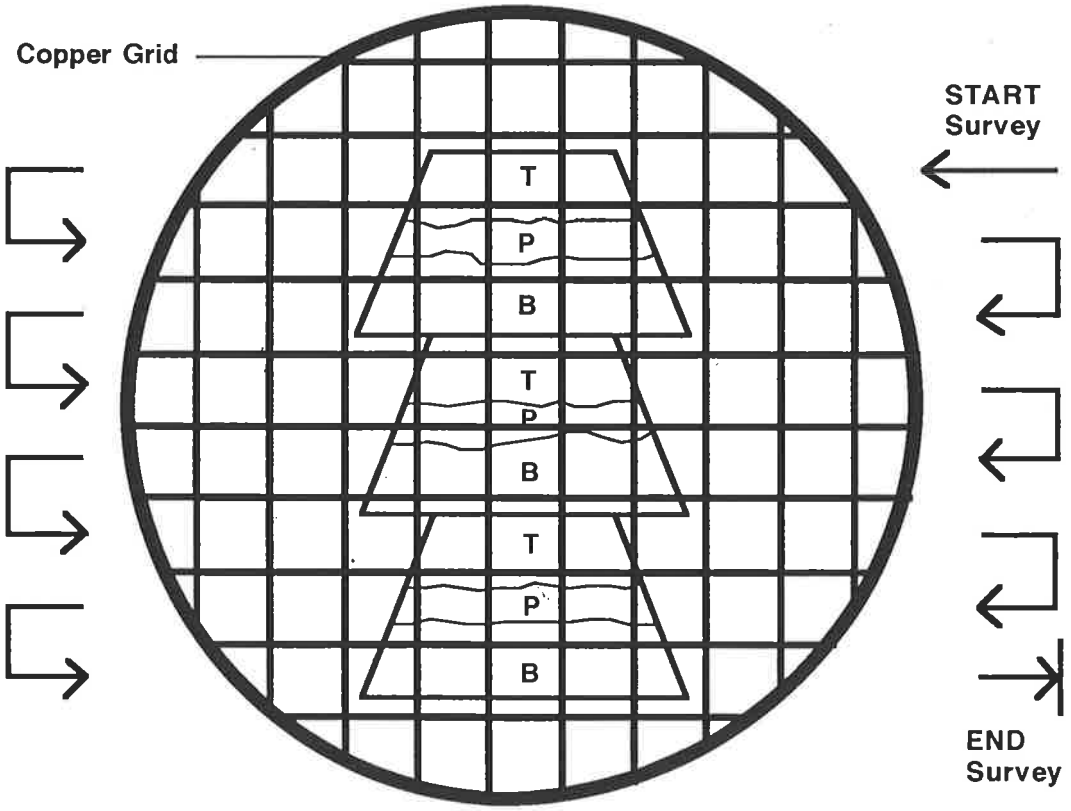

Fig. 4.5. The systematic way of surveying the sections for random selection of a square grid (quadrat) for sampling of the three circumferential thirds.

The square grid slot that was selected would be the FIRST slot surveyed to comprise the bone, middle and tooth circumferential thirds within the grid bars. The ligament of this first slot might or might not contain blood vessels or nerves. The presence or absence of BV/nerves should not be a criteria for selection as this would affect the random nature of selection. Each grid slot that was surveyed had a 0.5 probability of being the first slot to include the three circumferential thirds, and that did not have any tear along the entire portion of PDL.

Special circumstances:

When the ligament width was wider than the length of each square grid: The copper grid was oriented in a diagonal at ≈ 45° to the length of the periodontal ligament before picking the sections up. The length of the diagonal of the square grid might be sufficiently long to contain the ligament. In cases where the ligament width was even wider than the square diagonal, the sampling of the three circmferential thirds would involve two square grids lying adjacent to each other in a vertical direction. The tooth and bone circumferential thirds would lie in separate square grids with a grid bar intervening in the ligament. Provided the grid bar was not right in the middle of the ligament, the middle circumferential third might be positioned in the square grid containing the bone third or in the other grid containing the tooth third. Each photomicrograph of the circumferential thirds must follow a straight vertical from bone to tooth third or vice versa.

4.2.9 Photomicrography

When a square grid slot was selected, it must be ensured before taking photographs that the edges of tooth and bone surfaces were parallel to the long edge of photomicrographic view finder (at x3,000 magnification) designated by corner markings on the circular fluorescent plate of the Jeol 100S. If the surfaces were not parallel, the correct orientation was achieved by rotating the copper grid with a pair of tweezers until the correct orientation was obtained.

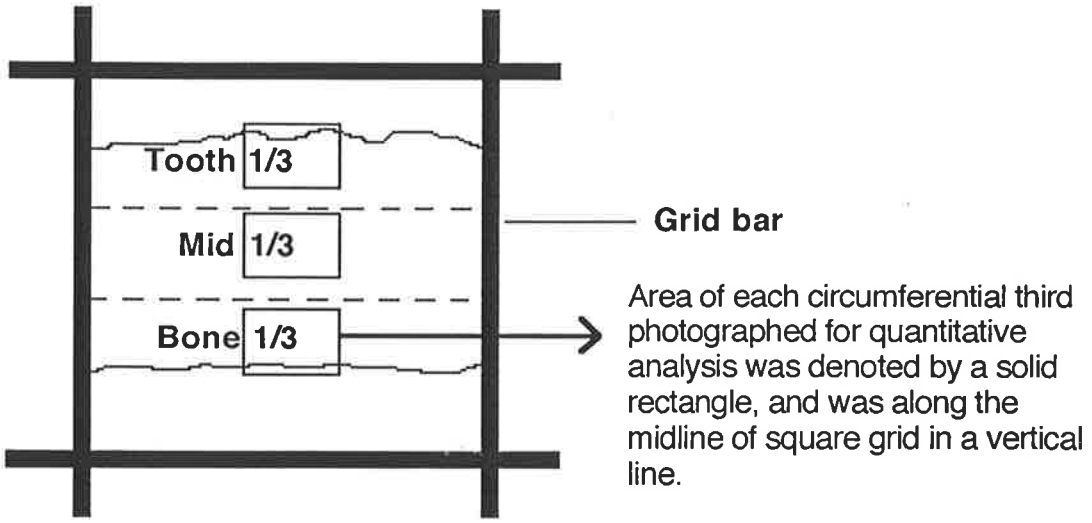

Fig. 4.6. The sampling carried out across the PDL width.

Photographs were taken of the tooth, middle, and bone circumferential thirds across the width of the PDL along the midline of the square grid slot (Fig. 4.6). Each photomicrograph of the circumferential thirds followed a straight vertical from bone to tooth third or vice versa. Ultramicrographs were obtained with Ilford Electron Microscope Film using the inbuilt photograph equipment of the Jeol 100S. This equipment had an automatic aperture setting and the exposure time was controlled by the operator. Focussing was assisted by the use of an image wobbler which was switched off immediately prior to micrograph exposure. An orientation micrograph of the whole ligament was taken at a magnification of x500 with an exposure time of two seconds. This orientation micrograph was used as an aid in identifying different types of blood vessels present. One micrograph was taken at a magnification of x3000 in each circumferential third, with an exposure time of three seconds. A picture of a replicating graticule was also taken at each magnification at x500 and x3000 at the end of each session. Features of special interest were also photographed at varying magnifications. When selection and photomicrography are completed for the present level, the process of randomly selecting a square grid began for the next segmental level. This regime continued to the most apical level for each segmental block.

4.2.10 Developing and Printing

Ultramicrographs were agitated in Kodak D19 Developer for 4 minutes at 20°C, rinsed in running water and fixed in Hypam Rapid Fixer at 20°C for 7-8 minutes. Following fixation, negatives were again washed under running water for 15 minutes and rinsed in a wetting agent and deionised water. After drying, negatives were identified and stored in plastic envelopes. All micrographs to be used for stereological analyses were printed at a final magnification of x8,500 using a Durst Laborator 54 enlarger. Replicating graticules were used to ensure magnifications were constant and that variation in magnification between micrographs was eliminated. The negatives were printed on Ilford Multigrade photographic paper, processed with Ilford Multigrade paper developer and fixed in Hypam rapid fixer for at least 15 minutes. The photomicrographs were then washed in clean running water for at least 30 minutes before being dried in a roller dryer, and stored for future point counting.

4.3 POINT COUNTING PROCEDURE

4.3.1 Criteria for point counting

Point counting was carried out for blood vessels and nerves using the concept of forbidden lines (Gundersen, 1977), as explained in Fig. 4.7. In those instances where a point of the test system laid on a boundary between two test profiles, the profiles above and to the right of the test point were scored.

4.3.2 Grid Area

Each x8,500 magnified photomicrograph print was covered with a 140 point square lattice grid, made up of 17 x 17 mm square grids (Fig. 4.8). A total of 10 x 14 such squares encompassed the area of the photomicrograph that was to be point counted for stereological data. This area of 170 x 238 mm^2 corresponded to an area of 20 x 28 μm^2 of PDL.

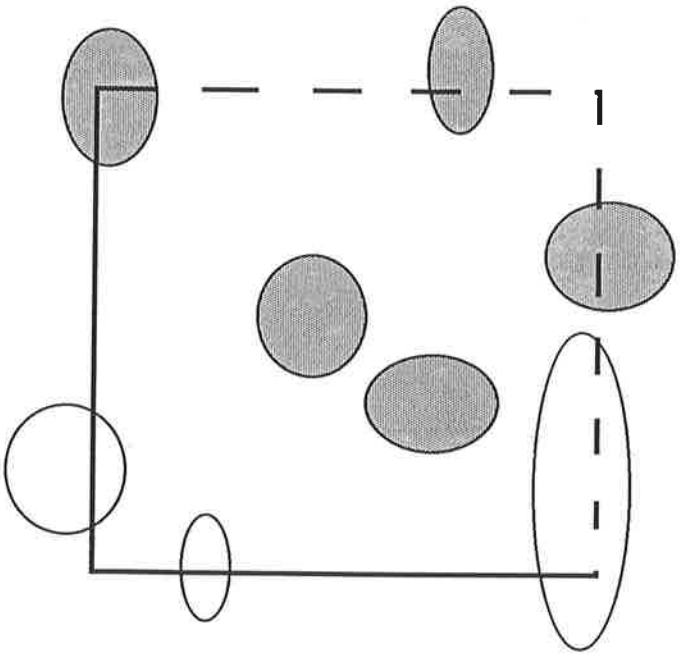

Fig. 4.7. A square test area with profiles. The shaded profiles were counted according to the manner below. The edge-effect arose when some profiles intersect the delineation of the test artea. The idea of inclusion / exclusion - edges was devised to prevent overestimation of the stereological parameter N_A. The number of profiles was estimated in the following manner: All profiles completely within the square were counted in addition to all profiles intersected by the upper and right border (inclusion-edges). All profiles intersected by the lower and left borders (exclusion edges) were disregarded. Profiles intersected by the upper left corner were counted but disregarded if intersected by the lower right corner. (Adapted from Gundersen, 1977)

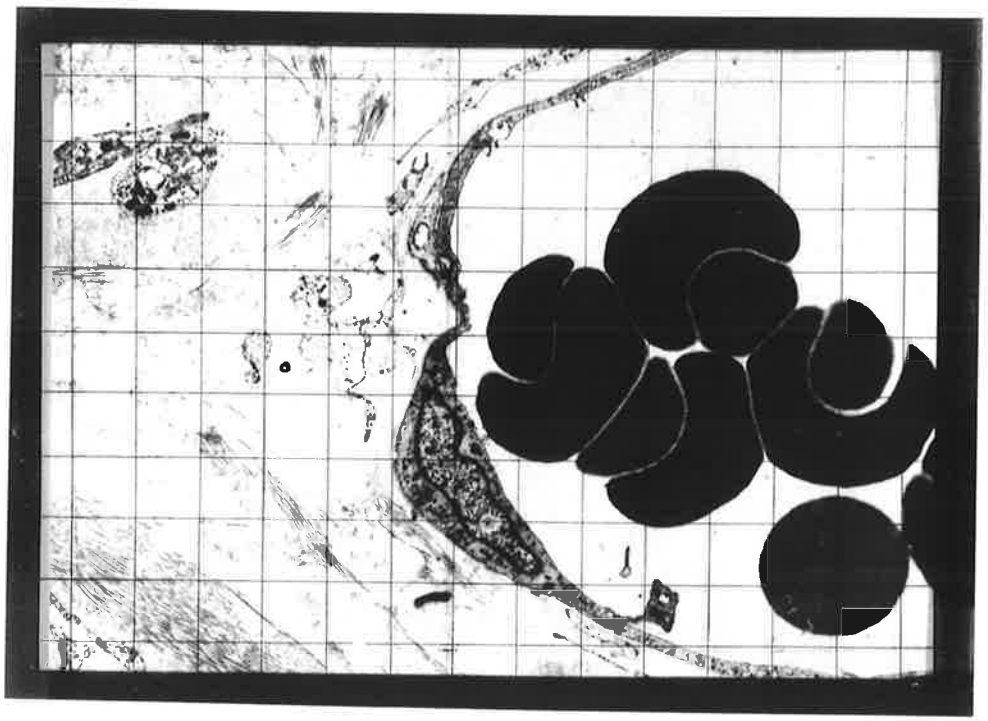

Fig. 4.8. A 140 point square lattice grid placed over a x8,500 magnification electron-micrograph (reduced) for point counting. Points were scored when the top right intersections fell over a profile.

4.3.3 Data Entry

The data were tabulated in a prescribed form and entered into the computer for stereological analysis (Appendix 15).

4.4 MORPHOMETRIC IDENTIFICATION

4.4.1 Identification of blood vessels

The blood vessels were identified according to the studies of Rhodin (1967,1968) (Fig. 4.9), Freezer and Sims (1987), and Cooper et al. (1990). Vessel lumina were categorized by diameter and wall thickness (Tang and Sims, 1992) according to stereological convention across the smallest axis. Cells were included in the outer vessel wall if the cell enclosed at least three quarters of the outer endothelial layer and the 'gap' between the cell membrane and outer endothelial layer was no greater than 1 μm.

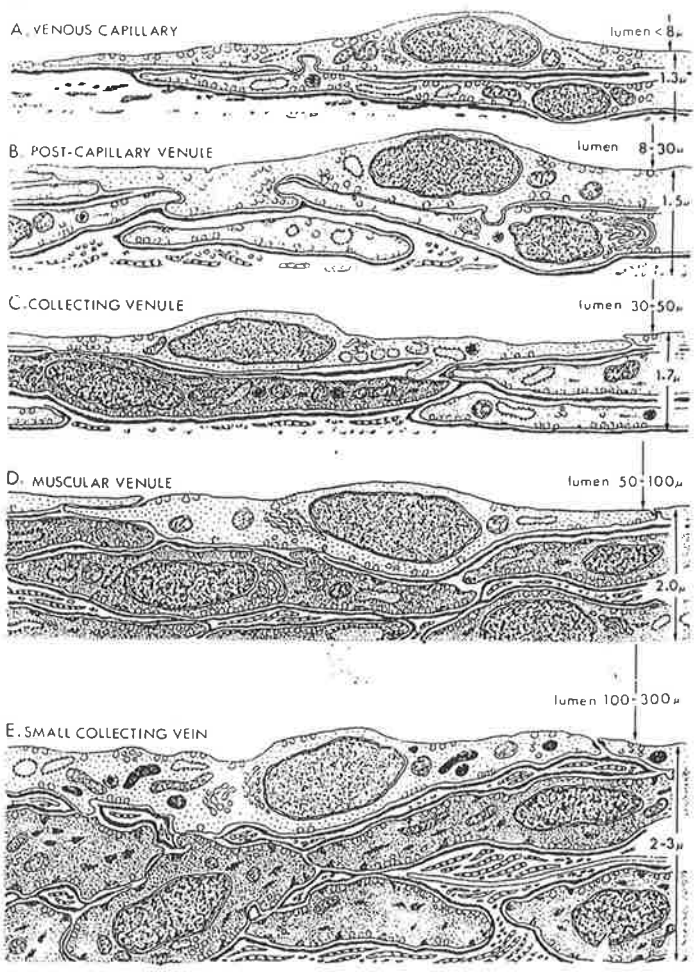

Fig. 4.9. Schematic drawing relating the luminal diameter and the thickness of venous blood vessel wall as described by and taken from Rhodin (1968).

4.4.2 Identification of nerve axons

Freezer (1984), Freezer and Sims (1988) and Crowe (1989) provided a classification of myelinated and unmyelinated nerve axons based on the location of the axons in the interstitial matrix of the PDL. Axons were either located in the parenchyma of the PDL or in close proximity to the endothelium of the blood vessel walls.

4.5 MEASUREMENT OF PDL WIDTH

The width of the PDL was measured on a straight line that passed through the middle of the test quadrats (rectangular areas photographed for point counting) across the zone of sampling. The measurement started from the junction between the ligament and the cementum in the tooth circumferential third, and ending in the bone third where the ligament and osteoid layer met. The measurement was made on the x500 magnification micrographs.

4.6 STATISTICAL ANALYSIS

A generalised linear regression model (McCullagh and Nelder, 1983) with binomial distribution was applied to the point counting data using the statistical package Genstat version 5 Release 2.2 from AT&T, USA. The binomial data obtained showed a variance that was greater than that was appropriate for a binomial distribution, which indicated an overdispersion. The standard error was calculated from iterative models using first-order approximations. The use of first order approximations suggested that the standard error obtained was only an approximation of the individual mean values. The analysis was devised to test for volumetric effects due to side of mouth (L v R), tooth (PM1 v PM2), and interaction between side of mouth and tooth. Taking into consideration the possible variation due to each tooth, volumetric effects were also tested due to side of tooth (Buccal v

Lingual), region (tooth, middle, bone thirds), and interaction between these two factors. In addition, an analysis of variance was performed to determine if there were any differences in luminal and abluminal vessel diameter as well as wall thickness due to tooth, side of tooth, and region, using the software Minitab Release 7 from from AT&T, USA. Statistical significance was assumed at the $p<0.05$ level. Stereological data were based on the following equations (Gundersen et al., 1988a,b; Nyengaard et al., 1988) :

$$V_v = \frac{V(lum)}{V(pdl)} \quad \text{.....1}$$

$$L_v = \frac{4V_v}{\overline{d}^2 \pi} \quad \text{.....2}$$

$$S_v = \overline{d}\,\pi L_v \quad \text{.....3}$$

V_v - volume density (luminal volume/PDL volume)
L_v - length density (luminal length/PDL volume)
S_v - surface density (luminal surface area/PDL volume)
V (lum) - luminal volume
V (pdl) - periodontal ligament volume
$\overline{d}$ - mean luminal diameter

CHAPTER 5 FINDINGS

5.1 THE PDL MICROVASCULAR BED

5.1.1 Non-pericytic Postcapillary-sized Venule

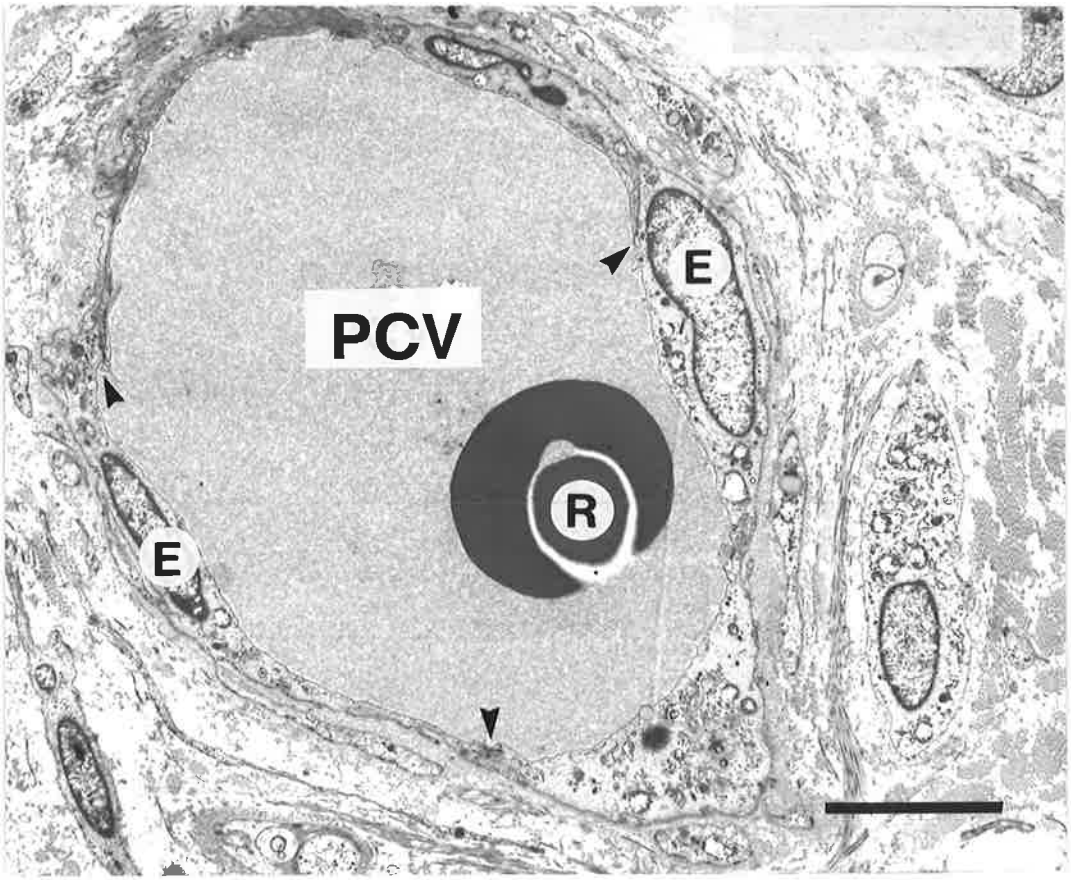

Fig. 5.1. A *non-pericytic postcapillary-sized venule* (PCV) with some erythrocytes (R) within. Arrows demarcate the intercellular junctions between the endothelial cells (E). Magnification : x4,500. Bar = 5.0 μm. Location : Buccal PDL, middle circumferential third, level 6 of RPM1.

5.1.2 Arterial Capillary

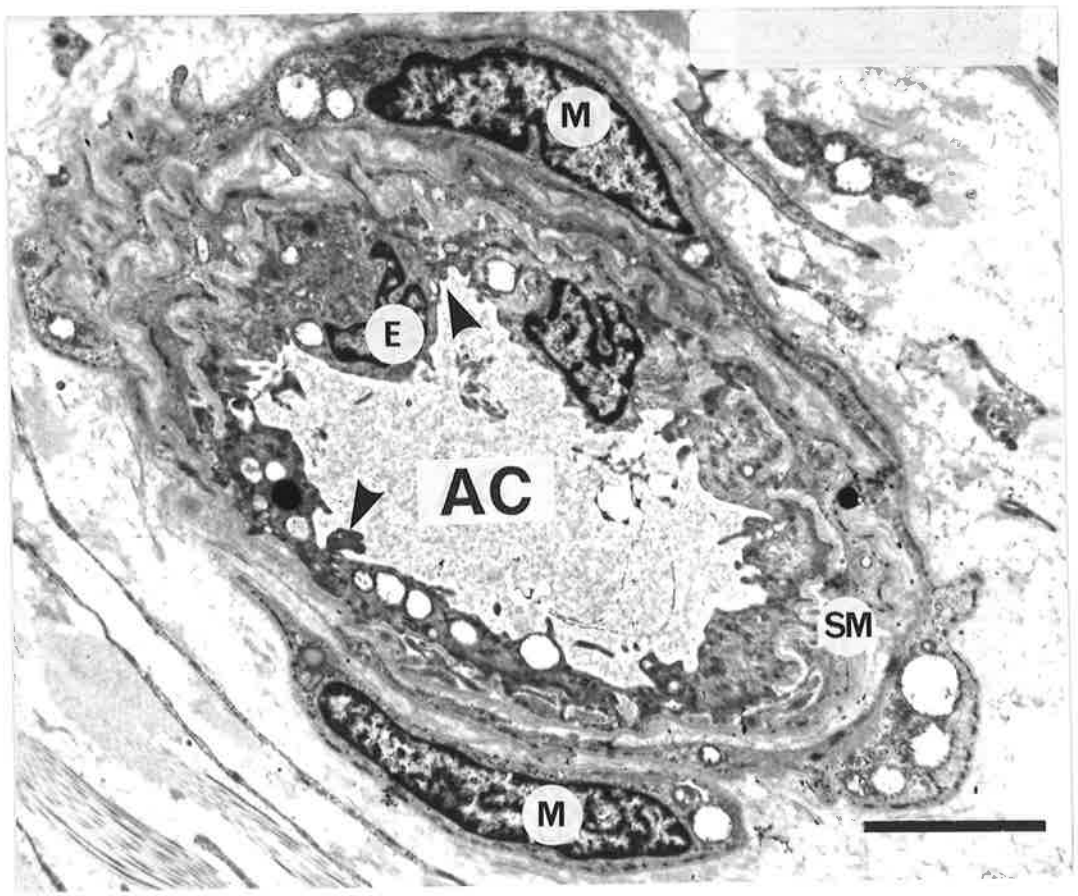

Fig 5.2. An *arterial capillary (AC)* with at least one layer of perivascular *smooth muscles* (tunica intima, SM) and *smooth muscle cells* (M). The endothelial cells (E) bulging into the lumen are a characteristic feature of arterial capillaries. Arrows denote intercellular junctions. x4,500. Bar = 5.0 μm. Location : Lingual PDL, bone circumferential third, level 7 of RPM2.

5.1.3 Presumptive Lymphatic Capillary

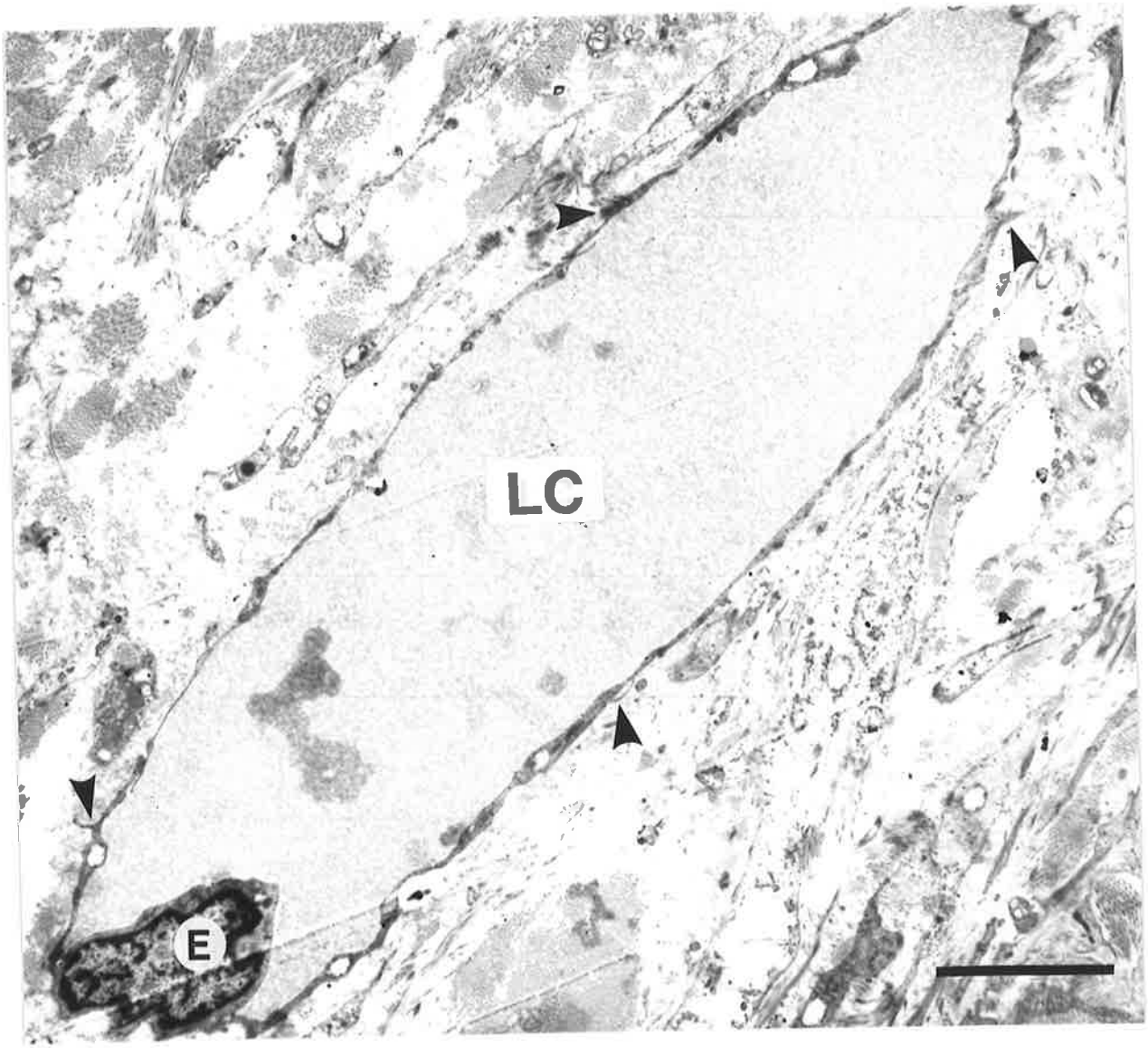

Fig 5.3. An extremely thin-walled presumptive *lymphatic capillary* (LC). Arrows denote abluminal projections. A high nuclear thickness to endothelial thickness ratio is shown in this photomicrograph. A characteristic of lymphatic capillaries is the luminal protruberance of the nucleus of the endothelial cell (E). All the lymphatic capillaries observed in this study were located in the apical (level 9) area and bone circumferential third of the PDL. x6,000. Bar = 4.0μm. Location : Lingual PDL, bone circumferential third, level 9 of LPM2.

5.2 PERIODONTAL NEURAL ELEMENTS

5.2.1 Unmyelinated Nerves

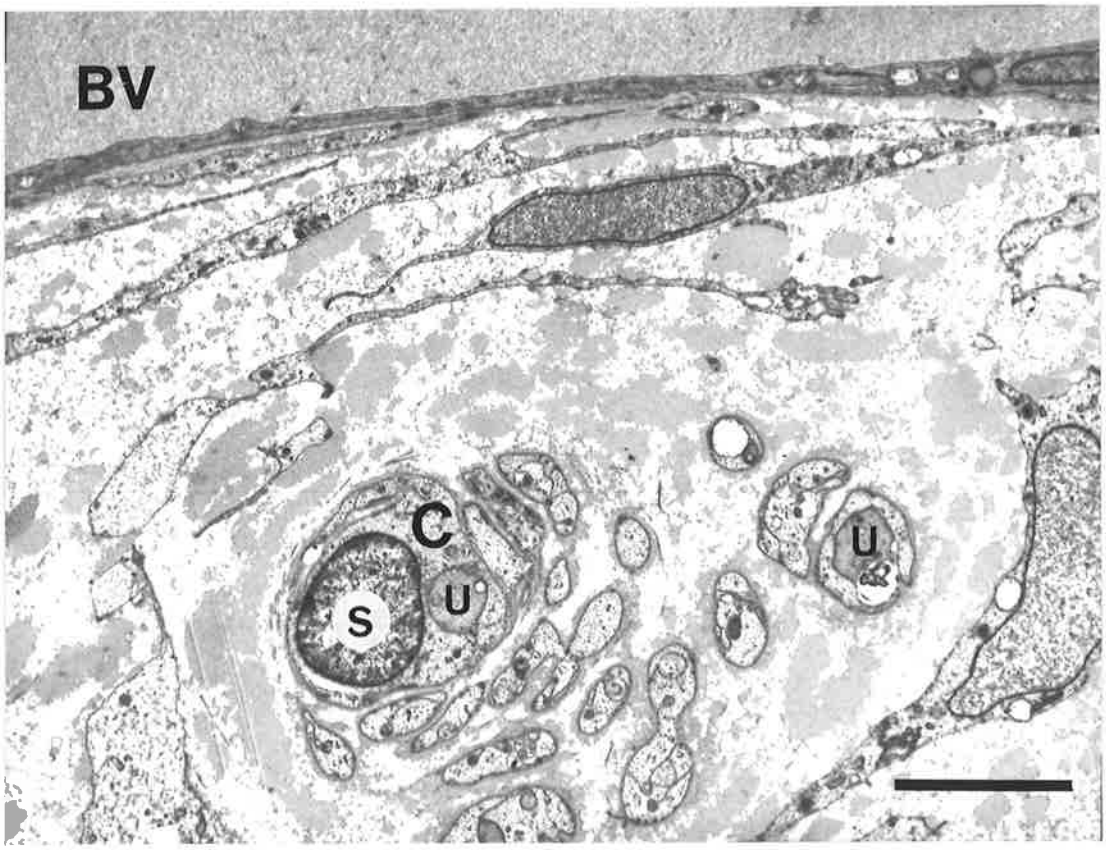

Fig. 5.4. A blood vessel (BV) in close proximity to a collection of *unmyelinated nerves* (U) surrounded by Schwann cell cytoplasm (C). Nucleus of Schwann cell (S) is located among the nerve collection. x4,500. Bar = 5.0 μm. Location : Buccal PDL, middle circumferential third, level 5 of RPM2.

5.2.2 Myelinated Nerves

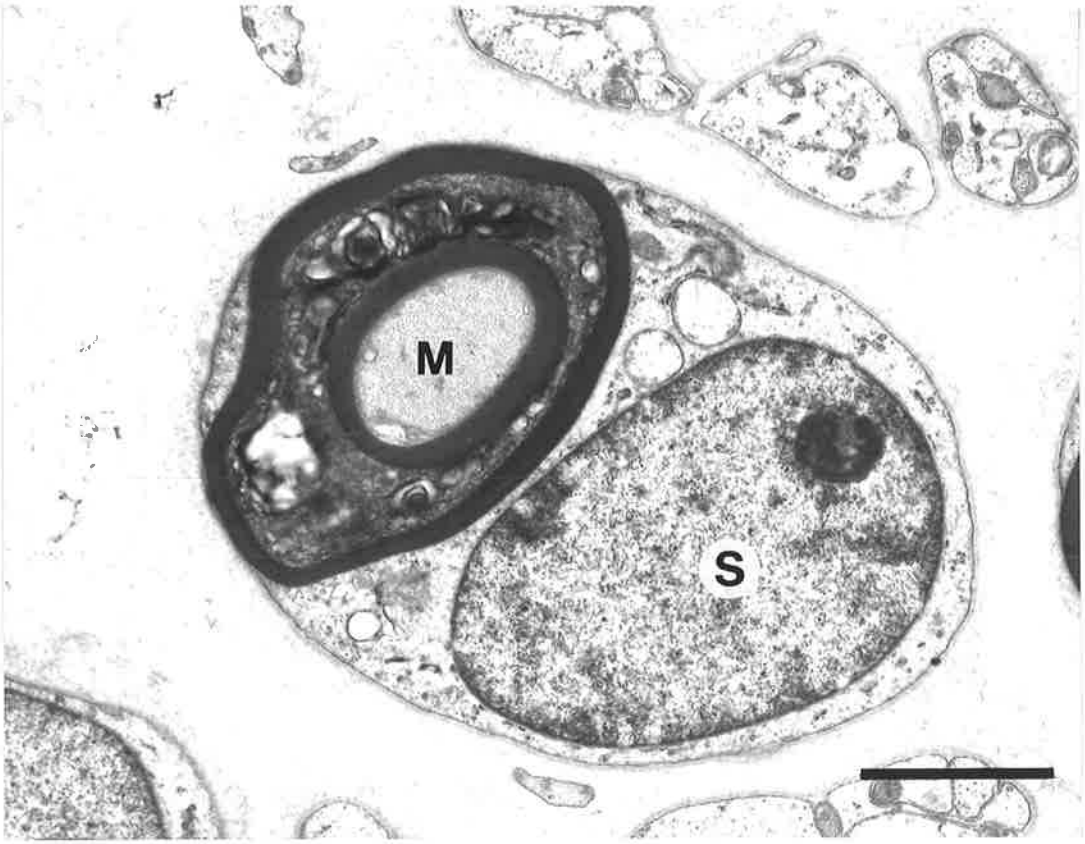

Fig. 5.5. A *Schwann cell nucleus* (S) and cytoplasm surrounding a *myelinated axon* (M). x12,000. Bar = 2.0 μm. Location : Buccal PDL, middle circumferential third, level 7 of LPM2.

5.3 VASCULAR VOLUMETRIC FINDINGS

5.3.1 Overall and Adjusted Volumes

The analyses of the point counts of the eight PDL samples provided an *overall mean* luminal volume of 8.97 ± 2.05%. The volume of endothelium and perivascular cells added another 3.40% to give an overall mean abluminal volume of 12.37 ± 2.45% (Table 5.1 and Fig. 5.6). No significant differences ($p<0.05$) in vessel luminal and abluminal volumes were observed between first and second premolars (PM), as shown in Table 5.2. (All values eg. ± 2.05% represent the standard error).

The total number of points counted for the vascular lumen in left first premolar (LPM1) buccal PDL sample appeared to be half that of the other seven PDL samples. This finding could be attributed to a collapse of a large number of blood vessels during surgical manipulation and TEM preparation. In considering the reduced number of points counted from the LPM1 buccal PDL sample to be outlying data, these point counts were removed from the data set. The point counts of the remaining seven PDL samples were re-evaluated to provide the ***adjusted*** mean luminal and abluminal volumes. Accordingly, the *adjusted mean* luminal and abluminal volumes increased to 9.52 ± 2.28% and 12.91 ± 2.76%, respectively, as shown in Table 5.1. No significant differences ($p<0.05$) were detected between the overall mean and adjusted mean luminal volumes, and between the mean abluminal volumes. The adjusted mean luminal and abluminal volumes were, therefore, chosen to represent the total luminal and abluminal volumes. The mean endothelial and perivascular cellular investment volume of the seven PDL samples appeared to remain the same at 3.39%. With this adjustment, the left and right premolar mean luminal vascular volumes showed a non-significant difference ($p<0.05$) at 9.66 ± 3.73% and 9.42 ± 2.99%, respectively, as shown in Table 5.3 and Fig. 5.7. No significant differences in vessel luminal and abluminal volumes were observed between the buccal and lingual PDL samples as shown in Table 5.4. No significant interactions were observed between tooth type (PM1 and PM2) and side of mouth.

A note of caution is sounded here in that three out of the eight PDL samples did not have root apices for evaluation (2 root apices were missing due to the surgical porcedure, and 1 root apex was misplaced before the present author started the experimentation); therefore point counting data for level 9 (root apex level) of these PDL samples had to be estimated from the samples with apices present and added to provide point counts representing the total grid count and vessel count for that level, so that total vascular volumes could be compared (Appendix 16).

VOLUME	Overall	Adjusted	p<0.05
Luminal	8.97±2.05	9.52±2.25	NS
Abluminal	12.37±2.45	12.91±2.76	NS

Table 5.1. *Overall mean* vascular volume ± SE (%) compared with *adjusted mean* vascular volume ± SE (%) calculated from the remaining seven PDL samples. The difference between adjusted and overall vascular volumes was not significant.

VOLUME	First Premolars	Second Premolars	p<0.05
Luminal	8.24±2.87	9.66±3.02	NS
Abluminal	12.39±3.58	12.35±3.51	NS

Table 5.2. *Overall mean* vascular volumes ± SE (%) between first and second premolar PDL were not significantly different. (NS - not significant)

VOLUME	LEFT	RIGHT	p<0.05
Luminal	9.66±3.73	9.42±2.99	NS
Abluminal	11.79±4.30	13.64±3.72	NS

Table 5.3. *Adjusted mean* vascular volumes ± SE (%) between left and right premolar PDL were not significantly different. (NS - not significant)

	Coronal	Middle	Apical	TOTAL
Buccal	1.36	3.7	4.59	9.65
Lingual	2.2	2.18	5.01	9.39
MEAN	1.78	2.94	4.8	9.52

Table 5.4. *Adjusted mean* luminal vessel volume (%) in the vertical thirds, separated into buccal and lingual sides. The lingual PDL sides had a greater luminal volume in the coronal and apical thirds than the buccal sides, while the buccal PDL sides appeared to carry more blood in the middle vertical third. Differences due to side and vertical levels were not statistically analysed.

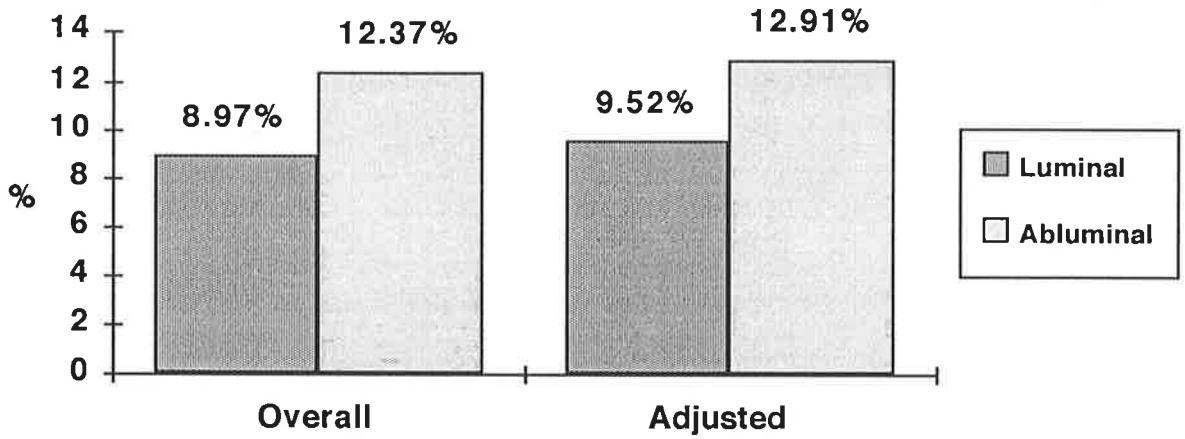

Fig. 5.6. *Overall mean* vascular (luminal and abluminal) volumes and *adjusted mean* vascular volumes. Statistically, there was no difference in vascular volumes between the two groups ($p<0.05$).

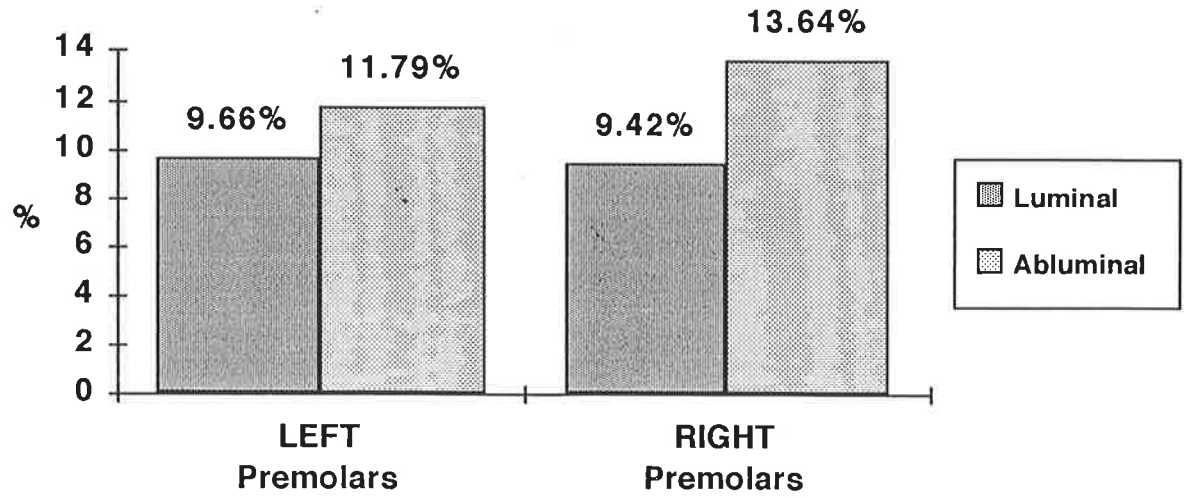

Fig. 5.7. The *adjusted mean* vascular volumes between left and right premolars do not differ significantly ($p<0.05$).

5.3.2 Regional Distribution

Most of the vessel volume was located in the middle circumferential third of the PDL which contributed 78.0 (12.0)% of the total luminal volume or 7.44 (1.13)% of the PDL volume (Fig. 5.8). The bone and tooth circumferential thirds held 13.0 (3.2)% and 9.0 (2.92)%, respectively, of the total luminal volume. Accordingly, the middle circumferential third contained 9 times more blood volume than the tooth third, and 6 times more than the bone third. (SE values are indicated in parentheses).

5.3.3 Vertical distribution

Levels 1 to 3, levels 4 to 6, and levels 7 to 9 of each PDL segment were designated the coronal, middle, and apical thirds, respectively, of the PDL. Statistical analysis was not performed to evaluate the differences in blood vessel volume in the vertical plane from the alveolar crest down to the root apex. However, the volumetric distribution from the alveolar crest down to the root apex was estimated using the principle of proportion. Ignoring the effects of side of mouth and tooth type, and LPM1 buccal PDL sample, it was concluded that the apical third of the PDL contained more than half of the total luminal volume at 50.4%. The coronal third held slightly less than one-fifth of the luminal volume at 18.7%. The middle vertical third accomodated 30.9% (Fig. 5.9). It appeared that the apical third of the PDL contained 1.6 times as much blood as the middle vertical third, and the middle vertical third contained 1.6 times as much blood as the coronal third.

5.3.4 Vessel Type and Proportion

Four morphologically distinct blood vessel types were identified in the human PDL. They were the venous capillaries (VC), the postcapillary-sized venules (PCV), the arterial capillaries (AC), and the collecting venules (CV). The VC and PCV were further subdivided into vessels with or without a partial cellular pericytic investment layer, ie. apericytic VC (*a*VC) and apericytic PCV (*a*PCV).

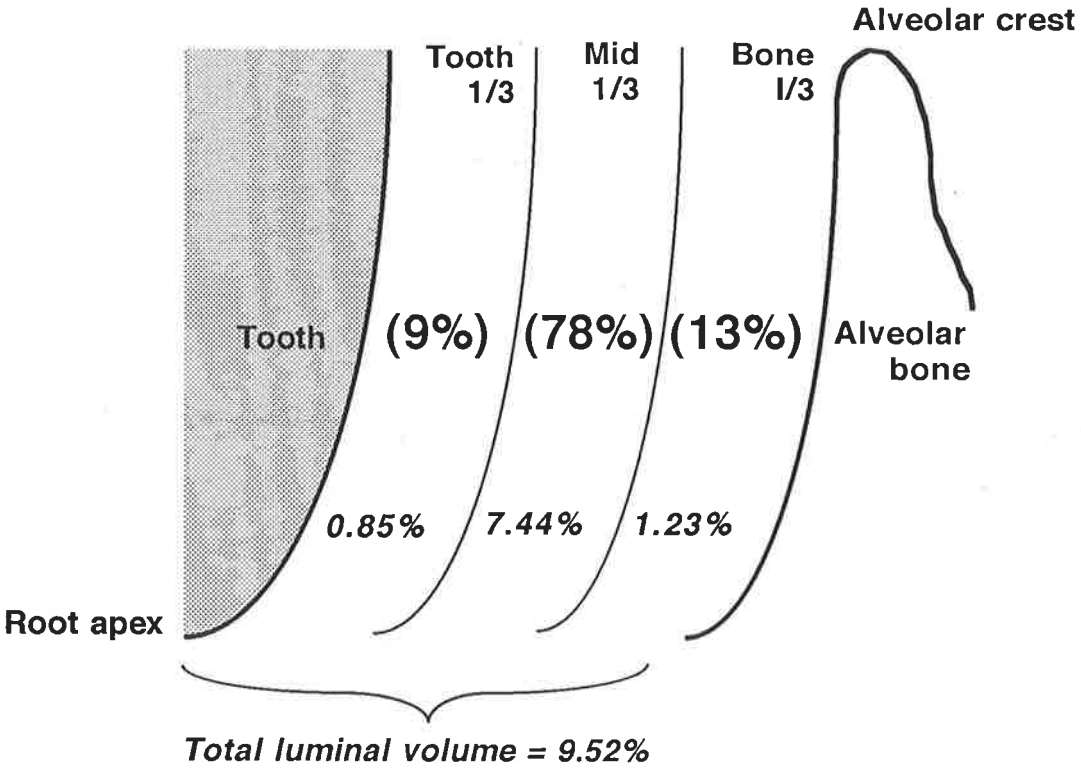

Numbers in parentheses represent the percentage of total luminal volume. The numbers in italics indicate the distribution of blood volume as a % of the PDL volume.

Fig.5.8 Distribution of luminal blood volume from tooth third to the bone third.

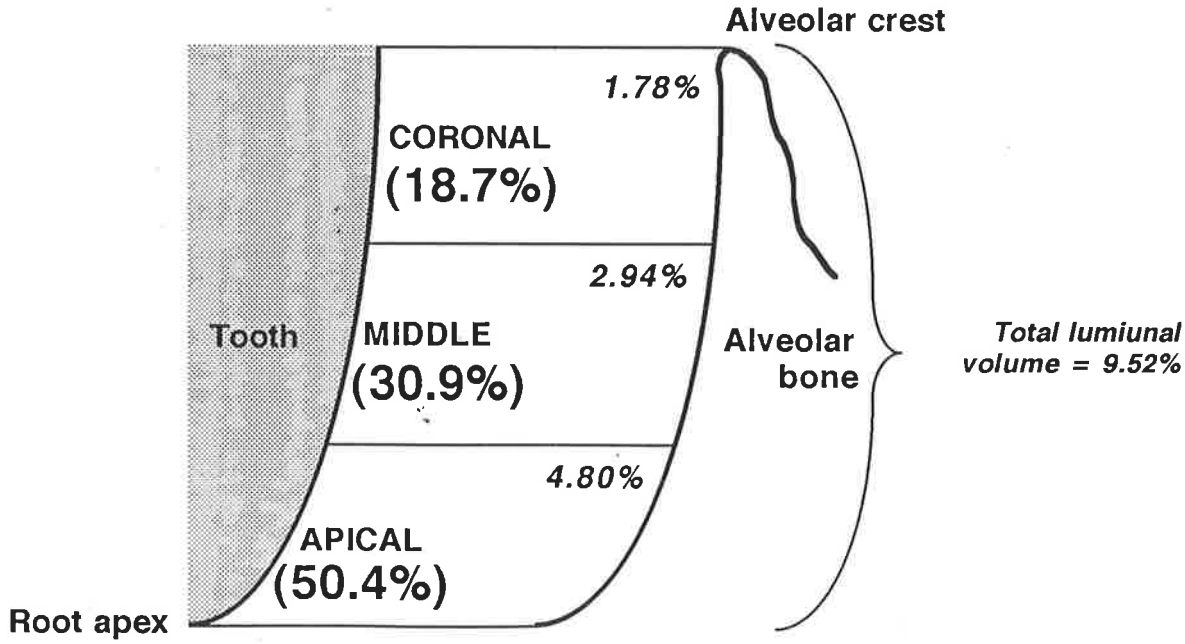

Numbers in parentheses represent the percentage of total luminal volume. The numbers in italics indicate the distribution of blood volume as a % of the PDL volume.

Fig. 5.9 Blood volume distribution from alveolar crest to root apex in the PDL.

a. Vascular Proportion

A distinction between pericytic and non-pericytic vessels was not always definitive. Numerically some observations for arterial capillaries and collecting venules were insufficient for analysis. The postcapillary - sized venules were the major contributors to the vascular volume, occupying about 69.1% of the total luminal volume. The venous capillaries contributed 14.9% while the collecting venules provided 12.4% of the vascular volume. The arterial capillaries were uncommon, and occupied only 3.6% of the vascular volume. Hence, venous blood volume (VC + PCV + CV) was 26 times that of arterial vlood volume (AC). The capillary - sized vessels (VC and AC) altogether made up 18.5% of the luminal volume while the venules contained the majority of blood volume at 81.5%. Fig. 5.10 shows the vessel type and proportion.

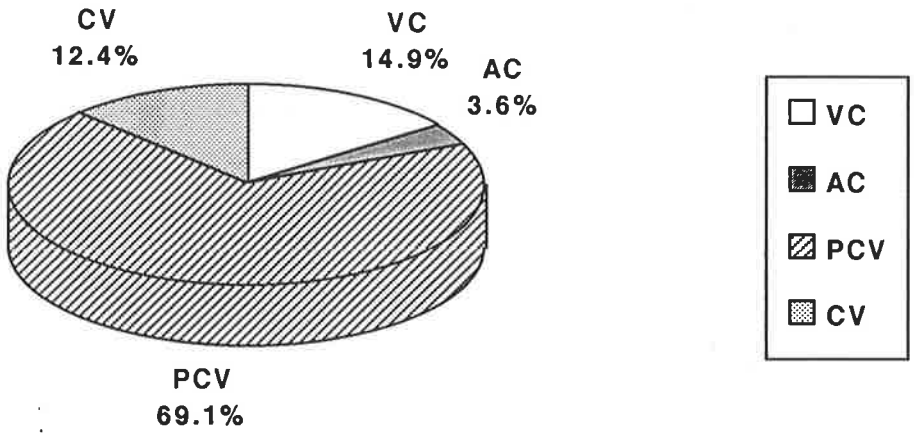

Fig. 5.10 Postcapillary - sized venules contained nearly 70% of the total luminal volume. Blood volume was least in the arterial capillaries which held less than 4% of total luminal volume.

PCV contained blood volume equivalent to 6.58% of the PDL volume while on the other extreme, the amount of blood contained in arterial capillaries was less than 0.5% of the total PDL volume as shown in Table 5.5.

Volume %	VC	AC	PCV	CV	p<0.05
Luminal	1.42±0.44	0.34±0.13	6.58±1.91	1.18±0.54	*
Abluminal	2.68±0.79	1.09±0.44	7.83±2.23	1.31±0.60	*

Table 5.5. The adjusted mean luminal and abluminal volumes ± SE (%) of the 4 distinct blood vessel types. Significant differences were observed between vascular volume and vessel type (*).

b. Regional distribution of vessel type

The venous vessels (the VC, PCV, and CV) predominated in the middle circumferential third of the PDL while the arterial capillaries were found mainly in the bone circumferential third. Fig. 5.11 and Table 5.6 show the distribution of vessel type in the tooth, middle, and bone circumferential thirds.

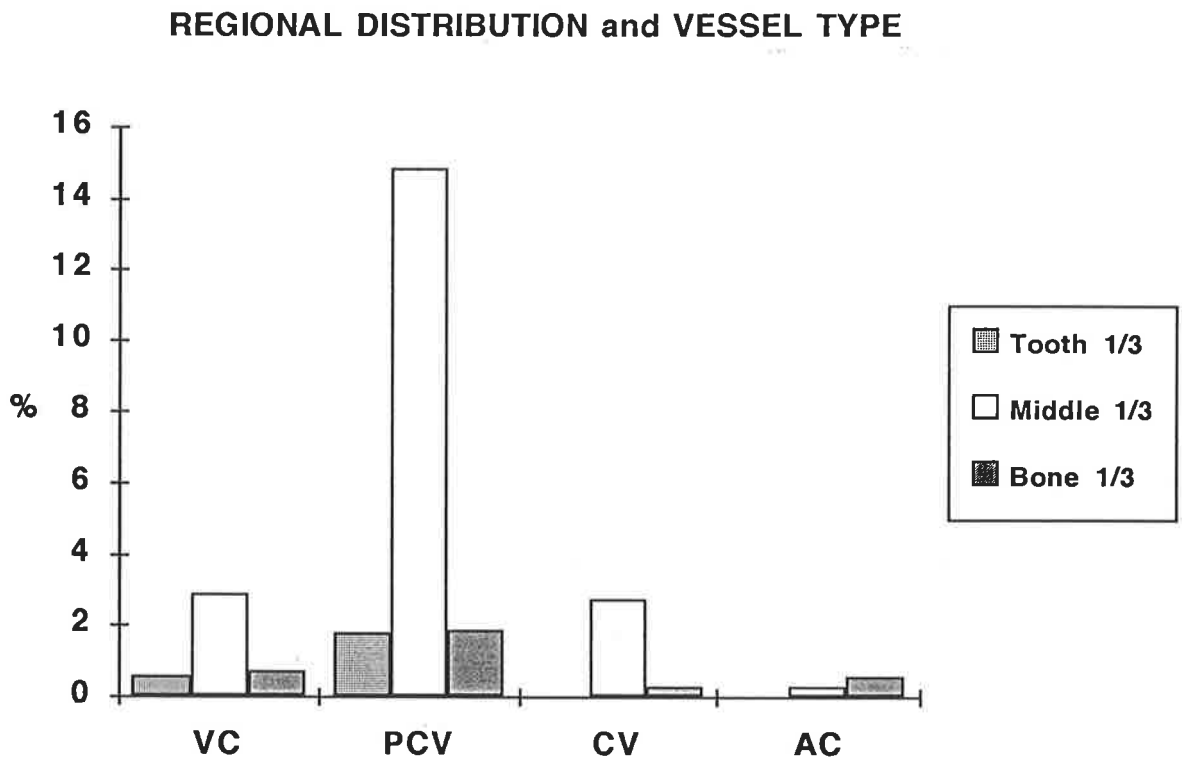

Fig. 5.11 The venous vessels were commonly found in the middle circumferential third, while the arterial capillaries were located mainly in the bone circumferential third. Both findings were statistically significant at $p<0.05$ level.

Vessel Type	Tooth 1/3	Middle 1/3	Bone 1/3	p<0.05
VC	0.59±0.39	2.9±0.85	0.73±0.43	*
PCV	1.79±1.20	14.83±3.18	1.87±1.21	*
CV	0.00	2.78±1.09	0.31±0.39	*
AC	0.00	0.29±0.17	0.57±0.24	*

Table 5.6 Regional distribution of luminal volumes ± SE (%) of the 4 vessel types. Venous vessels predominated in the middle circumferential third while arterial capillaries predominated in the bone circumferential third. Significant differences were observed between vessel type and regional variation (*).

5.3.5 Stereological Parameters of Blood Vessel Volume

a. Vascular proportion and Blood vessel type

Stereological parameters were applied to the 4 major blood vessel types as shown in Table 5.7. The total *luminal length density* was 14974.37 x 10^3 cm/cm^3. Venous capillaries occupied 71.5% while arterial capillaries made up 6.7% of the total luminal length density. Postcapillary - sized venules contributed 21.4% and collecting venules made a marginal contribution with 0.4%. The postcapillary - sized venules provided the major portion of the *luminal surface density* with 49.3%, while the collecting venules made the smallest contribution with 2.6%. Total capillary - sized vessels (VC and AC) made up 48.1% of the total luminal surface density, with venous capillaries contributing 41.8% while arterial capillaries made up the remainder with 6.3%. The total luminal surface density was 33024.55 cm^2/cm^3.

Venular - sized vessels (PCV and CV) contained four times more blood volume per unit surface area of endothelium than capillary - sized vessels (AC and VC). Similarly, venular - sized vessels contained 15.5 times more blood volume per unit length of blood vessel than capillary - sized vessels. However, capillary - sized vessels were three times as long as venular - sized vessels per unit volume of PDL tissue.

The total area of PDL tissue examined was 110,000 μm^2. The number of each blood vessel type per cm^2 of PDL tissue (N_A) was estimated by counting the total quantity of each vessel type and dividing by the number of total grid counts to give a proportional value out of 140 points or 560μm^2 (= 5.6 x 10^{-6} cm^2) of tissue (Table 5.7). The value obtained is then further divided by 5.6 x 10^{-6} to give the N_A value (per cm^2). Venous capillaries were the most common vessel type identified at 48.5% while PCV made up 39.4%. The numbers of CV and AC sampled were few, and contributed 3.1% and 9%, respectively.

	V_V (per cent)	L_V ($x10^3$ cm/cm^3)	S_V (cm^2/cm^3)	$\overline{d}$ (μm)	N_A Mean ($x10^4$ / cm^2)
Venous Capillaries	1.42±0.44 (14.9±4.6%)	10709.12 (71.5%)	13824.94 (41.8%)	4.11	2.86 (48.5%)
Arterial Capillaries	0.34±0.13 (3.6±1.3%)	1006.15 (6.7%)	2073.17 (6.3%)	6.56	0.54 (9.0%)
Postcapillary-sized Venules	6.58±1.91 (69.1±20.1%)	3212.72 (21.4%)	16297.21 (49.3%)	16.15	2.32 (39.4%)
Collecting Venules	1.18±0.54 (12.4±5.7%)	46.38 (0.4%)	829.93 (2.6%)	56.92	0.18 (3.1%)
TOTAL	**9.52±2.25**	**14974.37**	**33024.55**		

Table 5.7. The stereological values of the 4 blood vessel types. Venous capillaries had the highest length per unit volume of PDL tissue. Postcapillary - sized venules had the largest surface area per unit volume of PDL tissue.

b. Regional distribution and blood vessel type

i. Venous capillaries

The middle circumferential third contained the highest luminal volume density (V_v) at 69% while the bone and tooth circumferential thirds contributed 17% and 14%, respectively. The length and surface densities (L_v and S_v) were similarly distributed across the circumferential thirds. Table 5.8 shows the regional distribution of venous capillary stereological parameters.

ii. Postcapillary - sized venules

The middle circumferential third contains four-fifths of the luminal volume density while the bone and tooth circumferential thirds provided 10% of the total V_v each. The length and surface densities (L_v and S_v) are similarly distributed across the circumferential thirds. Table 5.9 shows the regional distribution of PCV stereological parameters.

Stereological Parameters of VENOUS CAPILLARIES:

Region	V_V (per cent)	L_V ($x10^3$ cm/cm^3)	S_V ($x10^3$ cm^2/cm^3)	N_A ($x10^5$ / cm^2)
Tooth	0.59±0.40	4461.24	5.74	5.59
	14±9.4%	14%	14%	
Middle	2.90±0.85	21928.16	28.25	17.70
	69±20.2%	69%	69%	
Bone	0.73±0.43	5519.84	7.11	6.52
	17±10%	17%	17%	

Table 5.8. Stereological parameters of luminal volume occupied by venous capillaries.

Stereological Parameters of POSTCAPILLARY - SIZED VENULES

Region	V_V (per cent)	L_V ($x10^3$ cm/cm^3)	S_V ($x10^3$ cm^2/cm^3)	N_A ($x10^5$ / cm^2)
Tooth	1.79±1.20	87413.01	4.43	3.73
	10±6.7%	10%	10%	
Middle	14.83±3.18	724209.49	36.73	16.75
	80±17.1%	80%	80%	
Bone	1.87±1.21	91319.74	4.63	3.76
	10±6.4%	10%	10%	

Table 5.9. Stereological parameters of luminal volume occupied by postcapillary - sized venules.

iii. *Collecting venules*

No collecting venules were identified in the tooth circumferential third. 90% of the luminal volume density was located in the middle circumferential third with the remaining 10% in the bone third. The length and surface densities (L_v and S_v) were similarly distributed across the circumferential thirds. Table 5.10 shows the regional distribution of collecting venule stereological parameters.

iv. *Arterial capillaries*

Unlike the venous vessels, the majority of lumen volume density was located in the bone circumferential third which contributed 66% of the total V_v. The remaining one third or 34% was located in the middle circumferential third. No AC was sampled in the tooth third. The length and surface densities (L_v and S_v) were similarly distributed across the circumferential thirds. Table 5.11 shows the regional distribution of arterial capillary stereological parameters.

From the arterial side to the venous reservoir of the microvascular bed (MVB), there was a sharp drop in the V_v, L_v, and S_v from 60% in the arterial capillaries to 10% of the PCVs and CVs in the bone circumferential third. By contrast, in the middle circumferential third, there was a progressive increase in the V_v, L_v, and S_v from 34% in the AC, rising to 69% in the VC, 80% in the PCV and topping at 90% for the CVs.

Arterial capillaries and collecting venules were not identified in the tooth third. There was a gradual reduction in the V_v, L_v, and S_v for the VC at 14% to the PCV at 10% in the tooth circumferential thirds, which was not unlike the gradual reduction in the same parameters for the VC at 17% to PCV at 10% in the bone circumferential thirds. The number of blood vessels per unit volume of PDL reflected the volumetric distribution of each vessel type across the tooth, middle and bone circumferential thirds.

Stereological Parameters of COLLECTING VENULES

Region	V_V (per cent)	L_V ($x10^3$ cm/cm^3)	S_V ($x10^3$ cm^2/cm^3)	N_A ($x10^5$ / cm^2)
Tooth	0	0	0	
	0%	0%	0%	
Middle	2.78±1.09	109.35	1.95	1.86
	90±35.2%	90%	90%	
Bone	0.31±0.37	12.19	0.22	0.93
	10±11.9%	10%	10%	

Table 5.10. Stereological parameters of luminal volume occupied by collecting venules.

Stereological Parameters of ARTERIAL CAPILLARIES

Region	V_V (per cent)	L_V ($x10^3$ cm/cm^3)	S_V ($x10^3$ cm^2/cm^3)	N_A ($x10^5$ / cm^2)
Tooth	0	0	0	
	0%	0%	0%	
Middle	0.29±0.17	858.24	1.76	2.79
	34±19.9%	34%	34%	
Bone	0.57±0.24	1686.88	3.47	3.73
	66±27.7%	66%	66%	

Table 5.11. Stereological parameters of luminal volume occupied by arterial capillaries.

5.4 BLOOD VESSEL DIAMETER AND WALL THICKNESS

5.4.1 Blood vessel diameter

The average luminal, abluminal diameters and wall thickness were estimated. An ANOVA was performed testing for the main effects of tooth, wedge, and region. Due to the small numbers of arterial capillaries and collecting venules in the sample, it was not possible to perform the ANOVA on these two vessel types. The ANOVA was only performed for the PCV and VCs No significant differences were found in luminal and abluminal diameters or wall thickness due to side of tooth, tooth and region. Table 5.12 illustrates the mean luminal and abluminal diameters and the mean wall thickness.

5.4.2 Wall thickness

In terms of wall thickness, the overall ratio of wall thickness to lumen volume was approximately 1 : 3, indicating that nearly one quarter of the space occupied by blood vessel consisted of endothelium and peri-endothelial cells (Fig. 5.12).

Arterial capillaries, due to their thick tunica intima and one or more layers of smooth muscle cells, had the thickest endothelial lining with a wall to lumen ratio of 1 : 0.43 for immersion - fixed tissues. On the other end of the spectrum, the CV showed the smallest wall to lumen ratio at 1 : 9.83. Postcapillary - sized venules had a wall to lumen ratio of 1 : 5.3, while the wall thickness of the venous capillaries was marginally smaller than the lumen at a ratio of 1 : 1.1 .

Vessel	Number	Mean Luminal diameter	1SE	Mean Abluminal diameter	1SE	Mean Wall thickness	±1SE
VC	32	4.11	0.43	6.26	0.38	2.16	0.25
PCV	24	16.15	1.06	18.00	1.12	1.85	0.20
AC	7	6.56	1.13	12.17	1.01	5.61	0.63
CV	3	56.90	12.9	58.50	13.10	1.6	0.20

Table 5.12. The mean luminal and abluminal diameters, and wall thickness (μm).

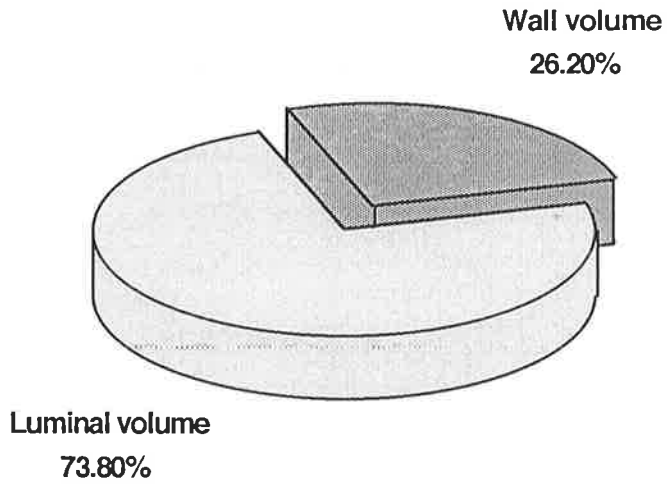

Fig. 5.12. Proportion of luminal volume and wall volume as a percentage of vascular volume.

5.5 NERVE VOLUME

The total number of points counted for axons were insufficient for statistical and stereological analyses; only morphometric nerve data are reported.

No nerves were identified within 1.0 μm of the blood vessel wall, the latter used as a criteria by Freezer (1984) for axon identification. Point counting data were however, obtained for axons beyond 1.0 μm of vessel walls. No axons were identified in two out of the eight PDL samples. Using the mathematical principle of proportion, the total axon volume worked out to be 0.52% of the PDL volume. The volume of Schwann cells and K-cells added another 0.48% to give a total nerve volume of 1.00% (Fig. 5.13). No attempt was made to add estimates of point counts for nerves to three of the PDL samples with missing root apices, as the number of nerves point counted were far too few to make any reasonable comparison.

The mean diameters of unmyelinated and myelinated axons were 0.55 μm and 3.2 μm, respectively. The majority of the axons identified were unmyelinated (85%), and the remaining 15% were myelinated axons. Adrenergic axons could not be

located. Encapsulated nerve terminals, characterised by a central core of myelinated axons and surrounded by cytoplasmic processes of Schwann cells and unmyelinated axons, were present. Complex nerve endings were also identified in close proximity to blood vessels.

The regional distribution of the axons in the human premolar PDL showed that 80% of the axons were located in the middle circumferential third, 15% in the bone circumferential third and 5% in the tooth third (Fig. 5.14). The distribution pattern of axons in the PDL from the alveolar crest to the root apex in the PDL samples with root apices showed that 70% of the axons were located in the apical third, 20% in the middle vertical third, and 10% in the coronal third (Fig. 5.15). The PDL samples without root apices were not assessed for the vertical distribution of axons.

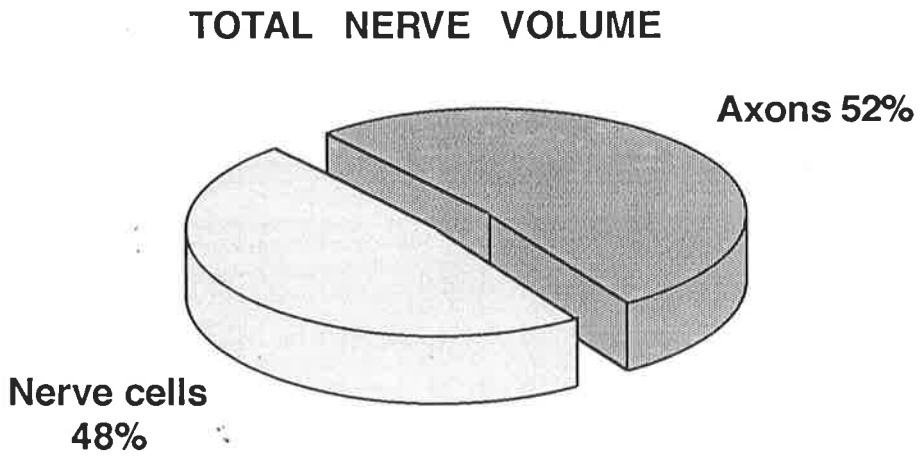

Fig. 5.13. Proportion of axons and nerve cells out of total nerve volume (%) in the PDL.

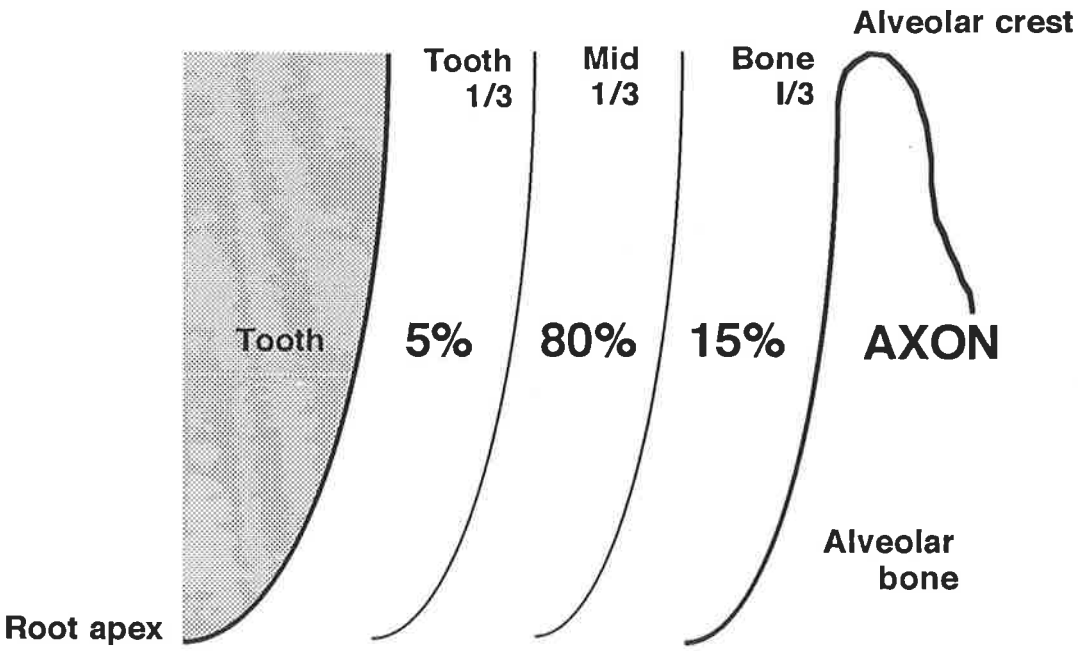

Fig. 5.14. Lateral distribution of axons showed that the middle circumferential third contained the majority of axons.

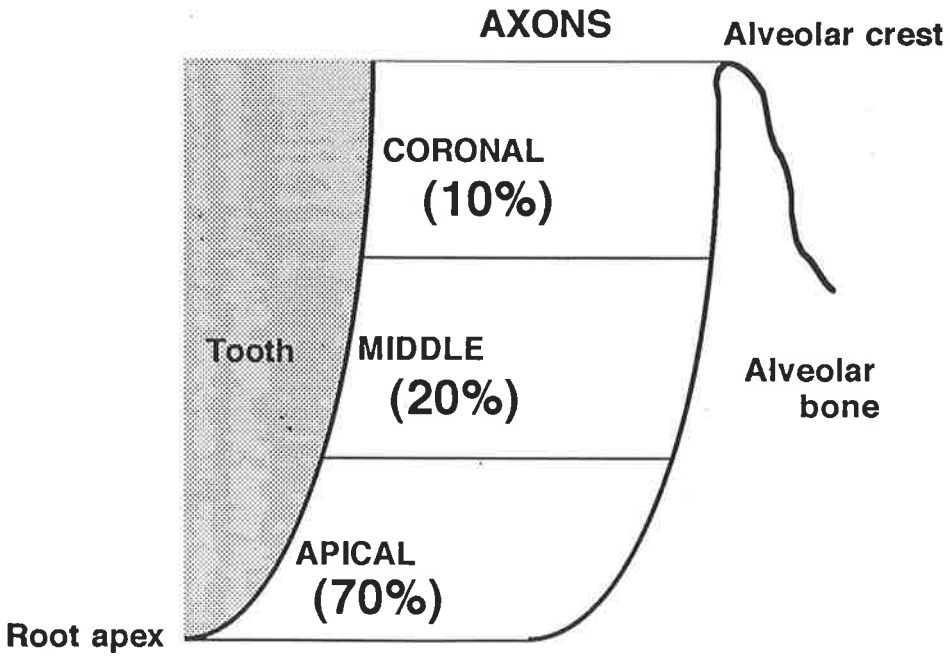

Fig. 5.15. Vertical distribution of axons showed that 70% of all axons were held in the apical third of the PDL.

5.6 WIDTH OF THE HUMAN PDL

No significant differences in mean PDL width were observed between the buccal and lingual samples of PDL ($p<0.05$). The width of the PDL was however, not uniform along the length of the ligament from the alveolar crest region to the root apex. Furthermore, the width of the ligament was observed to vary within each level. The PDL width among the eight PDL samples ranged from 16 μm to slightly under 250 μm. Table 5.13 provides mean values of the width of the PDL from the alveolar crest to the root apex.

Level	1	2	3	4	5	6	7	8	9
Mean Width (μm)	**131.3**	**97.6**	**80.4**	**61.8**	**61.8**	**82.5**	**78.4**	**108.6**	**120.1**

Table 5.13. Mean PDL width from alveolar crest to root apex.

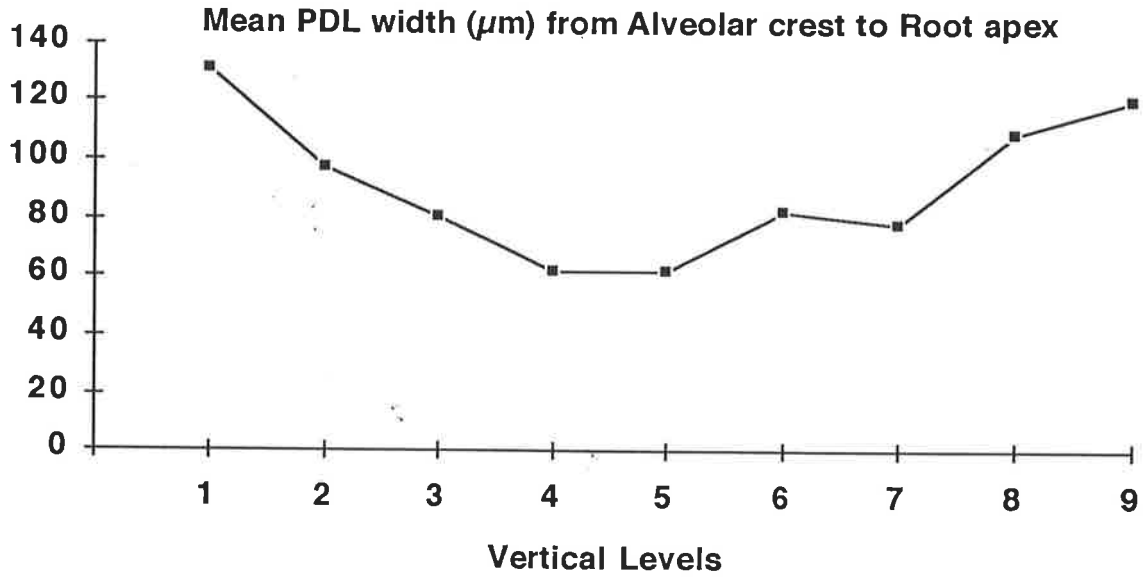

Fig 5.16. The V-shaped pattern of mean PDL width of the total PDL sample from alveolar crest to root apex.

A general pattern was observed in that the mean PDL width was widest at the cervical level, was narrowest at the midroot level, and widened again at the apical level. Figure 5.16 confirms the narrowing of the PDL at the middle vertical third.

5.7 PRODUCTS OF T.E.M. PREPARATION

Processing artefacts were observed within the human PDL specimen. Post mortem changes in the cells before fixation occured resulted in swelling of cells and organelles. The cytoplasm of many fibroblasts appeared patchy and contained vacuoles. Furthermore, shrinkage occured and this was evidenced by the scalloping of the nuclear membrane. The cell membranes might have also been damaged. It was not uncommon to find cellular refuse in the intercellular spaces: bits of cytoplasm and/or a bunch of membranous material. Oftentimes, whorls of myelin-like membranes were observed within myelinated nerves or in the endothelial lining of blood vessels. The amount of compression of the ultrathin sections after each cutting cycle was reduced by chloroform vapour. This procedure, however, did not remove all the compression and some rounded objects appeared flattened. Stain precipitates of lead carbonate formed by secondary staining with lead citrate were seen as black homogenous rectangular crystals on the photomicrograph. These crystals obscured important structures on the PDL, and when they covered part of the blood vessels or nerves, the sampling of the PDL would be moved to another part of the PDL where no artefacts interfered with the line of sampling.

CHAPTER 6 DISCUSSION

6.1 NATURE OF EXPERIMENTAL TISSUE

6.1.1 Surgical Preparation

The mandibular premolars were received with their PDL attached and surrounded by the alveolar bone. Any occlusal load applied in the form of mouth jacks to stabilise the mandible during the surgery would have caused displacement of blood from the compression side of the premolar PDL. Furthermore, any surgical manipulation near the PDL would have caused a transient vasodilation as well as vasoconstriction of other PDL microvessels.

The scarring which resulted from the extensive facial and cervical burns at 4 years of age produced a progressive open bite malocclusion and altered the facial form severely. The open-bite was so extensive that normal mastictory occlusal load would not have been possible on the mandibular premolars. The question would be, how did the subject obtain his nutritional requirements ? Pureed food, rather than solid food could have been taken through a straw or been simply swallowed. Furthermore, the experimental premolars would have been out of occlusion since eruption and were, therefore, considered to be non-functional teeth. Accordingly, they would also have undergone some degree of supra-eruption until resisted by the passive posture of the tongue.

6.2 THE T.E.M. METHOD

In its entirety, this human specimen presented a rare opportunity for a stereological study of the human PDL. However, conditions inherent in its preparation presented a non-ideal situation, and warranted a careful interpretation of the investigation results.

6.2.1. Fixative

Following surgical resection, the mandibular segments containing the premolars were immersion-fixed in gluteraldehyde. The experiment used a 2.5% cacodylate buffered solution of gluteraldehyde as a fixative. The tissues were post-fixed with osmium tetroxide. The components of the PDL which contained most lipids were the cellular membrane and the myelin sheath of nerves. Stein and Stein (1971) reported as much as 95% of the lipids in cellular tissues can be extracted by gluteraldehyde fixation unless processed with a second fixative like osmium tetroxide. Fortunately, the double fixation of the human specimen preserved most of these structures, thereby confirming the observations of Trump and Bulger (1966) that combination fixatives of gluteraldehyde and osmium tetroxide reduced the number of artefacts arising from lipid extraction and cellular shrinkage. Any distortion of cellular structures during this preparatory phase might have affected the accuracy of the volumetric data. However, if all the premolar teeth were prepared in exactly the same way and under the same conditions, any inherent distortion should not have altered the overall result significantly because the distortions would not be local but generalised.

6.2.2. Fixation method

Tissues fixed by the immersion fixation method showed closed blood vessel lumina. Hayat (1970) suggested that the presence of closed lumina was an artefact because of the slow penetration of osmium tetroxide into the deeper layers of the tissue. This viewpoint may not necessarily be true. The human PDL did, however show a number of collapsed blood vessels. It is known that not all blood vessels are patent at any one time in the microvascular bed. Depending on the functional requirements of the surrounding tissues, a selective and differential patency exists in all blood vessels. Arterial capillaries, with at least a layer of paravascular smooth muscles might constrict under neuro-humoral control. With the lumen of the arterial capillaries narrowed, the receiving venous capillaries, postcapillary - sized venules and collecting venules might have partially collapsed due to a lack of blood

flow. Accordingly, a non-functioning PDL (in this human specimen) was more likely to show more closed blood vessel lumina than in a functional ligament.

It was also possible that surgical resection performed near the site of the premolar PDL might have caused some vessels to reduce or increase their luminal size in response to bleeding and the loss of neuro-vascular tone, or to acute inflammation, respectively. This phenomenon was most visible in the right first premolar where the surgeons' bone cutter sectioned diagonally through the root. Having a portion of the blood vessels closed and others opened may not give an accurate representation of the vascular volume. Vascular perfusion under pressure with a fixative is considered to be the most ideal way of maintaining the patency of vessel lumen. However, perfusing a live human being is out of the question.

To overcome the limitations of immersion fixation, each of the two human mandible blocks, consisting of the premolars and their alveolar bone, was first reduced in size and immersion fixed with the primary fixative gluteraldehyde. Subsequently, smaller pieces representing the distal segment of the premolars were cut and secondarily fixed with osmium tetroxide. This procedure had the advantage of stabilising the tissue and giving it added mechanical strength to withstand shearing forces that might have damaged the PDL. The total volume of both blocks was approximately 10.0 cm^3 which was one-fifth the volume of fixative used. This ratio of fixative volume to tissue volume differed substantially from the 9 : 1 ratio recommended by Glauert (1978) , yet the tissues showed features of good fixation when viewed under the TEM.

6.2.3. Staining

Reynolds' lead citrate was used as a second stain in this experiment. Citrate, a chelating agent, was added in excess quantity to sequester all of the lead present. Therefore, lead was prevented from combining with carbonate, and resulted in an appreciable reduction in the formation of contaminants. In spite of the longer duration of staining with lead citrate, it was noted that there was no increase in the

amount of lead carbonate precipitate. This could be attributed to the three-fold increase in the number of sodium hydroxide pellets used, and to washing the grids vigorously in millipored filtered double-distilled water. The latter action was known to shake off any lead carbonate precipitates attached to the section.

6.2.4 Stereological Sampling

A blood vessel or a nerve is not a straight tube of constant diameter coursing through the ligament, but a winding tube of variable diameter (Fig. 6.1). The stereological principle of geometric probability proposes that, with random selection of blood vessel profiles for sampling, we can postulate that the cross-section area of a blood vessel profile is representative of the same blood vessel type in other sections. The random surveying of the trapezoidal sections assumes a blood vessel profile observed at one level has as much a probability of being included for counting, or excluded at subsequent levels, thereby minimising bias in determining blood volume. Similarly, taking the smallest vessel diameter would minimise this effect.

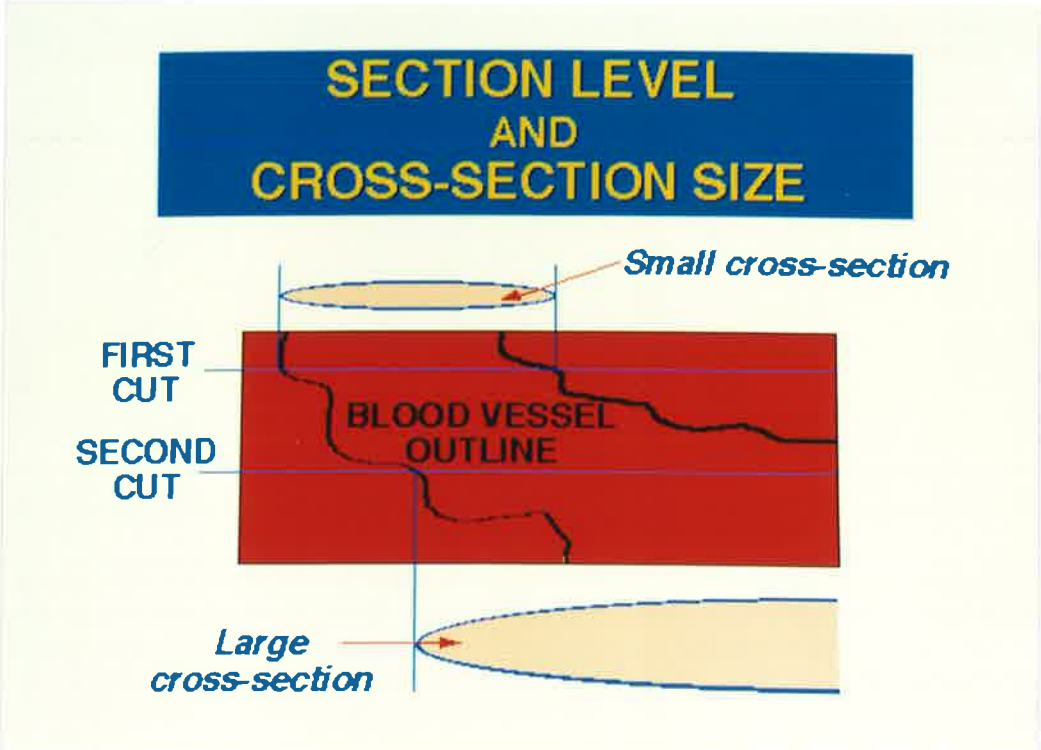

Fig. 6.1 Schematic drawing of a blood vessel coursing through the ligament space, and indicating variability in vessel cross-section area at different depths of sectioning.

6.2.5 Section thickness

The thickness of the sections influenced the visibility of important structures when viewed under the TEM. Some of the sections of a thickness corresponding to the silver-gold interference range (60 -80 nm) were very fragile under the electron beam. Even with the added caution of prior conditioning under the electron beam before viewing, tearing of the sections was frequently observed along the length of the PDL. Affected sections were discarded, and additional sections cut. Structures present at a higher level may not be visible at a lower level due to the tortous pathway of these structures as they course through the ligament space. Sampling performed on these sections would invariably produce an inaccurate picture of, for example, the volume of a certain blood vessel type. This feature was most visible in the LPM1 buccal PDL samples where the points counted for the overall vascular volume were approximately half those of other PDL samples.

6.3 POINT COUNTING OF BLOOD VESSELS AND NERVES

6.3.1 Blood Vessels

a. Arterial vessels

The arterial and venous components of the microcirculation were identified according to the classification provided by Rhodin (1967, 1968). According to Rhodin (1967), the criteria for determining a blood vessel as an arterial capillary are a luminal diameter of 7-15μm, and one or two layers of smooth muscle. Rhodin (1967) called this vessel type a "precapillary sphincter". The term "arterial capillary" included any metarteriole or precapillary sphincters, while the term "terminal arteriole" was a separate entity in itself in that this vessel type consisted of a larger luminal diameter from 16 μm to 49 μm with more than two layers of smooth muscle in its tunica intima. All the arterial capillaries found in the experimental human PDL comprised a layer of endothelial cells surrounded by one or two perivascular layers of smooth muscle, and a few smooth muscle cells. The nuclei of the

endothelial cells exhibited characteristic bulges into the lumen, thereby reducing the luminal cross-sectional area.

All the arterial volume in the human premolar PDL was provided by vessels corresponding to arterial capillaries or precapillary sphincters as defined by Rhodin (1967). This was not surprising as the human PDL consisted of a fine MVB sandwiched between two hard tissues (alveolar bone and dentine). Stanley (1993), using vascular castings of the marmoset PDL, found terminal arterioles only in the PDL region beneath the root apex. He showed that the arterioles gave off capillary branches which coursed occlusally through the PDL. As the distance of the cells was not far from the blood vessels, diffusion of substrates and fluids could easily occur between blood vessels and perivascular spaces for the maintenance of homeostasis and metabolic exchange. In terms of morphology and function, arterial capillaries with only one or two layers of smooth muscle would be more adept at capillary exchange than terminal arterioles which have thicker smooth muscle layers.

The absence of terminal arterioles in the sample did not mean that terminal arterioles did not exist in the human PDL. The sampling circumstance in the present study provided another reason to explain the absence of terminal arterioles throughout the length of the PDL. The wedge - shaped PDL tissues used for sampling might have been derived from a part of the PDL which was located in between the openings of transalveolar channels where the arterial component of the PDL supply came through. Therefore, the sampling of such a tissue would not have identified any terminal arterioles.

The percentage of the arterial capillary luminal volume amounted to approximately 3.6% of the total vascular volume or 0.34% of the total ligament volume. This value was considerably lower than the values provided by Parlange and Sims (1993) who reported that the arterial component (arterial capillary and terminal arterioles) of perfused marmoset PDL, following extrusion, was 23% of the

total vascular volume. Arterial volume from alveolar crest to root apex in the perfused mouse molar PDL was 12% (Freezer and Sims, 1987) which was also higher than the 3.6% reported presently. The small human PDL arterial component could be a reflection of the sampling circumstance, as described above, which resulted in the absence of terminal arterioles, and the small number of AC identified (n = 7). The present estimate for the arterial volume was, therefore, probably an underestimate. If the PDL tissues were perfused, were derived from functional teeth, and if more sections were sampled so that terminal arterioles were identified, the arterial component might increase substantially.

b. Venous vessels

Rhodin (1968) defined VCs as vessels with a luminal diameter of up to 8 μm. The present study redefined the luminal diameter of venous capillaries as up to 10μm. Blood vessels were unlike a water pipe with a fixed diameter throughout the entire length, but had a variable diameter. What might be defined as a venous capillary at one level might change its morphology and be classified as a postcapillary - sized venule at another level, and vice versa, although both measurements were taken of the same vessel. Therefore, it all balances out in a statistical sense.

Most of the blood volume in the PDL was contained within postcapillary - sized venules which had a luminal diameter ranging from 10 μm to 30 μm. This finding could be reflective of the quiescent nature of the PDL where the microcirculation was primarily "output". While the arterial component accounted for only 3.6% of the total vascular volume, and the venous component the remaining 96.4%, the amount of blood inflow would match the volume of blood outflow. This balance could only be explained by a much faster rate of blood flowing in from the arterial side, while the venous side appeared to exhibit the "pooling" of blood.

Freezer (1984) studied the mouse molar ligament, and defined pericytic venous vessels as vessels having a complete investment layer of pericytes and their processes while apericytic venous vessels had a partial covering or an absence of pericytic cell nuclei and processes. By contrast, none of the human PDL venous vessels observed had a complete pericytic covering. A venous vessel was termed "pericytic" when the nucleus and/or pericytic processes of a pericyte abutted the endothelial lining. The pericytic appendages were, however, enclosed by a basal lamina. Perivascular fibroblasts (veil cells) were distinguished from pericytes, which also approximated the endothelial lining, by the absence of a basement membrane. A non-pericytic venous vessel was one that did not show any pericytic processes along the periphery of the vessel wall. This classification was, however, a morphological means of distinguishing blood vessel profile types. What might appear to be an apericytic vessel at one particular level might form a pericytic vessel at another level, and vice versa. Furthermore, the plane at which the tissue block was sectioned might also determine whether one was observing a pericytic or apericytic state. Hence, if Freezer's (1984) definition of what constituted a pericytic venous vessel was adopted for the human specimen, all the venous vessel in the human PDL would be apericytic. This difference suggested a morphological and possibly a functional variability in blood vessels between mouse and human PDL, and warranted a separate vascular classification for the human PDL.

A blood vessel with pericytic cytoplasm covering only 1% of the vessel perimeter, and another blood vessel with the pericytic process covering 50% of the vessel perimeter are both anatomically pericytic blood vessels. However, the functional potential of the two vessels may be quite different as pericytes are known to have contractile properties regulating blood flow (Rhodin, 1968).

Collecting venules, with luminal diameter from 30 μm to 50 μm as an identification landmark, were found only in the apical sections of the LPM 1 lingual PDL sample. The number of collecting venules sampled (n = 3) was very small. For

the data to have any stereological significance, the number must be higher, and the minimal point count should be 100 (Gundersen et al., 1988a).

c. Initial Lymphatics

Presumptive lymphatic capillaries were rare and identified in only three out of the eight PDL samples. These extremely thin-walled (<0.3 μm) capillaries were located in the bone circumferential third of the apical level (level 9) of the PDL. This finding corroborated that of Crowe (1989) who showed the presence of presumptive lymphatic capillaries in the bone circumferential third of the apical PDL. However, a higher magnification in the order of x50,000 is needed to help identify accurately the nature of this vessel type. Further analysis of the PDL past the root apex may reveal a larger number of this vessel type.

The tissue channels (TC) of the PDL (Cooper et al., 1990; Tang and Sims, 1992), which form an extensive extravascular circulation, may serve to return interstitial fluid to the blood vessels instead of a lymphatic system, as suggested by Casley-Smith et al. (1975) for tissue channels found in other connective tissues. This explanation could account for a lack of definitive morphological evidence for the presence of lymphatic capillaries in the human PDL.

6.3.2 Nerves

From the morphometric data on nerves, the mean overall (axons and nerve cells) volumetric estimation of human PDL nerves was 1.00% of the total PDL volume. Nerve cells included Schwann cells and capsular fibroblasts. The mean axon volume (unmyelinated and myelinated nerves axons) was 0.52%, and this finding compared favourably with the reported mean axon volume of 0.50% in the mouse molar PDL by Freezer and Sims (1987) and also with the mean axon volume reported by Parlange and Sims (1993) in marmoset incisor PDL of 0.43%. A small volume of nerves however, did not imply a lack of physiological importance.

The diameters of myelinated and unmyelinated nerves were in close agreement with those reported by Griffin and Harris (1968) and Griffin (1972) for human PDL. The present findings of a mean diameter for unmyelinated axons of 0.55 μm and that for myelinated axons of 3.2 μm were comparable with those reported for the marmoset incisor PDL of 0.67 μm and 2.94 μm, respectively by Parlange and Sims (1993). While the myelinated axons of the human premolar PDL have a similar mean diameter to the myelinated axons of mouse molar PDL (3.3 μm), the mean diameter of unmyelinated axons in the mouse molar PDL was higher at 1.7 μm, though there was considerable variation in the mean axon diameters from 0.2 μm to 2.5 μm in the mouse PDL. The similarity in axon diameters between marmoset and human PDL could be attributed to the fact that the specimens used were single-rooted teeth, ie. incisors and mandibular premolars. Notwithstanding the similarity in myelinated axon diameters between mouse and human PDL, the difference in mean unmyelinated axon diameters could be attributed to differences in non-functional condition of the specimen teeth, and possibly to species differences.

The end ring or encapsulated nerve terminals, as described by Griffin (1972) were present. Complex nerve endings, arranged in a whorl-like pattern, were observed near blood vessels, and these neuro-vascular complexes might be part of a periodontal pressure/mechanoreceptor system. Lamellated corpuscles and bulbous-shaped mitochondria rich nerve terminals in the mouse molar PDL, reported by Freezer and Sims (1989) to be in abundance, were not identified in the human sample. Two out of the eight tooth segments did not have any point counts for nerves. This data void, however, did not imply that there was an absence of nerves. Nerves might be present at a level that was either above or below or to one side of the plane of sectioning. Adrenergic nerve fibres could not be identified. Nerve endings without the Schwann cell encasement were also difficult to identify. The paucity of nerve terminals in the present study could be attributed to sampling circumstance and to the fact that the tissues were immersion-fixed and, therefore, such endings might have undergone autolysis.

Nerve endings within 1.0 μm of vessel walls could not be located in the present sample. This finding contrasted with the report by Sims (1984b) who illustrated the presence of unmyelinated axons within 1.0 μm of vascular endothelium in the human PDL. This discrepancy arose due to the sampling circumstance. If more sections were sampled, the possibility of identifying more blood vessels and axons would be greater. Similarly, nerves within vessel walls could not be identified. Parlange (1991) and Chintavalakorn (1994) were also unable to locate nerve terminals within the vessel walls in marmoset PDL. Therefore, the criteria used by Freezer (1984) to describe the location of nerves for mice should be reassessed for human teeth using a coefficient of variation cut off of 5% to have an accurate assessment of human / marmoset PDL neural volume.

While the number of axons identified in the human sample were far too few for statistical analyses to compare vertical and horizontal third distribution, the point counting data on nerves showed that 85% of the total point counts were from unmyelinated axons while the remaining 15% were attributed to myelinated nerves. This relative distribution contrasted with the 95% of unmyelinated nerves and 5% of myelinated nerves reported by Freezer and Sims (1989). However, the present findings were comparable with the 89% and 11% distribution for unmyelinated and myelinated axons, respectively, in the marmoset PDL (Parlange and Sims, 1993), suggesting a similarity between man and the marmoset PDL model.

The lateral distribution of nerves showed that the majority of axons were located in the middle circumferential third of the human PDL. This finding corroborated the findings of Chintavalakorn (1994) and Parlange and Sims (1993) who showed that the majority of the nerve volume in the marmoset incisor PDL was located in the same region. By contrast, Freezer and Sims (1989) showed that 61% of the axon V_v density was located within the bone circumferential third. The present findings and those of Chintavalakorn (1994) and Parlange and Sims (1993) showed that both the vascular and neural volume were highest in the middle circumferential thirds while the studies of Freezer and Sims (1987, 1989) showed that the bone

circumferential third contained most of the nerve and vascular volumes. The difference in neurovascular distribution between human / marmoset and mouse PDL posed the suggestion of either a species or functional differential.

The significance of neurovascular association is further highlighted by the present findings. The regulation of blood vessel volume and blood flow through nervous control was reported by Rhodin (1968) who attributed the regulation of blood-fluid elements through vessel endothelium to pericytes. Similarly, Edwall and Kindlova (1971) showed that sympathetic nerve stimulation induced a reduction of 90% in the washout of periodontal tracer. However, Freezer and Sims (1988) argued that their findings represented changes in vessel permeability rather than through a reduction in lumen volume.

The vertical distribution of axons in the human premolar PDL showed that the apical innervation was approximately three times that of the middle vertical third. This pattern corroborated the findings of Freezer and Sims (1987) for the mouse molar PDL, and that of Parlange and Sims (1993) for the marmoset incisor PDL. However, the vertical distribution pattern of axons in the human PDL has to be viewed in the light of the small number of axons point counted.

The predominant distribution of PCVs in the middle circumferential third of the human PDL might be explained by the vascular concepts of Intaglietta and de Plombe (1973) who had defined microvessels as tube, or tunnel capillaries on the basis of the mechanisms controlling vessel permeability. Tube capillaries are vessels where the endothelium regulates the vessel permeability, whereas the permeability coefficient of tunnel capillaries is regulated by the hydrostatic pressure of the surrounding ground substance. Freezer and Sims (1988) have shown significant correlations between K-cells and both unmyelinated and myelinated axons which may indicate a biological association between K-cells and PDL innervation. Furthermore, statistically significant correlations have been shown between K-cells and apericytic PCV (Freezer and Sims, 1988). As the majority of PCV in the present

sample were apericytic according to Freezer's (1984) definition, then a biologically significant relationship between axons, K-cells and apericytic PCV could exist and might represent a periodontal regulator of vascular volume. If indeed that nervous control regulated vascular volume through changes in plasma membrane surface charges altering endothelial permeability, then the majority of PCV in the human PDL could be tube capillaries. This inference found support from the study of rat PDL by Tang and Sims (1992) who showed that the mean number of endothelial tissue channels increased markedly with orthodontic tension loading.

In summary, the morphometric data on human PDL nerves appeared to be similar to nerve data on marmoset PDL in terms of axon diameters, distribution by axon type, distribution by circumferential thirds, and distribution by neurovascular association. The common ground between the two suggests that the marmoset model may be the most reliable analogue for the study of neural morphology and function of the human PDL.

6.4 VASCULAR VOLUME

6.4.1 Analysis of vascular volume

The mean overall luminal volume of human mandibular premolar PDL of 8.97% , and the adjusted mean luminal volume at 9.52% were not significantly different ($p<0.05$). However, looking at the PDL samples individually, LPM1 buccal PDL sample contained the lowest blood volume at 4.9%. This reduction in vascularity could have resulted from a widespread collapse of blood vessels arising from surgical manipulation. With a low blood volume, it was suggested that the behavioural characteristics of this PDL sample was different from the other PDL samples, when subjected to any occlusal loading.

When wall thickness was taken into account, it added another 3.39% to the mean luminal volumes, which was 26.2% of the total vascular volume. This finding compared favourably with the 3.59% of vessel wall volume reported by Parlange and Sims (1993) or an equivalent of 24.1% of the marmoset total incisor luminal volume. Freezer and Sims (1987) did not report the abluminal volume, and a comparison with the mouse molar PDL cannot be made.

Histological estimation of blood vessel volume by Sims (1980) on human mandibular premolars approximated a mean of 11%, with regional estimates reaching 20% (Table 6.1). The 11% mean vascular volume reported by Sims (1980) was derived from immersion - fixed human PDL. In addition, the vascular volume estimate included the vessel wall volume. Granted that immersion-fixed tissues underwent shrinkage with processing, and assuming that the endothelial volume was removed from the 11% mean vascular volume, the projected luminal volume would then be ≈ 8%. This projected finding compared favourably with the overall mean luminal volume of 9.0% found in the present investigation of human premolar PDL. By contrast, the present investigation seriously questioned the volumetric estimations of human premolar vascular volume of 1.63% to 3.50% reported by Götze (1976, 1980). His histological estimation presumably included the vessel wall, and if the luminal volume was to be estimated from his data, the estimates would certainly be much lower. Therefore, in reviewing the studies of Götze (1976, 1980), the present investigation demonstrated that the vascular volume estimated from the stereological TEM technique was a more accurate method of estimating blood vessel volume than histology.

The mouse molar mesial PDL showed a mean vascular volume of ≈ 7.5% (Freezer and Sims, 1987) from alveolar crest to root apex. With the inclusion of blood volume beyond the root apex, Sims et al. (1994) showed that an additional 1.0% of blood volume resided in the PDL past the root apex to give a mean vascular volume of 8.5%. This finding was similar to the 8.4% estimated from histological sections by Douvartzidis (1984) on marmoset second molar PDL. Weir (1990) estimated the

STUDY	TOOTH (PDL SITE)	BV VOLUME	METHOD
HUMAN		Mean	
FOONG (1993)	Mandibular Premolars	8.97% - 9.52%	TEM Stereology
SIMS (1980)	Mandibular Premolars	11.00%	Histology
GÖTZE (1976, 1980)	Mandibular Premolars	1.63% - 3.50%	Histology
MONKEY			
WEIR (1990)	Maxillary Incisor (apical)	10.80%	TEM Stereology
PARLANGE & SIMS (1993)	Maxillary Incisor (mesial)	11.26%	TEM Stereology
MOUSE			
FREEZER & SIMS (1987)	Mandibular first molar (mesial)	7.50%	TEM Stereology
SIMS et al. (1994)	Mandibular first molar	8.50%	TEM Stereology

Table 6.1. ANIMAL and HUMAN PDL luminal vascular volume compared against methodology.

mean luminal volume of marmoset incisor subapical PDL at 10.80%. Parlange and Sims (1993) and Chintavalakorn (1994) determined the mean luminal volume of non-subapical PDL to be 11.26% and 10.79%, respectively. The differences observed in the above vascular volumes reported for the marmoset PDL can be ascribed to differences in methodology, site and tooth type. The mean 8.97% to 9.52% range of vascular volume obtained from the human premolar non-subapical PDL was lower but comparable with the findings of Weir (1991), Parlange and Sims (1993) and Chintavalakorn (1994). However, the difference in mean luminal volume between human mandibular premolar PDL and the mean luminal volume for marmoset incisor PDL was attributed to method of fixation, functional status of the teeth prior to experimentation, site of PDL examined and tooth type. The marmoset incisor PDL was perfusion-fixed which revealed the full cohort of the PDL microvessels. Immersion-fixed tissues, as mentioned previously, would have resulted in shrinkage and collapse of some blood vessels and, therefore, a lower V_v was observed for the human premolar PDL.

Furthermore, a non-functioning tooth would result in atrophy of the PDL (Klein, 1928) and a reduction in the number of ligament microvessels. Because the need to subserve the demands of rapid cellular turnover in a functioning PDL was diminished, vascular atrophy would lead to an overall reduction in blood volume. Therefore, had the human PDL tissues been fixed by perfusion and the premolars subjected to normal masticatory function prior to surgery, the mean luminal vascular volume of human mandibular premolar PDL might well have approximated that reported for the the marmoset incisor PDL.

Although the alternative studies have the element of animal variation to consider, the present investigation lacks this element. All the four mandibular premolar teeth were taken from a young male, where inter-tooth variation would be a consideration. The variation in vascular volumes could be attributed to the 4 premolar teeth and/or within each premolar PDL. The effect of side of mouth (L v R), tooth type (first v second premolars) and the PDL side (buccal v lingual) on the

vascular volumes might be important considerations. Statistical analyses of the sample available suggested that the differences in vessel volumes between first and second premolars, and between left and right premolars were not strongly significant ($p<0.05$). This was not an unexpected finding in view of the random sampling technique and that the four mandibular premolars had been out of occlusal function for a long time. Lack of occlusal stimulation might have resulted in anatomical and physiological uniformity in the PDL among the four premolars. However, facial and skeletal asymmetry did exist in the subject. The scarring was more severe on the left side. Any differences in the PDL would more likely be found in the left premolars. In fact, as mentioned earlier, the buccal PDL of LPM1 segment contained the lowest vascular volume, and this might be attributed to the existing asymmetry, in addition to the surgical and laboratory manipulation.

6.4.2 Regional Distribution of Volume and Vessel Type

The present study showed that the majority of blood volume was located in the middle circumferential third of the PDL. This conclusion was similar to the observations of Parlange and Sims (1993) in the marmoset incisor PDL where the blood volume was greatest in the middle circumferential third and occupied 8.8% of the total PDL volume or 78% of the total vascular volume. The present finding however, contrasted sharply with the results obtained for the mouse molar PDL by Freezer and Sims (1987) who reported that the majority of the blood volume was located in the bone circumferential third which occupied 68% of the total vascular volume. The findings of Freezer and Sims (1987) were consistent with those of Douvartzidis (1984) who also reported that most blood was located in the bone circumferential third in marmoset second molar PDL.

The middle circumferential third contained the majority of the blood volume, mostly in venous vessels. Postcapillary - sized venules were the most abundant vessel type in each of the three circumferential thirds in the human premolar PDL. By contrast, arterial capillaries were found mainly in the bone third. It was

postulated that the majority of the arterial blood input would have come from the alveolar bone. This was believed to account for a higher volume of arterial capillaries in the bone circumferential third. The findings of Birn (1966) lend support to the above postulate by his assumption that blood vessels entered the PDL through alveolar bone perforations. However, a note of caution is needed here in that the number of arterial capillaries sampled (n = 7) may be far too few to support the above hypothesis.

The arterial capillaries in the bone circumferential thirds changed to venous vessels in the middle circumferential thirds, which supported the finding that the majority of venous blood vessels were located in the middle circumferential PDL. These microvessels subserved the function of capillary exchange and also served to direct the blood flow apically. If these vessels were to function as tube or tunnel capillaries (Intaglietta and de Plombe, 1973) in the ligament, the mechanisms regulating vascular permeability in response to functional loading, may be of great significance.

The distribution of blood in the middle circumferential thirds of the human and marmoset PDL was strikingly similar at 78% of the total luminal volume. In the human mandibular premolar PDL, this was calculated to be 6 times more vascular than the bone circumferential third, and 9 times more vascular than the tooth circumferential third. With no blood vessels identified in the tooth circumferential third of the marmoset incisor PDL, Parlange and Sims (1993) showed that the middle third contained 3.5 times more blood than the bone circumferential third. By contrast, Freezer and Sims (1987) showed that the bone third was 13.4 times more vascular than the tooth third and 2.4 times more vascular than the middle circumferential third.

Concepts of functional compartments within the PDL and interstitial pressure gradients (Edwall, 1982) are relevant to orthodontic treatment, because changes in electrolyte balance and chemistry of the periodontal ground substance are known to

accompany changes in tooth movement (Tyler and Burn-Mordoch, 1976). With the greatest number of blood vessels identified in the middle circumferential third, it was assumed that the physiological exchange in this region to be the most efficient. On this basis, the greatest number of synthetic cells per unit volume of PDL tissue would reside in the middle circumferential third. This projected pattern of cellular distribution would create a differential in the concentration of periodontal ground substance between the three circumferential thirds, and subsequently alter the interstitial pressure gradient regulating vessel permeability. As mentioned earlier, the greatest number of axons were located in the middle third. Therefore, in the presence of an extravascular tissue pressure gradient, and the effect of nerve stimulation on the biochemistry of the perivascular ground substance or on vessel permeability, the present findings in non-functional teeth appeared to be viable for extrapolation to functional teeth when investigating functional tooth support and changes in tooth movement.

6.4.3 Vertical Distribution

Garfunkel and Sciaky (1971) showed vascular volume changes down the length in the rat molar PDL. Similarly, Götze (1976) reported a progressive increase in vascular volume from the cervical third to the apical third on the buccal and lingual sides of the human mandibular premolar PDL. This observation agrees with the present findings.

Sims (1987) found the effect of depth on vascular volumes to be quadratic in nature with the larger volumes at the cervical and apical regions. Parlange and Sims (1993) reported that the cervical third contained most of the blood volume at ≈ 45.5%, while blood volume was evenly distributed in the middle and apical thirds at 27.2% and 27.3%, respectively. The findings of Parlange and Sims (1993) corresponded with those observed in the mouse molar PDL (Sims, 1987). By contrast, the present study showed that more than 50% of the vascular volume resided in the apical third of the PDL while 31% of the blood volume was contained in the middle vertical third.

The least vascular portion of the PDL was in the cervical third, contributing less than 19% of the total blood volume. The vertical vascular proportions suggested that the apical third was roughly 1.6 times more vascular than the middle third, while the middle third was also 1.6 times more vascular than the cervical third. The present findings in man did not substantiate the claim of Sims (1987) that the effect of depth on vascular volume was quadratic. Rather, the vascular volume increased linearly with increasing depth. This finding however, had to be examined in the light of the differences in the available data, in that the human premolars used were non-functional.

The progressive increase in blood volume towards the apical third of the root suggested a flow of blood in the occluso-apical direction, resulting in a reservoir of blood in the apical third of the root. Certainly, this feature has contributed to the concept that the PDL acts as a cushion or dampener to axial loading on the tooth. Blood volume and interstitial fluid provide a fluid system that helps to maintain the integrity of the PDL during masticatory loading. Lew (1986), Cooper et al. (1990) and Tang and Sims (1992) have shown the presence of fenestrated capillaries in the apical third of the rat maxillary molar. The presence of fenestrations facilitates the rapid trans-endothelial transport of fluids into and out of the vascular system in response to occlusal load.

6.4.4 Vascular Proportion

Four morphologically distinct vessel types were identified within the human premolar PDL which contrasted to the 6 types of vessels identified in the marmoset incisor PDL reported by Parlange and Sims (1993). Not identified were the terminal arterioles and the arteriovenous anastomoses. Venous vessels (VC, PCV and CV) accounted for 96.4% of the blood volume while the arterial component carried 3.6%. This finding established that at any one time, there would be 26 times more blood on the venous side than on the arterial side. As mentioned before, the arterial component is believed to be responsible for pumping up the venous reservoir. The

venous vessels observed in the human PDL were thin-walled vessels which subserved functions such as metabolic exchange and cellular diapedesis. For the arterial vessels to pump up the venous reservoir, the relative rate of blood flowing through the arterial capillaries would therefore need to be 26 times greater than the outflow of blood from the venous vessels. Back pressure on the venous end would also help to maintain the arterial-venous differential.

The stereological findings on mouse molar mesial PDL (Freezer and Sims, 1987) showed that venular - sized vessels had a luminal surface density of 40% and contained 88% of the blood volume. On the other hand, capillary - sized vessels had a higher luminal surface density of 60% and contained only 12% of the blood volume. These data showed that in the mouse molar PDL, the venular - sized vessels carried 11 times more blood per unit area of endothelium than the capillary - sized vessels. By contrast, Parlange and Sims (1993) showed that venular - sized vessels contained 5 times more blood per unit area of endothelium than the capillary - sized vessels in the marmoset incisor PDL. The present study on human premolar PDL appeared to corroborate the latter findings. The venules, both PCV and CV had a combined luminal surface density of 51.9% and yet contained 81.5% of the blood volume. In contrast to the capillary - sized vessels, the AC and VC, the luminal endothelial surface area accounted for the remaining 48.1% but contained only 18.5% of the blood volume. These findings showed that the venules held more than 4 times the volume of blood per unit area of endothelium than the capillary - sized vessels. Therefore, with the relatively larger endothelial surface area exposed to a unit volume of blood, the capillary - sized vessels were considered to be more important exchange units than venular - sized vessels.

The mean wall thickness of the 4 distinct vessel types found in the human premolar PDL was 2.16 μm (VC), 1.85 μm (PCV), 5.61 μm (AC) and 1.60 μm (CV). These measurements were comparable to the respective vessel types reported for the marmoset incisor PDL (Parlange and Sims, 1993) as 2.82 μm, 2.19 μm, 4.74 μm and 2.50 μm. The similarity in vessel wall dimensions suggests that the vascular system

in the marmoset PDL has a similar function to that of the human PDL vascular system, and therefore may accurately reflect the physiological characteristics of the human PDL, provided that V_v, S_v, and L_v are comparable.

In summary, the mean luminal volume of the non-functional human premolar PDL ranged from 8.97% to 9.52%. The finding contrasted with the 1.63% to 3.50% histological estimation by Götze (1976, 1980). When considering that the vascular volumes obtained for man and other animal models, the findings by Götze must be considered to be erroneous. The pattern of vascular distribution across the circumferential thirds in the human premolar PDL compared favourably with that reported for the marmoset incisor PDL. Vascular volume was greatest in the apical third of the premolar PDL, which subserved the function of tooth support rather than as a means of providing nutrition. Venular - sized vessels carried more than 4 times the blood volume per unit area of endothelium than capillary - sized vessels but the latter were considered to be more efficient in providing physiological exchange.

6.5 PERIODONTAL LIGAMENT WIDTH

The fact that the PDL width varies according to functional demand, age and along the length of the root has been demonstrated by Klein (1928), Kronfeld (1931) and Coolidge (1937). It is known that masticatory forces impart a mesially directed force on individual teeth (Picton, 1964). The absence of masticatory forces on the experimental premolar PDL could be expected to result in a narrowing of the entire PDL space, due to a loss of transient tension and compression in the PDL. Klein (1928) and Kronfeld (1931) compared teeth with and without antagonists, and reported that in the latter, the width of the PDL is about one-half to one-third of that of the former. Klein (1928) reported that the mean PDL width of functional teeth was greatest at the alveolar crest at 390 μm, while the midroot region was narrowest at 170 μm. The apical region was intermediate at 210 μm. The present findings in the non - functional human premolar PDL showed that the mean PDL width at the

cervical level at 131.3 μm and at the midroot level at 61.8 μm corroborated their observations. The mean human PDL width for the apical level at 120.1 μm was more than one-half of the mean PDL width for functional teeth reported by Klein (1928). This difference might be attributed to variability in methodology and tooth type. The present study also confirmed the double-cone goblet shaped PDL space observed by Klein (1928) in functionless teeth.

The narrowing of the non-functional human premolar PDL could also have an effect on the V_v when compared with functioning teeth. Had the human tissues been perfusion-fixed and with the narrowing of the PDL, the V_v would have been higher due to a relatively smaller volume of PDL tissue. The shrinkage of blood vessels found in the immersion-fixed human PDL might have contributed to a lower V_v in spite of the constriction of the PDL width.

With such a minute space interposed between tooth and alveolar bone, the shock-absorbing capacity of the human PDL is not unlimited. Picton (1964) showed that the intermittent forces during masticating could depress and displace a tooth mesially into the tooth socket without remission throughout the chewing cycle. Picton and Davies (1967) reported a horizontal load of 500g during chewing would reduce the PDL width by 25 μm or 12% of the mean ligament width. While the fluid systems in the PDL were important in supporting the tooth when forces of less than 100g were applied, Wills et al. (1976) contended that the fibrous components played a greater role in force transmission with loads greater than 100g. Thus, the vascular volume, the proprioceptors located within the PDL, the collagen fibres, cells and spaces together help to maintain the PDL width during normal function.

6.6 IMPORTANCE OF PDL VASCULATURE

The PDL vasculature has been implicated in tooth support. Parfitt (1960) and Bien (1966) proposed that the pulsatile nature of blood flow (Mühlemann, 1967) is

responsible for supporting the tooth against axial loading. Using a mathematical model, Walker (1980) showed that the PDL blood vessels contributed measurably to the support of the teeth. The histomorphometric findings on vascular volume by Blauschild et al. (1992) affirmed the above observations that the abundance of blood volume in the apical half of the rat incisor served to act as a protective cushion for the continuously growing dental and periodontal tissues against occlusal load.

In addition to tooth support, Blauschild et al. (1992) reported that the extensive vascularization in the apical half of the rat incisor PDL provided for the high metabolism of actively dividing cells in that region. However, the human mandibular premolars are unlike rodent incisors of continuous eruption. While the present study reported more than 50% of the blood volume resided in the apical third of the premolar ligament, this finding suggested a pooling of blood to subserve the function of cushioning rather than as a means of providing nutrition.

Whether the blood vessels in the human PDL function as tube or tunnel capillaries, or as a combination is still not fully understood at present. On the basis of the evidence presented by Casley-Smith et al. (1975) for jejunal capillaries, the presence of fenestrated periodontal blood capillaries (Clark et al., 1990; Lew et al., 1989) may indicate that apericytic PCV (*a*PCV) function as tunnel capillaries in some regions of the ligament.

Freezer and Sims (1988) have shown statistically significant associations between *a*PCV, K-cells and oxytalan fibres. If *a*PCV do function as tunnel capillaries in the vicinity of K-cells, oxytalan fibres and nerve complexes, then these structures may represent anatomical mechanisms which regulate the biochemical properties of perivascular ground substance or PDL vascular permeability. On the basis of evidence provided by Chintakanon (1990), Cooper et al. (1990) and Tang and Sims (1992), these anatomical mechanisms may be implicated in vascular changes during tooth movement.

The majority of microvessels identified in the human mandibular premolar PDL were PCV. In addition, Cooper et al. (1990) and Tang and Sims (1992) have shown that PCV in the tensioned rat molar ligament contributed most to the increase in the mean number of tissue channels. These findings accord with other studies where the PCV are considered to be the most functionally sensitive vessels to stimuli (Casley-Smith, 1983; Simionescu and Simionescu, 1984; Lew et al., 1989) and, therefore, may be the most important vessels during tooth movement.

6.7 AREAS FOR FUTURE RESEARCH

From the above findings, the following areas of further investigation are suggested:

1. The present investigation analysed the most distal segment of PDL from the alveolar crest to the root apex. Future research should include the portion of ligament beyond the root apex to give a more comprehensive picture of the PDL blood vessels and nerves.

2. An investigation of the PDL vascular and neural reconstitution following periodontal disease and periodontal surgery to complement the ongoing research in guided tissue regeneration.

3. Orthodontic tooth movement is often called "controlled inflammation". Research may be advanced in the direction of the PDL blood vessel, nerve and mast cell interaction in response to mechanical stimulation.

4. With the increasing prevalence of adults seeking orthodontic treatment, research should be conducted to compare the PDL blood vessel endothelial morphology and function of young and old subjects, and its regulation of fluid into and out of blood vessels during mechanical loading. This research may be performed using a non-human primate model, eg. the marmoset or the macaque monkey.

5. The response of the vascular and neural components to orthodontic tooth intrusion and extrusion has been studied (Weir, 1991; Parlange, 1991; Parlange and Sims, 1993; Chintavalakorn, 1994). Further investigation into the PDL vascular and neural behaviour following other types of controlled tooth movement, and their effect on the duration of retention may be carried out.

6. Root resorption is a common feature of orthodontic tooth movement. Investigations should be undertaken to analyse the function of the ligament microvascular bed in the repair of damaged root surfaces.

CHAPTER 7 CONCLUSIONS

1. The present investigation was the first TEM stereological analysis of a non-functional human mandibular premolar PDL. Quantitative data on vascular and nerve volume were obtained. This study also reviewed the work of Götze (1976), and found his methodology wanting in accuracy in the light of the present findings.

2. The mean luminal volume in the human mandibular premolar PDL ranged from **8.97% to 9.52%** of the total PDL volume. When wall thickness was included, it added another ≈3.4% to the luminal volume to give a mean abluminal volume range of **12.37% to 12.91%**. This range contrasted with the histologically determined vascular volume of 1.63% to 3.50% reported by Götze (1976, 1980) for human mandibular premolars. In view of the close similarities in vascular volume, determined from TEM stereology, between human, marmoset and mouse PDL, it is inferred that the histological estimations of vascular volume from human cadaver premolar PDL by Götze (1976, 1980) are highly erroneous.

3. Four vessel types were identified from the blood vessel sample - venous capillaries (VC), postcapillary-sized venules (PCV), collecting venules (CV), the arterial capillaries (AC). The most common vessel type was the PCV, which contained 69.1% of the total blood volume. The second most common vessel type was the VC which held 14.9% of the total blood volume. Collecting venules and arterial capillaries were few in number but contained 12.4% and 3.6%, respectively, of the total blood volume.

Venous vessels (VC, PCV and CV) accounted for 96.4% of the blood volume while the arterial component (AC) accomodated the remaining 3.6%. This finding implied that at any one moment, there were ≈ 26 times more blood volume on the venous side than on the arterial side, and suggests a slower rate of blood flow in the venous microvessels.

4. The distribution of blood volume within circumferential thirds showed significant differences across the PDL ($p<0.05$). The middle circumferential third was 9 times more vascular than the tooth third, and 6 times more vascular than the bone circumferential third. The predominance of blood vessels in the middle circumferential third suggested a regionalization of vascular function in the human PDL.

5. The blood volume along the length of the PDL from the alveolar crest to the root apex showed great variation among the vertical thirds. More than half of the blood volume (50.4%) was located in the apical third of the PDL. The middle third contained approximately one third (30.9%) of the blood volume while the coronal third was the least vascular contributing less than one - fifth of the volume at 18.7%. The trend of vertical vascular distribution agreed with the findings of Götze (1976) who showed that blood volume increased towards the apical third of the human mandibular premolar PDL. This observation suggested an occluso-apical direction of blood flow in the human PDL. However, the present pattern was not repeated in the marmoset incisor PDL model which showed that most of the blood volume was contained in the coronal third (Parlange and Sims, 1993).

Blood volume in the human PDL was shown to increase 1.6 times between the vertical thirds with increasing depth. The linear pattern of increasing volume with depth refuted the claim of Sims (1987) that the effect of depth on vascular volume was quadratic.

6. Venular - sized vessels (PCV and CV) in the human premolar PDL contained more than 4 times the blood volume per unit area of endothelium than capillary - sized vessels (AC and VC). Similar findings were observed in the marmoset incisor PDL where venules contained 5 times more blood per unit area of endothelium than capillary - sized vessels (Parlange and Sims, 1993). The accord in relative vascularity between human and marmoset PDL suggested similar functional patterns in both PDL.

7. The mean axon volume was **0.52%** of the total PDL volume, which was comparable to the mouse molar PDL (Freezer and Sims, 1987, 1988) and marmoset incisor PDL (Parlange and Sims, 1993). When the Schwann cells were included, they added another 0.48% to give an overall mean volume of 1.00% of the total PDL volume. The mean axon diameters reported for the present study were in accord with those reported for the marmoset incisor PDL (Parlange and Sims, 1993). Further similarities in the distribution pattern of axons by type and region to the marmoset incisor PDL suggested comparable neural function between man and marmoset. Difference in axon location between human premolar PDL and mouse molar PDL reflected structural and functional differences between mouse and man.

8. The mean widths of the human PDL measured from the cervical level to the root apex in all eight PDL samples revealed a consistent narrowing in the midroot region. The mean apical and cervical PDL widths were found to be approximately twice that at the midroot level, and this variability in PDL width supported the concept of a double-cone goblet shaped PDL space proposed by Klein (1928). The present data corroborated the findings by Klein (1928) and Kronfeld (1931) in that the PDL widths in non-functional teeth were approximately one-third to one-half of functioning teeth.

9. The findings of the present study confirmed the anisotropic nature of the PDL (Freezer and Sims,1987). In addition, they complemented the existing knowledge on the role of the PDL microvascular bed in the homeostasis and regeneration of the PDL. Further research is needed to assess the PDL of normal functioning teeth, so that changes occuring during controlled tooth movement may be compared against this data. At present, the animal model which most accurately reflected the vascular and neural characteristics of the human PDL would be the marmoset PDL model.

CHAPTER 8 APPENDICES

Appendix 1

Demineralisation end points for the four premolar specimens:
- Tooth 34 - 21 months
- Tooth 35 - 21 months
- Tooth 44 - 13 months
- Tooth 45 - >21 months

Appendix 2

	Procedure and chemicals	Duration
1.	*Post-fixation*	
	4% osmium tetroxide in double distilled (d.d.) water	(1 hr)
2.	*Wash*	
	0.06M Cacodylate buffer	(20 mins)
3.	*Wash*	
	70% ethanol	(20 mins)
4.	*Block stain*	
	1% uranyl acetate in 70% ethanol	(1 hr)
5.	*Wash*	
	70% alcohol	(30 mins)
6.	*Dehydration*	
	70% ethanol	(2 x 20 mins)
	80% ethanol	(2 x 20 mins)
	90% ethanol	(2 x 20 mins)
	100% anhydrous ethanol	(2 x 20 mins)
	propylene oxide I	(2 x 20 mins)
	propylene oxide II	(2 x 20 mins)
	propylene oxide III	(30 mins)
	propylene oxide IV	(30 mins)

All diluted alcohols were prepared with double-distilled water.

7. *Infiltration*

Infiltration agar 100		
WPE 145 1:2 (DDSA:MNA=1:2)		
Propylene oxide : agar 100	1:1	(≈ 16 hours)
Propylene oxide : agar 100	1:3	(4 hours)
Agar 100 embedding resin		(4 hours)
Agar 100 embedding resin		(20 hours)

Appendix 3 **FIXATION SOLUTION**

Solution: 2.5% Glutaraldehyde

Preparation: 10 ml of 25% Glutaraldehyde
90 ml of 0.06M Cacodylate buffer

Divide resulting solution into two labelled jars , one used as a rinse for excess blood and the other as the fixation solution. Tissue is placed in the latter jar for at least 12 hours but no longer than 36 hours.

Appendix 4 **GLUTARALDEHYDE SOLUTION**

Solution: TAAB Glutaraldehyde 25% for electron microscopy.

Preparation: Use stock solution

Shelf life: 6 months at 4°C.

Appendix 5 **CACODYLATE BUFFER**

Solution: 0.06M Sodium Cacodylate Buffer

Preparation: 25.68 g Sodium Cacodylate in 2000 ml double distilled (d.d.) water.
Adjust to pH 7.4 using 1M HCL at 20°C.

Shelf life: 7 days at 4°C.

Cacodylate buffer is made from an arsenic compound and should not be inhaled or skin contact made. Wash thoroughly if contact is made.

Appendix 6 **DECALCIFYING SOLUTION**

Solution: 0.1M EDTA in 2.5% Glutaraldehyde, adjust to pH 6 using 1M HCL.

Preparation: 74.4 g EDTA (Ethylenediaminetetraacetic acid)
1800 ml 0.06M Cacodylate buffer pH 7.4
200 ml 25% Glutaraldehyde
Dissolve EDTA in 0.06M Cacodylate buffer by gently heating. Cool to 4°C, add Glutaraldehyde and adjust to pH 6.0 at 4°C using 1M HCL.

Shelf life: 7 days at 4 °C.

Appendix 7 OSMIUM TETROXIDE SOLUTION

Solution: 4% Osmium Tetroxide.

Preparation: Place 2 g of Osmium Teroxide in 50 ml d.d. water. Remove labels from the ampoule. Place the ampoule in hot water to melt the Osmium Tetroxide crystals. Remove from water and rotate the ampoule to form an even film of melted Osmium Tetroxide around the inside. When the Osmium Tetroxide has again solidified thoroughly clean the outside of the ampoule with Ethyl alcohol. Place the ampoule into a thick-walled screw bottle containing d.d. water. Ensure the lid is firmly secured and shake the bottle to the break the ampoule. Wrap in foil to exclude light and leave in a fume cupboard at room temperature to dissolve overnight. If the solution is exposed to light it will oxidise rendering it useless.

Shelf life: 7 to 10 days. This solution can only be used when clear. If it becomes straw coloured, or darker, then its fixative properties are greatly reduced and it should be discarded. Refrigeration is not advised as it increases the rate of oxidation and because Osmium Tetroxide is highly toxic.

Appendix 8 URANYL NITRATE

Solution: 1% Uranyl Nitrate in 70% alcohol.

Preparation: 1 g Uranyl Nitrate.
70 ml Ethyl alcohol.
30 ml d.d. water.
Exclude light with foil.

Shelf life: 7 days at room temperature.

Appendix 9 ALCOHOL DEHYDRATE

Alcohols are made up by diluting absolute alcohol with d.d. water.

Appendix 10 EMBEDDING MEDIUM

From Ladd Research Industries, Inc. The ratio of anhydride to epoxy resin can be varied to obtain blocks of different hardness. Because of the nature of the tissue to be sectioned, a hard embedding medium is selected. The ratio of anhydride to epoxy equivalent is, therefore, 0:7:1. The two anhydrides used are MNA (Methyl Nadic Anhydride) (MW = 178) and DDSA (Dodecenyl Succinic Anhydride) (MW = 266). The total quantity of resin required from each anhydride is varied in the ratio of DDSA: MNA at 1:2. The weight per epoxide (W.P.E.) of the epoxy resin batch used was 145. Volumetric rather than gravimetric measurements were used although this did not adversely affect the quality of the embedding medium.

Preparation: For a total volume approximating 200 ml.

Mixture A: 34 ml Agar 100, 43.66 ml (i.e. 34/145 x 266 x 0.7)
DDSA. (Shaken vigorously for 10 minutes).

Mixture B: 68 ml Agar 100, 58.43 ml (i.e. 68/145 x 178 x 0.7)
MNA (Shaken vigorously for 10 minutes).

Mixture C: A + B + 2.86 ml (ie. 0.14/10 x (34 + 43.66 + 68 + 58.43) BBMA (Benzyldimethylamine).
Thorough mixing is essential, otherwise blocks with poor sectioning properties will be obtained.

Precautions: Agar 100 is a suspected carcinogen and hence should be handled with great care. Agar, MNA, DDSA, and BBMA are all toxic if swallowed and can cause irritation to the skin. Work with these components must be carried out in a fume cupboard and protective clothing must be worn. There should be avoidance of exposure to vapours and contact with skin, eye and clothing.

Appendix 11 LIGHT MICROSCOPIC STAINS

(i) <u>0.05% Toluidine Blue</u>

Solution: 0.05% Toluidine Blue in d.d. water.

Preparation: 0.05 g Toluidine Blue.
100 ml d.d. water.
Dissolve by stirring.

Shelf life: 6 months at room temperature.

Precautions: Avoid contact with skin.

(ii) <u>1% Borax</u>

Solution: 1% Borax in d.d. water.

Preparation: 1 g Sodium Thiosulphate (borax).
100 ml d.d. water.
Dissolve be stirring.

Shelf life: 6 months at room temperature.

Precautions: Avoid contact with skin.

Appendix 12 GRID STAINS

(i) 0.5% Uranyl Acetate

Solution: 0.5% Uranyl Acetate in 70% Alcohol.

Preparation:
0.125 g Uranyl Acetate
7.5 ml Ethyl alcohol.
17.5 ml d.d. water.
Shake to dissolve.
Exclude light by wrapping with foil.

Shelf life: 1 month at room temperature.

(ii) Modified Reynolds' Lead

Preparation:
(i) 1.33 g Lead Nitrate
1.76 g Sodium Citrate
30 ml d.d. water
(ii) 8 ml 1M Sodium Hydoxide.
Shake vigorously (i) for i monute and allow to stand for 30 minutes, shaking intermittently. Add (ii) then dilute to 50 ml with d.d. water, mixing by inversion.

Shelf life: 1 month at 4°C. Final solution should be clear, with pH less than 14. Discard if pH drops below 11. (Use pH test paper, not the electrode).

Appendix 13 RADIOGRAPHIC EQUIPMENT

1. Kodak ultraspeed film 57 x 76 mm.
2. Siemens Heliodent machine.
   a. accelerating voltage: 50 kV.
   b. tube current: 7 mA.
   c. exposure time: 0.24 s.
   d. film distance from the tube: 17cm.

Appendix 14 TRANSMISSION ELECTRON MICROSCOPE

JEOL 100S (Jeol Ltd., Tokyo, Japan).

1. Accelerating voltage of 60 kV.
2. Beam current of 50 mA.
3. Gun bias setting of 5.
4. Objective lens aperture of 1.
5. Field aperture setting of 2.

APPENDIX 15 COMPUTERISED DATA ENTRY FORM FOR POINT COUNTING DATA

								VESSEL	POINTS		CELLS		
Human No.	Side	Level	Region	Film No.	Grid Count	Vessel type	Lumen	Endo	Nucl	MV	SM,Peri,Veil	Axons 1.0μm	Vessel No.

VESSELS		INTERSECTS					VESSEL SIZES			
Lumen	Endo	Nucleus	MV	Cells	Axons	BV Junctions	Lumen	Endo	Cells	Nucleus No.

Appendix 16 ESTIMATION OF POINT COUNTING DATA FOR TEETH WITH MISSING ROOT APEX

The PDL segments with missing root apices (level 9) are RPM1 lingual (Li) and buccal (Bu), and RPM2 lingual PDL segments. Certain ***assumptions*** have to be made when comparing with RPM2 buccal PDL segment (has full PDL length from level 1 to 9) to estimate missing values for the root apices. They are:

1. The number of *total grid count* for level 9 (root apex) of RPM2 lingual PDL segment is identical for each circumferential third to that of the number of total grid count for level 9 of RPM2 buccal PDL segment.

2. The sum of the *point counts of blood vessel (BV) lumen* in the apical third (levels 7 to 9) of the PDL of RPM2 buccal PDL segment is identical to that of the sum of point counts of BV lumen in the apical third (levels 7 to 9) of RPM2 lingual PDL segment. This assumption will give the number of points counted for BV lumen in *level 9 of RPM2 lingual segment*. The estimated number of points counted for level 9, when divided by the total number of grid counts from level 1 to level 9 in RPM2 lingual PDL segment, will give the estimated luminal vascular volume at the root apex of RPM2 lingual PDL segment.

3. The BV volume of level 9 of RPM2 lingual PDL segment is identical to that of level 9 for RPM1 buccal and lingual PDL segments. By simply adding the luminal vascular volume of level 9 of RPM2 lingual PDL segment to the existing luminal volumes of RPM1 lingual and buccal PDL segments (levels 1 to 8), one is able to derive the number of points counted for BV luminal volume for level 9 of RPM1 buccal and lingual PDL segments.

4. The estimated BV luminal volume of level 9 of RPM2 buccal, and RPM1 buccal and lingual PDL segments follow the *same mean regional distribution* of luminal volume from levels 1 to 8 in the respective PDL segments.

5. The wall thickness of the different BV types found in RPM2 buccal PDL segment is identical to that of BV types in RPM2 lingual, and RPM1 buccal and lingual PDL segments.

6. The vessel types found in level 9 of RPM2 buccal PDL segment are equally represented in level 9 of RPM2 lingual and RPM1 buccal & lingual PDL segments.

Summary of Calculations:

The total number of grid counts from levels 7 to 9 (apical third) of RPM2 Bu and RPM2 Li PDL segments are 1217 and 1229, respectively. The number of points counted in the apical third for RPM2 Bu and RPM2 Li are 180 and 121+X, respectively, where X represents the missing BV lumen point count for level 9 of RPM2 Li PDL segment. By proportion, X has a value of 61, which translates to a 1.6% of BV luminal volume for RPM2 Li level 9, ie. (X/ total grid count from levels 1 to 9 of RPM2 Li) = 61/3655 ≈ 0.016 or 1.6%.

Add this *1.6%* to the existing luminal vascular volumes (levels 1 to 8) of RPM1 Bu and RPM1 Li PDL segments:

RPM1 Buccal PDL segment : *7.6% + 1.6%* = **9.2%**

RPM1 Lingual PDL segment : *6.8% + 1.6%* = **8.4%**

To calculate the number of point counts for level 9 (Y) of RPM1 Buccal PDL segment:

Add the number of points counted from levels 1 to 8 to Y, and divide by the total number of grid counts from levels 1 to 9; multiply by 100 and this is equivalent to the 9.2% of luminal blood volume.

[(229 + Y) / 3417] x 100% = 9.2%; the value of Y will be 86. The Y value is then distributed according to the respective circumferential / regional thirds according to the mean regional luminal volume determined from levels 1 to 8 of RPM1 buccal PDL segment.

Following on from assumption 6 above, the estimated point counting value for each circumferential third of level 9 may then represent the most common vessel type found in level 9 of RPM2 buccal PDL segment.

The same procedure is then repeated for level 9 of RPM1 lingual PDL segment.

Chapter 9 BIBLIOGRAPHY

ANDERSON D.J. and HECTOR M.P. (1987)
Periodontal mechanoreceptors and parotid secretion in animals and man.
J. Dent. Res. **66**:518-523

AUSTEN K.F. (1974)
Reaction mechanisms in the release of mediators of immediate hypersensitivity from human lung tissue.
Fed. Proc. **33**:2256-262

AVERY J.K., CORPRON R.E., LEE S.D. and MORAWA A.P. (1975)
Ultrastructure of terminal blood vessels in mouse periodontium.
J. Dent. Res. Special Issue (Abstract) **54**:108

AZUMA M., ENLOW D.H., FREDRICKSON R.G. and GASTON L.G. (1975)
A myofibroblastic basis for the physical forces that produce tooth drift and eruption, skeletal displacement of sutures, and periosteal migration.
In: McNamara JA (ed) Determinants of mandibular form and growth. Monograph 4.
University of Michigan, Ann Arbor, pp 179-207

BADDELEY A. J., GUNDERSEN H.J.G. and CRUZ-ORIVE L.M. (1986)
Estimation of surface area from vertical sections.
J. Microsco. **142**:259-276.

BAEZ S., FELDMAN S.M. and GOOTMAN P.M. (1976)
Integrated response of the microvasculature to stimulation of the CNS in the rat.
In: Microcirculation-Blood vessel interactions system in special tissues. Vol. I

BARKER J.H. (1979)
A morphometric atlas of the human periodontal ligament.
M.D.S Thesis, The University of Adelaide, South Australia

BEERTSEN W. and EVERTS V. (1977)
The site of remodelling of collagen in the periodontal ligament of the mouse incisor.
Anat. Rec. **189**:479-498

BEERTSEN W., EVERTS V. and van den HOOFF A. (1974a)
Fine structure of fibroblasts in the periodontal ligament of the rat incisor and their possible role in tooth eruption.
Archs. Oral Biol. **19**:1087-1098

BELLOWS C.G., MELCHER A.H. and AUBIN J.E. (1981)
Contraction and organization of collagen gels by cells cultured from periodontal ligament, gingiva and bone suggest functional difference between cell types.
J. Cell Sci. **50**:299-314

BELLOWS C.G., MELCHER A.H., BHARGAVA U. and AUBIN J.E. (1982b)
Fibroblasts contracting three-dimensional collagen gels exhibit ultrastructure consistent with either contraction or protein secretion.
J. Ultrastruct. Res. **78**:178-192

BENNET H.S., LUFT J.H. and HAMPTON J.C. (1959)
Morphological classifications of vertibrate blood capillaries.
Am. J. Physiol. **196**:381-390.

BERKOVITZ B.K.B. (1990)
The structure of the periodontal ligament: an update.
Eur. J. Orthod. **12**:51-76.

BERKOVITZ B.K.B. and SHORE R.C. (1978)
High mitochondrial density within peripheral nerve fibres of the periodontal ligament of the rat incisor.
Archs. Oral Biol. **23**:207-213.

BERKOVITZ B.K.B. and SHORE R.C. (1982)
Cells of the periodontal ligament.
In: The periodontal ligament in health and disease.
(eds: Berkovitz B.K.B., Moxham B.J. and Newman H.N.)
Pergamon Press, Oxford, Ch. 2, pp. 25-50.

BERKOVITZ B.K.B., WEAVER M.E., SHORE R.C. and MOXHAM B.J. (1981)
Fibril dameters in the extracellular matrix of the periodontal tissues of the rat.
Connect Tissues Res. **8**:127-132

BERNICK S. (1957)
Innervation of the teeth and periodontium after enzymatic removal of collagenous elements.
Oral Surg. **10**:323-332

BERNICK S. (1962)
Age changes in the blood supply of molar teeth of rats.
Anat. Rec. **144**:265-274

BERNICK S. and LEVY B.M. (1968B)
Studies on the biology of the periodontium of marmosets : IV. Innervation of the periodontal ligament.
J. Dent. Res. **56**:1409-1416

BERTRAM J.F. (1989)
Stereological Methods for Histopathology.
Tissue Talk Vol. **2** (2)

BEVELANDER G. and NAKAHARA H. (1968)
The fine structure of the human periodontal ligament.
Anat. Rec. **162**:313-326.

BIEN S.M. (1966)
Fluid dynamic mechanisms which regulate tooth movement. In: Staple P H (ed.), Advances in oral biology. Academic Press, New York, pp. 173-201

BIENKOWSKI R.S. (1983)
Intracellular degradation of newly synthesized secretory proteins.
Biochemical Journal **214**:1-10

BIENKOWSKI R.S., COWAN M.J., McDONALD J.A. and CRYSTAL R.G. (1978)
Degradation of newly synthesized collagen.
J. Biol. Chem. 253:4356-4363

BIRN H. (1966)
The vascular supply of the periodontal membrane.
J. Periodont. Res. 1:51-68.

BLACK G.V. (1887)
A study of the histological characters of the periosteum and peridental membrane.
Keener, Chicago

BLAUSCHILD N., MICHAELI Y. and STEIGMAN S. (1992)
Histomorphometric study of the periodontal vasculature of the rat incisor.
J. Dent. Res. **12**:1908-1912

BONE Q. and DENTON E.J. (1971)
The osmotic effects of electron microscope fixatives.
J. Cell Biol. **49**:571

BONNAUD A., PROUST J.P. and VIGNON C. (1978)
Terminaisons nerveuses buccales chez le chat.
J. Biol. Buccale **6**:111-120

BOX K.F. (1949)
Evidence of lymphatics in the periodontium.
J. Canadian Dent. Assoc. **15**:8-19

BOYER C.C. and NEPTUNE C.M. (1962)
Patterns of blood supply to teeth and adjacent tissues.
J. Dent.Res. **41**:158-171

BOYKO G.A., MELCHER A.H. and BRUNETTE D.M. (1981)
Formation of new periodontal ligament by periodontal ligament cells implanted *in vivo* after culture *in vitro*. A preliminary study of transplanted roots in the dog.
J. Period. Res. **16**:73-88

BRASHEAR A.D. (1936)
The innervation of teeth. An analysis of nerve fiber components of the pulp and periodontal tissues and their probable significance.
J. Comp. Neurol. **64**:169-185

BRUNS R.R. and PALADE G.E. (1968a)
Studies on blood capillaries. I. General organization of blood capillaries in muscles.
J. Cell Biol. **37**:244-276

BUCHANAN R.A. and WAGNER R.C. (1990)
Association between pericytes and capillary endothelium in the eel rete mirabile.
Microvasc. Res. **39**:60-76

BURNSTOCK G. and BELL C. (1974)
Peripheral autonomic transmission. In: The peripheral nervous system, J I Hubbard (ed), pp 277-327. London, Plenum Press

BUTLER W.T., BIRKEDAL-HANSEN H., TAYLOR R.E. and CHUNG E. (1975)
Proteins of the periodontium. Identification of collagens with the $a1(I)_2$ a2 and $[a1(III)]_3$ structures in bovine periodontal ligament.
J. Biol. Chem. **250**:8907-8912

BYERS M.R. (1985)
Sensory innervation of periodontal ligament of rat molars consists of unencapsulated Ruffini-like mecahanoreceptors and free nerve ending.
J. Comp. Neurol. **231**:500-518.

BYERS M.R. and HOLLAND G.R. (1977)
Trigeminal nerve endings in gingiva, junctional epithelium and periodontal ligament of rat molars as demonstrated by autoradiography.
Anat. Rec. **188**:509-523

BYERS M.R. and MATTHEWS B. (1981)
Autoradiographic demonstration of ipsilateral and contralateral sensory nerve endings in cat dentine, pulp and periodontium.
Anat. Rec. **201**:249-260.

BYERS M.R., O'CONNOR T.A., MARTIN R.F. and DONG W.K. (1986)
Mesencephalic trigeminal sensory neurones of cat. Axon pathways and structure of mechanoreceptive endings in periodontal ligament.
J. Comp. Neurol. **250**:181-191.

CARMICHAEL G.G. and FULLMER H.M. (1966)
The fine structure of the oxytalan fiber
J. Cell Biol. **28**:33-36

CARRANZA F.A., ITOIZ M.E., CABRINI R.L. and DOTTO C.A. (1966)
A study of periodontal vascularization in different laboratory animals.
J. Periodont. Res. **1**:120-128

CASLEY-SMITH J.R. (1968)
The dimensions and numbers of small vesicles in blood and lymphatic endothelium and in mesothelium.
J. Anat. **103**:202-203 (Abstract)

CASLEY-SMITH J.R., O'DONOGHUE P.J. and CROCKER K.W.J. (1975)
The quantitative relationships between fenestrae in jejunal capillaries and connective tissue channels: proof of "Tunnel Capillaries".
Microvasc. Res. **9**:78-100

CASLEY-SMITH J.R. (1977a)
Lymph and Lymphatics. In: G. Kaley and B. Altura (eds), Microcirculation , Vol. 1, (University Park Press, Baltimore , London), pp 421-502

CASLEY-SMITH J.R. (1983)
The structure and functioning of the blood vessels, interstitial tissues, and lymphatics.
In : Lymphangiology. Eds: Foldi M. and Casley-Smith JR, Stuttgart-New York : Schattauer Verlag, pp 27-169

CASTELLI W.A (1963)
Vascular architecture of the human adult mandible.
J. Dent. Res. 42:786-792

CASTELLI W.A. and DEMPSTER W.T. (1965)
The periodontal vasculature and its responses to experimental pressures.
J. Am. Dent. Ass. 70:890-905.

CHAMBERS R.W., BOWLING M.C. and GRIMLEY P.M. (1968)
Glutaraldehyde fixation in routine histopathology.
Arch. Path. **85**:18

CHINTAKANON K. (1990)
An ultrastructural study of vascular endothelial junctions in normal and tensioned rat PDL.
M.D.S. Thesis, The University of Adelaide, South Australia

CHINTAVALAKORN S. (1994)
A T.E.M. stereological study of marmoset PDL vasculature and nerves following orthodontic extrusion and long-term retention.
M.D.S. Thesis, The University of Adelaide, South Australia

CLARK A.B. (1986)
A quantitative analysis of the effects of intrusion on apical PDL fenestrae of the rat maxillary molar
M.D.S. Thesis, The University of Adelaide, South Australia

CLARK A.B., SIMS M.R. and LEPPARD P.I. (1990)
An analysis of the effect of tooth intrusion on the microvascular bed and fenestrae in the apical periodontal ligament of the rat molar.
AJO-DO **99**(1):21-29

CLIFF W.J. (1976)
Blood Vessels.
Cambridge University Press; pp. 31-36, 68-72

COHEN L. (1959a)
The venous draniage of the mandible.
Oral Surg **12**:1447-1449

COOLIDGE E.O. (1937)
The thickness of the human periodontal membrane.
J. Am. Dent. Ass. **24**:1260- 1276.

COOPER S.M., SIMS M.R., SAMPSON W.J. and DREYER C.W. (1990)
A morphometric, electron microscopic analysis of tissue channels shown by ionic tracer in normal and tensioned rat molar apical periodontal ligament.
Archs Oral Biol 7:499-507

CORPRON R.E., AVERY J.K., MORAWA A.P. and LEE S.D. (1976)
Ultrastructure of capillaries in mouse periodontium.
J. Dent. Res. **55**:551.

COTRAN R.S., GUTTUTA M.L. and MAJNO G. (1965)
Studies on inflammation. Fate of intramural vascular deposits induced by histamine.
Am. J. Path. **45**:261-281

CROWE P.R. (1989)
The marmost ligament: A TEM morphometric analysis following incisor crown fracture, root canal therapy and orthodontic extrusion.
M.D.S. Thesis, The University of Adelaide, South Australia

CRUZ-ORIVE L.M. (1987)
Particle number can be estimated using a dissector of unknown thickness: the selector.
J. Microsc. **145**:121-142

DELESSE, M.A. (1848).
Procede mecanique pour determiner la composition des roches. C.R. Acad. Sci. (Paris) 25, 544

DEPORTER D.A., SVOBODA E.L.A., MOTRUK W. and HOWLEY T.P. (1982)
A stereological analysis of collagen phagocytosis by periodontal ligament fibroblasts during occlusal hypofunction in the rat.
Archs. Oral Biol. **27**:1021-1025

DOUVARTZIDIS I., (1984)
A morphometric examination of the periodontal ligament vasculature of the marmoset molar.
M.D.S. Thesis, The University of Adelaide, South Australia.

DUBLET B., DIXON E., de MIGUEL E. and van der REST M. (1988)
Bovine type XII collagen: amino acid sequence of a 10kDa pepsin fragment from periodontal ligament reveals a high degree of homology with the chicken a_1(XII) sequence.
Federation of European Biochemical Societies **233**: 177-180

DUBNER R., SESSLE B.J. and STOREY A.T. (1978)
The neural basis of oral and facial function.
New York, Plenum Press.

DUNCAN G.W., YEN E.H.K., PRITCHARD E.T. and SUGA D.M. (1984)
Collagen and prostaglandin synthesis in force-stressed periodontal ligament in vitro
J. Dent. Res. **63**:665-669

EDWALL L.G.A. (1982)
The vasculature of the periodontal ligament.
In: The periodontal ligament in health and disease.
(eds: Berkovitz BKB, Moxham BJ and Newman HN) Pergamon Press, Oxford, pp. 151-171.

EDWALL L. and KINDLOVA M. (1971)
The effect of sympathetic nerve stimulation on the rate of disappearance of tracers from various oral tissues.
Acta Odontol. Scand **29**:387-400

EVERTS V., BEERTSEN W. and van der HOOFF A. (1977)
Fine structure of the end-organs in the periodontal ligament of the mouse incisor.
Anat. Rec. **189**:73-89.

FARQUHAR M.G. and PALADE G.E. (1962)
Functional evidence for the existence of a third cell type in the renal glomerulus.
J. Cell Biol. **13**:55-87

FAWCETT D.W. (1959)
The fine structure of capillaries, arterioles and small arteries.
In: The microcirculation, Symposium on factors influencing exchange of substances across capillary wall, (eds) SRM Reynolds and BW Zweifach. University of Illinois press. pp 1-27

FAWCETT D.W. (1963)
Comparative observations on the fine structure of blood capillaries. In: The Peripheral Blood Vessels, JL Orbison and DE Smith (eds). Williams and Wilkins, Baltimore pp 17-41

FERNANDO N.V.P. and MOVAT H.Z. (1964)
The fine structure of the terminal vascular bed.
Exp. Mol. Pathol. **3**:87-97

FOLKE L.E.A. and STALLARD R.E. (1967)
Periodontal microcirculation as revealed by plastic microspheres.
J. Periodont. Res. **2**:53

FOONG K.W.C. (1993)
A TEM stereological analysis of blood vessels and nerves of human premolar PDL.
The First Year Report, The University of Adelaide, South Australia

FRANK R.M., FELLINGER E. and et STEUER P. (1976)
Ultrastructure du ligament alveolo-dentaire du rat.
J. Biol. Buccale 4:295-313.

FREEZER S.R. (1984)
A study of periodontal ligament mesial to the mouse mandibular first molar.
M.D.S. Thesis, The University of Adelaide, South Australia.

FREEZER S.R. and SIMS M.R. (1987)
A transmission electron microscope stereological study of the blood vessels, oxytalan fibres and nerves of mouse-molar periodontal ligament.
Archs Oral Biol. **32**:407-412.

FREEZER S.R. and SIMS M.R. (1988)
Statistical correlations between blood vessels, oxytalan fibres and cells with normal mouse PDL using transmission electron microscopy.
Aust. Orthod. J. **10**:227-230

FREEZER S.R. and SIMS M.R. (1989)
Morphometry of neural structures in the mouse preiodontal ligament mesial to the mandibular first molar.
Aust. Orthod. J. **11**:30-37

FROHLICH E. (1958)
Entwicklung und Morphologie der Weichgewebe des Paradontiums.
Dt Zahnartl Z **13**:121-240

FULLMER H.M., SHEETZ J.H. and NARKATES A.J. (1974)
Oxytalan connective tissue fibers
J. Oral Pathol. 3:291-316

FURSETH R., SELVIG K. and MJOR I.A. (1986)
The periodontium.
In: Human Oral Embryology and Histology.
(eds: Mjor I.A. and Fejerskov O.) 1st edition. Munksgaard, Copenhagen pp. 131-176.

GARFUNKEL A. and SCIAKY I (1971)
Vascularization of the periodontal tissues in the adult laboratory rat.
J. Dent. Res. **50**:880-887

GATHERCOLE L.J. and KELLER A. (1982)
Biophysical aspects of the fibres of the periodontal ligamental.
In: Berkovitz BKB, Moxham BJ, Newman HN (eds) The periodontal ligament in health and disease. Pergamon Press, Oxford, pp 103-117.

GILCHRIST D.R. (1978)
Ultrastructure of periodontal blood vessels.
M.D.S. Thesis, The University of Adelaide, South Australia

GILLARD G.C., MERRILEES M.J., BELL-BOOTH P.G., REILLY H.C. and FLINT M.H. (1977)
The proteoglycan content and the axial periodicity of collagen in tendon.
Biochemical Journal **163**:145-157

GLAUERT A.M. (1978)
In: Fixation, Dehydration and Embedding of Biological Specimens.
Ed. A.M. Glauert, North-Holland Publishing Company; pp. 5-85

GÖTZE von W. (1965)
Über Alternsveränderungen des Parodontiums (Volumenbestimmung der Gewebeanteile nach Hennig)
Ds Janhgang **1**:467-469

GÖTZE von W. (1976)
Quantitive untersuchungen zur verteilung der blutgefaßen im desmodont.
Dt. Zahnartztl. Z. **31**:428-430.

GÖTZE von W. (1980)
Uber den Volumenanteil von Faserbundelabschnitten und Blutgefaßen im Desmodont menschlicher Frontzahne.
Dt. Zahnarztl. Z. **35**:1103-1104

GOULD T.R..L. (1983)
Ultrastructural characteristics of progenitor cell populations in the periodontal ligament of mouse molar stimulated by wounding.
Anat. Rec. **188**:133-142

GOULD T.R.L., MELCHER A.H. and BRUNETTE D.M. (1977)
Location of progenitor cells in the periodontal ligament of mouse molar stimulated by wounding.
Anat. Rec. **188**:133-142

GOULD T.R.L., MELCHER A.H. and BRUNETTE D.M. (1980)
Migration and division of progenitor cell populations in the periodontal ligament after wounding.
J. Periodont. Res. **15**:20-42

GRANT D.A. and BERNICK S. (1970)
Arteriosclerosis in periodontal vessels of ageing humans.
J. Periodont. **41**:170-173

GRANT D.A. and BERNICK S. (1972b)
The periodontium of ageing humans.
J. Periodont. **43**:660-667

GRIFFIN C.J. (1972)
The fine structure of end-rings in human periodontal ligament.
Archs. Oral Biol. **17**:785-797

GRIFFIN C.J. and HARRIS R. (1968)
Unmyelinated nerve endings in the periodontal membrane of the human teeth.
Archs. Oral Biol. **13**:1207

GRIFFIN C.J. and SPAIN H. (1972)
Organisation and vasculature of human periodontal ligament mechanoreceptors.
Archs. Oral Biol. **17**:913-921.

GUNDERSEN H.J.G (1977)
Notes on the estimation of the numerical density of arbitrary profiles: the edge effect.
J. Microsc. **111**:219-223

GUNDERSEN H.J.G. (1986)
Stereology of arbitrary particles: a review of unbiased number and size estimators and the presentation of some new ones.
In memory of William R. Thompson, J. Microsc. **43**:3-35

GUNDERSEN H.J.G. and JENSEN E.B. (1985)
Stereological estimation of the voulume-weighted mean volume of arbitrary particles observed on random sections.
J. Microsc. **138**: 127-142

GUNDERSEN H.J.G., BENDTSEN T.F., KORBO L. MARCUSSEN A., NIELSEN K.M., NYENGAARD B., PAKKENBERG B., SORENSEN F.B., VESTERBY A. and WEST M.J. (1988a)
Some new, simple and efficient stereological methods and their use in the pathological research and diagnosis.
Acta Pathologica Microbiologica et Immunologica Scandinavia (A.P.M.I.S.) **96**:379-394

GUNDERSEN H.J.G., BAGGER P., BENDTSEN T.F., KORBO L. MARCUSSEN A., MOLLER A., NIELSEN K.M., NYENGAARD B., PAKKENBERG B., SORENSEN F.B., VESTERBY A. and WEST M.J. (1988b)
The new stereological tools: Dissector, fractionator, nucleator and point sampled intercepts and their use in pathological research and diagnosis.
A.P.M.I.S. **96**:857-881

HANCOX N.M. (1972)
The osteoclasts. In: The biochemistry and physiology of bone, Vol. 1 (2nd ed) GH Bourne (ed), pp 45-69. New York, Academic Press

HANNAM A.G. (1976)
Periodontal mechanoreceptors.
In: Mastication. (eds: Anderson D.J. and Matthews B.) Wright, Bristol pp. 43

HANNAM A.G. (1979a)
Neuromuscular control of overdentures. In: Precision attachments in dentistry (3rd ed.), HW Prieskel (ed), pp 156-161, London, Kimpton

HANNAM A.G. (1982)
The innervation of the periodontal ligament.
In: The periodontal ligament in health and disease.
(eds: Berkovitz B.K.B., Moxham B.J. and Newman H.N.)
Pergamon Press, Oxford, pp. 173-196.

HARRIS R. and GRIFFIN C.J. (1974b)
Innervation of the human periodontium. IV. Fine structure of the complex mechanoreceptors and free nerve endings.
Aust. Dent. J. **19**:326-331.

HAYAT M.A. (1969)
Uranyl acetate as a stain and a fixative for heart tissue.
Proc. 27th Ann. Meet. Electron Microsc. Soc. Am. pp 412
Claitor's Publishing Division, Baton Rouge

HAYAT M.A. (1970)
Principles and techniques of electron microscopy : Biological application, Vol. **1**.
Van Nostrand Reinhold Co., New York-Cincinnatti-Toronto-London-Melbourne.

HAYAT M.A. (1975)
In: Positive Staining for Electron Microscopy.
pp 1-47, Van Nostrand Reinhold Co., New York-Cincinnatti-Toronto-London-Melbourne.

HEERSCHE J.N.M. and DEPORTER D.A. (1979)
The mechanism of osteoclastic bone resorption: a new hypothesis.
J. Periodont. Res. **14**:266-267

HERMAN I.M. and JACOBSON S. (1988)
In situ analysis of microvascular pericytes in hypertensive rat brains.
Tissue Cell **20**:1-12

HOLTROP M.E. and WEINGER J.M. (1972)
Ultrastructural evidence for a transport system in bone. In: Calcium parathyroid hormone and the calcitonins, RV Talmage & PL Munson (eds) pp 365-374, Amsterdam, Excerpta Medica

HOPWOOD D. (1967a)
Some aspects of fixation with gluteraldehyde: a biochemical and histochemical comparison of the effects of formaldehyde and gluteraldehyde fixation on various enzymes and glycogen, with a note on penetration of gluteraldehyde into liver.
J. Anat. **101**:83

HYNES R.O. (1985)
Molecular biology of fibronectin.
Annual Review of Cell Biol **1**:67-90

INTAGLIETTA M. and PLOMBE E.P. de (1973)
Fluid exchange in tunnel and tube capillaries.
Microvasc. Res. **6**:153-168

JENSEN KJEILEN J.C., BRODIN P., AARS H. and BERG T. (1987)
Parotid salivary flow in response to mechanical and gustatory stimulation in man.
Acta Physiol. Scand. **131**:169-175

JONAS I.E. and RIEDE U.N. (1980)
Reaction of oxytalan fibers in human periodontium to mechanical stress.
J. Histochem. Cytochem. **28**:211-216

JONES G.E., ARUMUGHAM R.G. and TANZER M.L. (1986)
Fibronectin glycosylation modulates fibroblast adhesion and spreading.
J. Cell Biol. **103**:1663-1670

JOYCE N.C., DeCAMILLI P., and BOYLES J. (1984)
Pericytes, like vascular smooth muscle cells, are immunocytochemically positive for cyclic GMP- dependent protein kinase.
Microvasc. Res. **28**:206-219

JOYCE N.C., HAIRE M.F. and PALADE G.E. (1985a)
Contractile proteins in pericytes. I. Immunoperoxidase localization of tropomyosin.
J. Cell Biol. 100:1379-1386

JOYCE N.C., HAIRE M.F. and PALADE G.E. (1985b)
Contractile proteins in pericytes. II. Immunocytochemical evidence for the presence of two isomyosins in graded concentration.
J. Cell. Biol. 100:1387-1395

JYVASJARVI E., KNIFFKI K-D and MENGEL M.K.C. (1988)
Functional characteristics of afferent C-fibres from tooth pulp and periodontal ligament.
Progress in Brain Research **74**:237-245

KAHN A.J. and PATRIDGE N.C. (1987)
New concepts in Bone remodelling: An expanding role for the osteoblast.
American J. Otolaryngology **8**:258-264

KALLIO D.M., GARANT P.R. and MINKIN C. (1971)
Evidence of coated membranes in the ruffled border of the osteoclast.
J. Ultrastruct. Res. **37**:169-177

KANOZA R.J.J., KELLEHER L., SODEK J. and MELCHER A.H. (1980)
A biochemical analysis of the effect of hypofunction on collagen metabolism in the rat periodontal ligament.
Archs. Oral Biol. **25**:663-668

KELLER G.J. and COHEN D.W. (1955)
India ink perfusions of the vascular plexus of oral tissues.
Oral Surg. **8**:539-542

KENNEDY J. (1969)
Experimental ischaemia in monkeys. II. Vascular response.
J. Dent. Res. **48**:888-894

KINDLOVA M. (1965)
The blood supply of the marginal periodontium in the Macacus rhesus.
Archs. Oral Biol. **10**:869-874

KINDLOVÁ M. and MATENA V. (1959)
Blood circulation of the rodent teeth of the rat.
Acta Anat. **37**:163-192

KINDLOVÁ M. and MATENA V. (1962)
Blood vessels of the rat molar.
J. Dent. Res. **41**:650-660

KISHI Y. and TAKAHASHI K. (1977)
A scanning electron microscope study of the vascular architecture of the periodontal membrane.
Jap. J. Oral Biol. **28**:247-252

KLEIN A. (1928)
Systematische Untersuchungen über die Periodontalbriete.
Z. Stomat. **26**:417-439

KRONFELD R. (1931)
Histologic study of the influence of function on the human periodontal membrane.
J. Nat. Dent. Ass. **18**:1242-1274

KRONFELD R. (1936)
Structure, function and pathology of the human periodontal membrane.
New York J Dent **6**: 112-122

KUBOTA K. and OSANAI K. (1977)
Periodontal sensory innervation of the dentition of the Japanese shrew mole.
J. Dent. Res. **56**:531-537

LAMBRICHTS I., CREEMERS J. and van STEENBERGHE D. (1992)
Morphology of neural endings in the human periodontal ligament: An electron microscopic study.
J. Periodont. Res. **27**:191-196

LeBEUX Y.J. and WILLEMOT J. (1978)
Actin- and myosin-like filaments in rat brain pericytes.
Anat. Rec. **190**:811-826

LEE D., SIMS M.R., SAMPSON W.J. and DREYER C.W. (1990)
Stereo-pair three-dimensional imaging of microvascular architecture in primate dental tissues
Aust. Ortho. J. **11**:251-255

LEEDHAM M.D., SAMPSON W.J. and LINDSKOG S. (1990)
The relationship between the epithelial cell rests of Malassez and experimental root resorption and repair in Macaca fascicularis.
B.Sc. in Dentistry (Honors) Thesis, The University of Adelaide, South Australia

LEESON T.S., LEESON C.R. and PAPARO A.A. (1988)
Text/Atlas of Histology.
pp 126-158, 263-287, 309-323, 401-408, 669-674
W.B. Saunders International Edition.

LENZ (1968)
Zur Gefäßstruktur des marginalen Paradontiums-rasterelektronenmikroskopische Untersuchungen.
Dt Zahnärztl Z **29**:868-881

LEVY B.M. and BERNICK S. (1968b)
Studies on the biology of the periodontium of marmosets: V. Lymphatic vessels of the periodontal ligament.
J. Dent. Res. **47**:1166-1170

LEVY B.M., DREIZEN S. and BERNICK S. (1972a)
Effect of ageing on the marmoset periodontium.
J. Oral Pathol. **1**:61-65

LEVY B.M., DREIZEN S. and BERNICK S. (1972b)
The marmoset periodontium in health and disease.
In: Monographs in oral science vol **1**. Karger, Basel

LEW K.K.K. (1986)
Microvascular changes in the rat molar PDL incident to orthodontic toot extrusion with special reference to fenestrae.
M.D.S. Thesis, The University of Adelaide, South Australia

LEW K.K.K., SIMS M.R. and LEPPARD P.I. (1989)
Tooth extrusion effects on microvessel volumes, endothelial areas, and fenestrae in molar apical PDL.
AJO-DO **96**(3):221-231

LEWINSKY W. and STEWART D. (1937)
The innervation of the periodontal membrane of the cat with some observations on the function of the end-organs found in that structure.
J. Anat. **72**:531-536

LIMEBACK H.F., SODEK J. and BRUNETTE D.M. (1978)
Nature of collagens synthesised by monkey periodontal ligament fibroblasts in vitro.
Biochem. J. **170**:63-71

LIMEBACK H.F., SODEK J. and AUBIN J.E. (1983)
Variation in collagen expression by cloned periodontal ligament cells.
J. Periodont. Res. **18**:242-248

LINDEN R.W.A. (1990)
An update on the innervation of the periodontal ligament.
Eur. J. Orthodont. **12**:91-100.

LINDEN R.W.A. and SCOTT B.J.J. (1989a)
Distribution of mesencephalic nucleus and trigeminal ganglion mechanoreceptors in the periodontal ligament of the cat.
J. Physiology. **410**:35-44.

LINDHE J. (1985)
Textbook of clinical periodontology.
Munksgaard, Copenhagen; pp 63, 423-428

LINDSKOG J., BRANEMARK P. and LUNDSTROM J. (1968)
Biomicroscopic evaluation of micro-angiographic methods.
In: Hardes H (ed) Advances in microcirculation. Karger, Basel, pp 152-160

LUFT J.H. (1965)
The ultrastructural basis of capillary permeability.
In: The inflammatory process, ed. by BW Zweifach, L Grant and RT McCluskey
Academic Press, N.Y. and London, pp 121-159

LUFT J.H. (1973)
Capillary permeability. I. Structural considerations.
In "The inflammatory process". edited by BW Zweifach, L Grant, RT McCluskey
2nd ed. Vol 2. Chapter 2 pp 47-93, academic Press, New York

LUND J.P., McLACHLAN R.S. and DELLOW P.G. (1971)
A lateral jaw movement reflex.
Expl. Neurol. **31**:189-199

MAJNO G. (1965)
Ultrastructure of the vascular membrane.
In Handbook of Physiology, Sect 2, Circulation, Vol. 3, ed. W.F. Hamilton and P. Dow Am. Physiol. Soc., Washington. pp 2293-2375

MAJNO G., GABBIANI G., HIRSCHEL B.J, RYAN G.B. and STATKOV P.R. (1971)
Contraction of granulation tissue in vitro : Similarity to smooth muscle.
Science **173**:548-550

MAJNO G. and PALADE G.E. (1961)
Studies on inflammation. I. The effect of histamine and serotonin on vascular permeability: an electron microscopic study.
J. Biophys. Biochem. Cytol. **11**:571-605

MALASSEZ L. (1884)
Sur l'existence de masses epitheliales dans le ligament alveolodentaire chez l'homme adulte et al'etat normal.
Comp. Rend Soc. Biol. **36**:241-244

MATTHEWS B. and ROBINSON P.P. (1979)
The course of post-ganglionic sympathetic fibers to the face and jaws in the cat.
J. Physiol. (London) **293**:46P

MATTHEWS B. and ROBINSON P.P. (1980)
The course and post-ganglionic sympathethic fibers supplying the mandibular region in the cat.
J. Dent Res (Special Issue) 59:1840

MAUNSBACH A.B., MADDEN S.C. and LATTA H. (1962)
Variations in fine structure of renal tubular epithelium under different conditions of fixation.
J. Ultrastruct. Res. 6:511

McCULLAGH P. and NELDER J.A. (1983)
Generalised linear models.
Chapman and Hall, New York

McCULLOCH C.A.G. and MELCHER A.H. (1983b)
Cells density and cell generation in the periodontal ligament.
Am. J. Anat. 167:43-58.

McCULLOCH C.A.G. and MELCHER A.H. (1983c)
Cell migration in the periodontal ligament of mice.
J. Periodont. Res. 18:339-352

MEI N., HARTMANN F. and AUBERT M. (1977)
Periodontal mechanoreceptors involved in pain.
In: Pain in the trigeminal region. (eds: Anderson D.J. and Matthews B.)
Elsevier, Amsterdam, pp.103-110.

MELCHER A.H. and BEERTSEN W. (1977)
The physiology of tooth eruption.
In: McNamara JA (ed) The biology of occlusal development. Monograph No. 7
Craniofacial growth series. Centre for Human Growth and Development
University of Michigan, Ann Arbor pp 1-23

MEYER M. and TSCHETTER T. (1966)
A qualitative measure of pulpal blood flow using plastic microspheres.
IADR Abstract No. 381 pp 134

MIURA F. (1993)
Presentation on superelasticity at the 14th ASO Congress in Adelaide

MOFFAT D.B. (1967)
The fine structure of the blood vessels of the renal medulla with particlar reference to the control of the medullary circulation.
J. Ultrastruct Res 19:532-545

MORETZ R.C., AKERS C.K. and PARSONS D.F. (1969)
Use of small angle X-ray diffraction to investigate disordering of membranes during preparation for electron microscopy. I. Osmium tetroxide and potassium permanganate.
Biochem. Biophys. Acta 193,1

MOVAT H.V. and FERNANDO N.V.P. (1964)
The fine structure of the terminal vascular bed. IV. The venules and their perivascular cells (pericytes, adventitial cells).
Exp. Mol. Pathol. 3:98-114

MOXHAM B.J., SHORE R.C. and BERKOVITZ B.K.B. (1985)
Fenestrated capillaries in the connective tissues of the periodontal ligament.
Microvasc. Res. 30:116-124

MÜHLEMANN H.R. (1967)
Tooth mobility : a review of clinical aspects and research findings.
J. Periodont. 38:686-708

MUNEMOTO K., IWAYAMA Y., YOSHIDA M., SERA M., AONO M. and YOKOMIZO I. (1970)
Isolation and characterization of acid mucopolysaccharides of bovine periodontal membrane.
Archs. Oral Biol. **15**:369-382

NAKAMURA T.K., NAKAHARA H., NAKAMURA M., KIYOMURA H. and TOKIOKA T. (1992)
Fine structure of adrenergic nerve fibres in human periodontal ligament.
J. Periodont. Res. **27**:569-574

NYENGAARD J.R., BENDTSEN T.F. and GUNDERSEN H.J.G. (1988)
Stereological estimation of the number of capillaries, examplified by renal glomeruli.
APMIS Suppl. **4**:92-99

OWEN M. (1971)
Cellular dynamics in bone. In: The biochemistry and physiology of bone, Vol III (2nd ed.) GH Bourne (ed) pp 271-298. London, Academic Press

OWEN M. and SHETLAR M.R. (1968)
Uptake of 3-H glucosamine by osteoclasts.
Nature **220**:1335-1336

PALADE G.E. (1956)
The fixation of tissues for electron microscopy.
Proc. 3rd Int. Congr. Electron Microscopy, London, p 129

PALADE G.E. (1960)
Transport in quanta across the endothelium of blood capillaries.
Anat. Rec. **136**:254 (Abstract)

PARFITT G.J. (1960)
Measurement of the physiological mobility of individual teeth in an axial direction.
J. Dent. Res. **39**:608-618

PARLANGE L.M. (1991)
A TEM stereological analysis of blood vessels and nerves in marmoset PDL following orthodontic extrusion.
M.D.S. Thesis, The University of Adelaide, South Australia

PARLANGE L.M. and SIMS M.R. (1993)
A TEM stereological analysis of blood vessels and nerves in marmoset PDL following endontics and magnetic incisor extrusion.
Eur. J. Orthod. **15**:33-44

PEACHEY L.D. (1960)
Section thickness and compression.
Proc. 4th Intern. Congress Electron Micro. (Berlin)
2P-72 Springer-Verlag-Berlin

PEARSON C.H. (1982)
The ground substance of the periodontal ligament
In: Berkovitz BKB, Moxham BJ, Newman HN (eds) The periodontal ligament in health and disease.
Pergamon Press, Oxford, pp 119-149

PEARSON C.H. and GIBSON G.J. (1979)
Proteoglycans of the periodontal ligament and dermis.
In: Schauer R, Boer P, Buddecke E, Kramer MF, Vliegenthart JFG, Wiegandt H (eds)
Glycoconjugates. Thieme, Stuggart, pp 559-560

PICTON D.C.A. (1964)
Some implications of normal tooth mobility during mastication.
Archs. Oral Biol. **9**:565-573

PICTON D.C.A. and DAVIES W.I.R. (1967)
Dimensional changes in the periodontal membrane of monkeys (macaca irus) due to horizontal thrusts applied to the teeth.
Archs. Oral Biol. 12:1635-1643

PROVENZA D.V., BIDDIX J.C. and CHENG T.C. (1960)
Studies on the etiology of periodontosis.
II. Glomera as vascular components in the periodontal membrane
Oral Surg. **13**:157-164

QUINTARELLI G. (1959)
The normal vascular architecture of the mandibular periodontal membrane and gingiva in dog.
Alabama Dental Review **7**; Winter

RAPP R., KIRSTINE W.D. and AVERY J.K. (1957)
A study of neural endings in the human gingiva and periodontal membrane.
J. Canadian Dent. Assoc. **23**:637-643.

REEVE C.M. and WENTZ F.M. (1962)
The prevalence, morphology and distribution of epithelial rests in the human periodontal ligament.
J. Oral Med, Oral Surg, Oral Path **15**:785-793

RENKIN E.M. (1977)
Multiple pathways of capillary permeability.
Cir. Res. **41**:735-743

RHODIN J.A.G. (1962b)
The diaphragm of capillary endothelial fenestrations.
J. Ultrastruct Res **6**:171-185

RHODIN J.A.G. (1967)
The ultrastructure of mammalian arterioles and precapillary sphincters.
J. Ultrasruct. Res. **18**:181-223.

RHODIN J.A.G. (1968)
Ultrastructure of mammalian venous capillaries, venules and small collecting veins.
J. Ultrastruct. Res. **25**:452-500.

RHODIN J.A.G. (1974)
Cardiovascular system. In: Histology. A Text and Atlas.
Chapter 16, Oxford Univ. Press, London and New York

RHODIN J.A.G. (1980)
Architecture of the vessels wall.
Handbook Physiol. Sect. 2, **2**:1-31

RHODIN J.A.G. (1981)
Anatomy of the Microcirculation.
In: Microcirculation, Academic Press; Chapter 2, pp. 11

RHODIN J.A.G. and LIM SUE S. (1979)
Combined intravital microscopy and electron microscopy of the blind endings of the mesenteric lymphatic capillaries of the rat mesentery.
Acta Physiol. Scand. Suppl. **463**:51-58

RIPPIN J.W. (1976)
Collagen turnover in the periodontal ligament under normal and altered functional forces. I. Young rat molars.
J. Periodont. Res. **11**:101-107

ROBERTS W.E., MOZSARY P.G. and KLINGLER E. (1982)
Nuclear size as a cell-kinetic marker for osteoblast differentiation.
Am. J. Anat. **165**:373-384

ROBINSON P.P. (1979)
The course, relations and distribution of the inferior alveolar nerve and its branches in the cat.
Anat. Rec. **195**:265-272

RUBEN M.P., PRIETO-HERNANDEZ J.R., GOTT F.K., KRAMER G.M. and BLOOM A.A. (1971)
Visualization of lymphatic microcirculation of oral tissues. II. Vital retrograde lymphography.
J. Periodont. **42**:774-784

SAMPSON W.J. (1979)
A comparative light microscopic evaluation of oxytalan fiber staining with a variety of dye substances.
Stain Technol. **54**:181-191

SAUNDERS R.L. de C.H. (1966)
X-ray microscopy of the periodontal and dental pulp vessels in the monkey and man.
Oral Surg. **22**:503-518

SCHROEDER H.E. (1986)
The Periodontium.
(eds: Oksche A. and Vollrath L.)
Springer-Verlag, Berlin - Heidelberg - New York - Toronto pp. 170-231.

SCHUBACK P. and GOLDMAN H. (1957)
Technic for radiographic visualization of the vascular system of the periodontal tissues.
J. Dent. Res. **36**:245-248

SCHWEITZER G. (1907)
Über die Lymphgefäße des Zahnfleisches und der Zähne beim Menschen und Zähne.
Archs. Mikrosk. Anat. **69**:807-908

SEVERSON J.A., MOFFETT B.C., KOKICH V. and SELIPSKY H. (1978)
A histologic study of age changes in the adult human periodontal joint (ligament).
J. Periodont. **49**: 189-200

SHACKELFORD J.M. (1971)
Scanning electron microscopy of the dog periodontium.
J. Periodont. Res. **6**:45-54

SHORE R.C. and BERKOVITZ B.K.B. (1979)
An ultrastructural study of periodontal ligament fibroblasts in relation to their possible role in tooth eruption and intercellular collagen degradation in the rat.
Archs. Oral Biol. **24**:155-164

SHORE R.C., MOXHAM B.J. and BERKOVITZ B.K.B. (1982)
A quantitative comparison of the ultrastructure of the periodontal ligaments of impeded and unimpeded rat incisors.
Archs. Oral Biol. **27**:423-430

SHORE R.C., BERKOVITZ B.K.B. and MOXHAM B.J. (1984)
Histological study, including ultrastructural quantification, of the periodontal ligament in the lathyritic rat mandibular dentition.
Archs. Oral Biol. **29**:263-273

SHUTTLEWORTH C.A. and SMALLEY J.W. (1983)
Periodontal ligament.
International Review of Connective Tissue Research **10**:211-247.

SICHER H. (1966)
Orban's oral histology and embryology.
6th Edition, Saint Louis, Mosby

SIMIONESCU M. and SIMIONESCU N. (1984)
Ultrastructure of the microvascular wall: functional correlations. In: Handbook of physiology. (eds) Renkin EM, Michel CC. Bethesda: American Physiological Society, pp 41-101

SIMIONESCU N., SIMIONESCU M. and PALADE G.E. (1975)
Permeability of muscles capillaries to small heme-peptides : evidence for the existence of patent transendothelial channels.
J. Cell Biol. **64**:586-607

SIMPSON H.E. (1965)
The degeneration of the rests of Malassez with age as observed by the apoxestic technique.
J. Periodont. **36**:288-291

SIMPSON H.E. (1966)
Innervation of the periodontal membrane as observed by the apoxestic technique.
J. Periodont. **37**:374-376.

SIMPSON H.E. (1967)
A three dimensional approach to the microscopy of the periodontal membrane.
Proceedings of the Royal Society of Medicine **60**:537-542.

SIMS M.R. (1973)
Oxytalan fiber system of molars in the mouse mandible
J. Dent. Res. **52**:797-802

SIMS M.R. (1975)
Oxytalan-vascular relationships observed in histologic examination of the periodontal ligaments of man and mouse.
Archs. Oral Biol. **20**:713-716

SIMS M.R. (1977b)
The oxytalan fiber system in the mandibular periodontal ligament of the lathyritic mouse.
J. Oral Pathol. **6**:233-250

SIMS M.R. (1980)
Angular changes in collagen cemental attachment during tooth movement.
J. Periodont. Res. **15**:638-645

SIMS M.R. (1983)
Electron-microscope affiliation of oxytalan fibres, nerves and microvasculature bed in the mouse periodontal ligament.
Archs. Oral Biol. **28**:1017-1024.

SIMS M.R. (1984a)
Ultrastructural analysis of the microfibrillar component of mouse and human periodontal oxytalan fibers.
Connect Tissue Res. **13**:59-67

SIMS M.R. (1984b)
Ultrastructural evidence of nerve and oxytalan fibre associations in the endoneurium of human periodontal ligament.
Archs Oral Biol. **29**:565-567

SIMS M.R. (1987)
A model of the anisotropic distribution of microvascular volume in the periodontal ligament of the mouse mandibular molar.
Aust. Orthod. J. **10**:21-24.

SIMS M.R. and WEEKES W.T. (1985)
Resorption related to orthodontics and some morphological features of the periodontal microvascular bed.
Int. Endo J. **18**:140-145

SIMS M.R., LEPPARD P.I., SAMPSON W.J. and DREYER C.W. (1994)
Microvascular luminal changes in aged mouse periodontal ligament.
(Unpublished data)

SLOAN P. (1978)
Scanning electron microscopy of the collagen fibre architecture of the rabbit incisor periodontium.
Archs. Oral Biol. **23**: 567-572

SLOAN P. (1982)
Structural organization of the fibres of the periodontal ligament.
In: Berkovitz BKB, Moxham BJ, Newman HN (eds) The periodontal ligement in health and disease. Pergamon Press, Oxford, pp 51-72

SODEK J. (1976)
A new approach to assessing collagen turnover by using a microassay.
Biochem. J. **160**:243-246

STANLEY C. (1993)
Corrosion cast SEM stereopair study of marmoset periodontal ligament.
M.D.S. Thesis, The University of Adelaide, South Australia

STEIN O. and STEIN Y. (1971)
Light and electron microscopic radioautoradiography of lipids: techniques and biological applications.
Adv. Lipid Res. **9**:1

STERIO D.C. (1984)
The unbiased estimation of number and sizes of arbitary particles using the dissector.
J. Microsc. **134**:127-136

STOPAK D. and HARRIS A.K. (1982)
Connective tissue morphogenesis by fibroblast traction. I. Tissue culture observations.
Developmental Biology **90**:383-398

SUTTON J.S. and WEISS L. (1966)
Transformation of monocytes in tissue culture into marophages, epitheloid cells and multinucleate giant cells. An electron microscopic study.
J. Cell Biol. **28**:303-332

TAKITA K., OHSHAKI Y., NAKATA M. and KURISU K. (1987)
Immunofluorescence localization of type I and type III collagen and fibronectin in mouse dental tissues in late development and during eruption.
Archs. Oral Biol. **32**:273-279

TANG M.P.F and SIMS M.R.S (1992)
A TEM analysis of tissue channels in normal and orthodontically tensioned rat molar periodontal ligament.
Eur. J. Orthod. **14**:433-444

TEN CATE A.R. (1965)
The histochemical demonstration of specific oxidative enzymes and glycogen in the epithelial cell rests of Malassez.
Archs. Oral Biol. **10**:207-213

TEN CATE A.R. (1967)
The formation and function of the epithelial cell rests of Malassez.
In: The mechanisms of tooth support. Wright, Bristol, pp 80-83

TEN CATE A.R. (1972b)
Morphological studies of fibrocytes in connective tissue undergoing rapid remodelling.
J. Anat. **112**:401-414

TERTEL-KALWEIT D. and DONATH K. (1985)
Histologische Untersuchungengen zur Verteilung Malassezscher Epithelnester zwischen dem 10. and 90. Lebensjahr.
Dt Zahnärztl Z **40**:551-554

TRUMP B.F. and ERICSSON J.L.E. (1965)
The effect of the fixative solution on the ultrastructure of cells and tissues.
Lab. Invest. **14**:1245-1323

TRUMP B.F. and BULGER R.E. (1966)
New ultrastructural characteristics of cells fixed in a gluteraldehyde-osmium tetroxide mixture.
Lab. Invest. **15**:368

TURNER H., RUBEN M.P., FRANKL S.N., SHEFF M. and SILBERSTEIN S. (1969)
Visualization of the microcirculation of the periodontium.
J. Periodont. **40**:222-230

TYLER D.W. and BURN-MURDOCH R. (1976)
Tooth movements in an *in vitro* model system. In: The eruption and occlusion of teeth. (eds) Poole DFG and Stack MV. Butterworths, London pp 302-304

UNDERWOOD, E.E. (1970)
Quantitative Stereology (Addison Wesley, Massachusett)

VALDERHAUG J. and NYLEN M.U. (1966)
Function of the epithelial rests as suggested by their ultrastructure.
J. Periodont. Res. **1**:69-78

VALDERHAUG J. and ZANDER H.A. (1967)
Relationship of "epithelial rests of Malassez" to other periodontal structures.
Periodontics **5**:254-258

van STEENBERGHE (1979)
The structure and function of periodontal innervation.
J. Periodont. Res. **14**:185-203.

WALKER T.W. (1980)
A model of the periodontal vasculature in tooth support.
J. Biomech. **13**:149-157

WAERHAUG J. (1954)
Over-og underkjevens karsforsyning med saerlig henblikk på gingiva, tennene og deres støttev.
Norske Tandlaegforen Tid **64**:159-170

WATANABE S. and DAWES C. (1988)
A comparison of the effects of tasting and chewing foods on the flow rate of whole saliva in man.
Archs. Oral Biol. **33**:761-764

WEEKES W.T. (1983)
Vascular morphology of rat molar periodontium.
M.D.S. Thesis, University of Adelaide, South Australia

WEEKES W.T. and SIMS M.R. (1986b)
The vasculature of the rat molar periodontal ligament.
J. Periodont Res **21**:186-194

WEIBEL E.R. and PALADE G.E. (1964)
New cytoplasmic components in arterial endothelia.
J. Cell Biol. **23**:101-112

WEIBEL E.R. (1974)
Point counting methods.
In: Stereological methods Vol. I
Academic Press, London, New York, Toronto, Sydney, San Francisco pp. 101-120, 237-256.

WEIBEL E.R. (1981)
Stereological Methods in cell biology.
J. Histochem. and Cytochem. **29** (9): 1043-1052

WEIDEMAN M.P. (1963)
Dimensions of blood vessels from distributing artery to collecting vein.
Circulation Res. **12**:375-378

WEIR A. (1990)
A stereological analysis of the marmoset incisor periodontal ligament following root canal treatment, orthodontic extrusion and after prolonged retention.
M.D.S. Thesis, The University of Adelaide, South Australia

WHITTLE B.J.R. (1977)
Prostaglandins and mast cell histamine. In: Prostaglandins and thromboxanes, F Berti, B Samuelsson, GP Velo (eds)
pp 345-352, New York, Plenum Press

WILLMER E.N. (1945)
Growth and form in tissue cultures. In: Essays on Growth and Form, ed WEL Clark and PB Medawar. Clarendon Press, Oxford. pp 264-294

WILLS D.J., PICTON D.C.A. and DAVIES W.I.R. (1976)
A study of the fluid systems of the periodontium in macaque monkeys.
Archs. Oral Biol. **21**:175-185.

WOLFF J.R. (1964)
Ein Beitrag zur Ultrastruktur der Blutapillaren: Das nahtlose Endothel.
Z. Zellforsch **64**:290-300

WOLFF J.R., GOERZ C., BAR T. and GULDNER F.H. (1975)
Common morphogenetic aspects of various organotypic microvascular patterns.
Microvasc. Res. **10**:373-395

WONG R.S.T. and SIMS M.R. (1983)
Morphology of the enamel-cemental microvascular junction of the mouse incisor
Aust. Ortho. J. **8**:49-50

WONG R.S.T. and SIMS M.R. (1987)
A scanning electron-microscopic, stereo-pair study of methacrylate corrosion casts of the mouse palatal and molar periodontal microvasculature.
Archs. Oral Biol. **32**:557-566

YAMASAKI A, ROSE G.G., PIRERO G.J. and MAHAN C.J. (1987)
Ultrastructural and morphometric analyses of human cementoblasts and periodontal fibroblasts.
J. Periodont. **58**:192-201

ZWARYCH P.D. and QUIGLEY M.B. (1965)
The intermediate plexus of the periodontal ligament: History and further observations.
J. Dent. Res. 44: 383-391

ZWEIFACH B. (1961)
Functional behaviour of the microcirculation.
Springfield, Thomas.